

AEDC-TR-92-18

C.2

Effects of Spacecraft Materials Outgassing Products on Cryogenic Surfaces

W. T. Bertrand and B. E. Wood
Calspan Corporation/AEDC Operations

March 1993

Final Report for Period February 28, 1989 – July 27, 1992

Approved for public release; distribution is unlimited.

**TECHNICAL REPORTS
FILE COPY**

**PROPERTY OF U.S. AIR FORCE
AEDC TECHNICAL LIBRARY**

**ARNOLD ENGINEERING DEVELOPMENT CENTER
ARNOLD AIR FORCE BASE, TENNESSEE
AIR FORCE MATERIEL COMMAND
UNITED STATES AIR FORCE**



NOTICES

When U. S. Government drawings, specifications, or other data are used for any purpose other than a definitely related Government procurement operation, the Government thereby incurs no responsibility nor any obligation whatsoever, and the fact that the Government may have formulated, furnished, or in any way supplied the said drawings, specifications, or other data, is not to be regarded by implication or otherwise, or in any manner licensing the holder or any other person or corporation, or conveying any rights or permission to manufacture, use, or sell any patented invention that may in any way be related thereto.

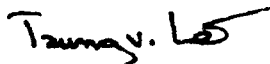
Qualified users may obtain copies of this report from the Defense Technical Information Center.

References to named commercial products in this report are not to be considered in any sense as an endorsement of the product by the United States Air Force or the Government.

This report has been reviewed by the Office of Public Affairs (PA) and is releasable to the National Technical Information Service (NTIS). At NTIS, it will be available to the general public, including foreign nations.

APPROVAL STATEMENT

This report has been reviewed and approved.



TRUNG V. LE
Space Systems Division
Directorate of Aerospace Flight Dynamics Test
Deputy for Operations

Approved for publication:

FOR THE COMMANDER



DAVID C. BOND
Chief, Space Systems Division
Directorate of Aerospace Flight Dynamics Test
Deputy for Operations

REPORT DOCUMENTATION PAGE			Form Approved OMB No. 0704-0188	
Public reporting burden for this collection of information is estimated to average 1 hour per response, including the time for reviewing instructions, searching existing data sources, gathering and maintaining the data needed, and completing and reviewing the collection of information. Send comments regarding this burden estimate or any other aspect of this collection of information, including suggestions for reducing this burden, to Washington Headquarters Services, Directorate for Information Operations and Reports, 1215 Jefferson Davis Highway, Suite 1204, Arlington, VA 22202-4302, and to the Office of Management and Budget, Paperwork Reduction Project (0704-0188), Washington, DC 20503.				
1. AGENCY USE ONLY (Leave blank)	2. REPORT DATE March 1993	3. REPORT TYPE AND DATES COVERED Final - February 1989 - July 1992		
4. TITLE AND SUBTITLE Effects of Spacecraft Materials Outgassing Products on Cryogenic Surfaces		5. FUNDING NUMBERS PE - 921F01		
6. AUTHOR(S) Bertrand, W. T. and Wood, B. E. Calspan Corporation/AEDC Operations				
7. PERFORMING ORGANIZATION NAME(S) AND ADDRESS(ES) Arnold Engineering Development Center/DOT Air Force Systems Command Arnold Air Force Base, TN 37389-9011		8. PERFORMING ORGANIZATION REPORT NUMBER AEDC-TR-92-18		
9. SPONSORING/MONITORING AGENCY NAME(S) AND ADDRESS(ES) Air Force Wright Laboratory (AFWL) Wright-Patterson Air Force Base, OH 45433		10. SPONSORING/MONITORING AGENCY REPORT NUMBER		
11. SUPPLEMENTARY NOTES Available in Defense Technical Information Center (DTIC).				
12a. DISTRIBUTION/AVAILABILITY STATEMENT Approved for public release; distribution is unlimited.		12b. DISTRIBUTION CODE		
13. ABSTRACT (Maximum 200 words) Optical property measurements of condensed contaminant films on cryogenically cooled substrates were reported in AEDC-TR-87-8 and AEDC-TR-89-2. Measurements for five additional materials and three material mixtures are presented in this report. Infrared spectral transmittance measurements were made for thin films of contaminant deposited on a 77 K germanium window under vacuum conditions. Material temperatures were controlled at 125°C to provide the outgassing source. The objective of this report is to present the refractive and absorptive indices of the condensed outgassing products of satellite materials which have been determined from the experimental measurements of infrared transmittance, and to describe an effort to combine optical property data from two materials to provide values that can be used to calculate the surface effects for contaminant mixtures.				
14. SUBJECT TERMS spacecraft materials, outgassing products, cryogenic surfaces, refractive indices, contamination, optical properties		15. NUMBER OF PAGES 64		
		16. PRICE CODE		
17. SECURITY CLASSIFICATION OF REPORT UNCLASSIFIED	18. SECURITY CLASSIFICATION OF THIS PAGE UNCLASSIFIED	19. SECURITY CLASSIFICATION OF ABSTRACT UNCLASSIFIED	20. LIMITATION OF ABSTRACT SAME AS REPORT	

PREFACE

The work reported herein was performed by the Arnold Engineering Development Center (AEDC), Air Force Materiel Command (AFMC) under Program Element 62102F. The results were obtained by Calspan Corporation, AEDC Operations, technical services contractor for Aerospace Flight Dynamics Testing at AEDC, AFMC, Arnold Air Force Base, Tennessee, under AEDC Project No. CP94VW (V41V-23). The project was sponsored by the Air Force Wright Laboratory (AFWL), Wright-Patterson AFB, Ohio. The AFWL Project Manager was Capt. Michele Jones, and the AEDC Project Manager was Mr. Trung Le.

The authors would also like to express their appreciation to Bill Hobbs and Winfred Johnson for their help with the chamber assembly, operation, and instrumentation. This report was submitted for publication on January 27, 1993.

DTIC QUALITY INSPECTED 4

Accession For	
NTIS	<input checked="" type="checkbox"/>
DTIC	<input type="checkbox"/>
Unannounced	<input type="checkbox"/>
Justification	
By	
Distribution/	
Availability Codes	
Dist	Avail and/or Special
A-1	

CONTENTS

1.0 INTRODUCTION	7
2.0 EXPERIMENTAL TEST APPARATUS	8
2.1 Contaminant Optical Properties (COP) Chamber	8
3.0 EXPERIMENTAL TEST PROCEDURE	11
3.1 Film Thickness Measurement	11
3.2 Material Documentation and Preparation	12
3.3 Contaminant Optical Properties Chamber Test Procedures	12
4.0 DATA REDUCTION	13
4.1 Optical Properties of Satellite Materials Outgassing Products	13
4.2 Transmittance Calculations Using CALCRT	14
5.0 RESULTS AND DISCUSSION	15
5.1 Torrseal Sealant	15
5.2 Polyclad Laminate	15
5.3 NVF Laminate	16
5.4 Uralane®	16
5.5 RTV-566	16
5.6 Mixtures	17
6.0 SUMMARY	17
REFERENCES	18

ILLUSTRATIONS

<u>Figure</u>	<u>Page</u>
1. Schematic of COP Chamber	21
2. Schematic of COP Chamber Components	22
3. Transmittance of Bare Germanium Window at 77 K	23
4. Optical Properties for Torrseal	24
5. Transmittance for 0.12- μ m-Thick Torrseal	25
6. Transmittance for 0.61- μ m-Thick Torrseal	25
7. Transmittance for 1.82- μ m-Thick Torrseal	26
8. Transmittance at 800 cm^{-1} for Torrseal	26
9. Transmittance at 2,000 cm^{-1} for Torrseal	27
10. Transmittance at 3,250 cm^{-1} for Torrseal	27
11. Optical Properties for Polyclad	28
12. Transmittance for 0.13- μ m-Thick Polyclad	29
13. Transmittance for 0.92- μ m-Thick Polyclad	29
14. Transmittance for 2.90- μ m-Thick Polyclad	30

<u>Figure</u>	<u>Page</u>
15. Transmittance at 800 cm^{-1} for Polyclad	30
16. Transmittance at 2,000 cm^{-1} for Polyclad	31
17. Transmittance at 3,250 cm^{-1} for Polyclad	31
18. Optical Properties for NVF	32
19. Transmittance for 0.13- μm -Thick NVF	33
20. Transmittance for 1.05- μm -Thick NVF	33
21. Transmittance for 4.21- μm -Thick NVF	34
22. Transmittance at 800 cm^{-1} for NVF	34
23. Transmittance at 2,000 cm^{-1} for NVF	35
24. Transmittance at 3,250 cm^{-1} for NVF	35
25. Optical Properties for Uralane	36
26. Transmittance for 0.11- μm -Thick Uralane	37
27. Transmittance for 0.45- μm -Thick Uralane	37
28. Transmittance for 0.91- μm -Thick Uralane	38
29. Transmittance at 1,100 cm^{-1} for Uralane	38
30. Transmittance at 2,000 cm^{-1} for Uralane	39
31. Transmittance at 3,250 cm^{-1} for Uralane	39
32. Optical Properties for RTV-566	40
33. Transmittance for 0.11- μm -Thick RTV-566	41
34. Transmittance for 0.68- μm -Thick RTV-566	41
35. Transmittance for 1.48- μm -Thick RTV-566	42
36. Transmittance at 1,100 cm^{-1} for RTV-566	42
37. Transmittance at 2,000 cm^{-1} for RTV-566	43
38. Transmittance at 3,250 cm^{-1} for RTV-566	43
39. Optical Properties for Mix 1	44
40. Transmittance for 0.11- μm -Thick Mix 1	45
41. Transmittance for 1.02- μm -Thick Mix 1	45
42. Transmittance for 2.50- μm -Thick Mix 1	46
43. Transmittance at 1,100 cm^{-1} for Mix 1	46
44. Transmittance at 2,000 cm^{-1} for Mix 1	47
45. Transmittance at 3,250 cm^{-1} for Mix 1	47
46. Optical Properties for Mix 2	48
47. Transmittance for 0.11- μm -Thick Mix 2	49
48. Transmittance for 0.79- μm -Thick Mix 2	49
49. Transmittance for 1.59- μm -Thick Mix 2	50
50. Transmittance at 1,100 cm^{-1} for Mix 2	50
51. Transmittance at 2,000 cm^{-1} for Mix 2	51
52. Transmittance at 3,250 cm^{-1} for Mix 2	51

FigurePage

53. Optical Properties for Mix 3	52
54. Transmittance for 0.12- μm -Thick Mix 3	53
55. Transmittance for 0.83- μm -Thick Mix 3	53
56. Transmittance for 1.66- μm -Thick Mix 3	54
57. Transmittance at 1,100 cm^{-1} for Mix 3	54
58. Transmittance at 2,000 cm^{-1} for Mix 3	55
59. Transmittance at 3,250 cm^{-1} for Mix 3	55
60. Transmittance for 1.02- μm -Thick Combined Mix 1	56
61. Transmittance for 2.50- μm -Thick Combined Mix 1	57
62. Transmittance for 0.91- μm -Thick Combined Mix 2	58
63. Transmittance for 1.59- μm -Thick Combined Mix 2	59
64. Transmittance for 0.95- μm -Thick Combined Mix 3	60
65. Transmittance for 1.66- μm -Thick Combined Mix 3	61

1.0 INTRODUCTION

As satellite applications become more sophisticated and satellite lifetimes are extended, the roles of contamination prediction and control become increasingly important. Contamination can alter the spectral characteristics of cryogenically cooled optical systems, increase the solar absorptance of thermal control surfaces, causing the spacecraft to overheat, or degrade the power output of solar cells.

A spacecraft designer must predict effects of contamination with a very limited amount of data. The ASTM 595 (Ref. 1) outgassing test has been the industry standard for screening materials. The total mass loss (TML) and the collected volatile condensable material (CVCM) are used as guides. These parameters are determined by heating a sample to 125°C for 24 hr under vacuum. The TML is found from the measurements of the sample weight before and after heating. The CVCM is determined by weighing a 25°C collector surface which was positioned above the heated sample, before and after the 24-hr heating cycle. From the ASTM 595 criteria, a material, to be space rated, must have a TML of less than 1 percent and a CVCM of less than 0.1 percent. These criteria do not take into account the effect of a contaminant on a spacecraft optical surface.

The objectives of the AFWL contamination program at AEDC are to establish a centralized Air Force surface effects facility for determining optical properties of satellite material outgassing products, determine refractive (n) and absorptive (k) indices for contaminant films condensed on cryogenic surfaces, and establish a database for satellite material categories such as paints, adhesives, films, composites, etc.; and provide computational-analytical thin-film programs for calculating contaminant effects on the transmittance/reflectance of cryogenically cooled optical components using derived contaminant n 's and k 's.

The experimental investigations of cryogenically condensed contaminant films were carried out in the AEDC Contaminant Optical Properties (COP) Chamber. The materials were heated to 125°C under vacuum and the outgassed products were frozen as thin films on a 77 K germanium window. A scanning Michelson interferometer was used to measure the infrared transmittance over the 4,000-450 cm^{-1} wavenumber range. From the recorded infrared transmittance data, the refractive and absorptive indices of the contaminant films were determined using a computational program (TRNLIN) (Ref. 2) which is based on a thin-film interference model. These n and k values can then be used with CALCRT (Ref. 2), another program developed at AEDC, to calculate the transmittance or reflectance of other optical components contaminated with the outgassing products of the same satellite material as a function of contaminant film thickness, wavenumber, and incidence angle.

Infrared transmittance of contaminants condensed from 17 satellite materials and the calculated optical properties were previously reported in AEDC technical reports (Refs. 2, 3). In this report infrared spectra and optical properties of contaminant gases condensed on a 77 K germanium window are presented for five additional materials and three mixtures. An effort to combine optical property data from two materials to provide values that can be used to calculate the surface effects for contaminant mixtures is described. Tabulated n, k data for the materials investigated have been input to the NASA Marshall MAPTIS material database. The data and the CALCRT program are also available from AEDC.

2.0 EXPERIMENTAL TEST APPARATUS

2.1 CONTAMINANT OPTICAL PROPERTIES (COP) CHAMBER

Infrared transmittance measurements were made of satellite material outgassing contamination products on cryogenic surfaces in the AEDC COP Chamber (Figs. 1-2). The pumping system consisted of a turbomolecular pump with a mechanical forepump and a liquid nitrogen (LN_2)-cooled chamber liner. The turbo pump and the cryopanel were necessary to provide a near contaminant-free vacuum. With this pumping system a vacuum in the mid- 10^{-7} torr range could be routinely achieved. Thermocouple and ion gauges were used to monitor the chamber pressure. An effusion cell heated the materials to 125°C to provide the source of contamination. The test surface was a germanium window mounted in the center of the chamber. It was cooled to near 77 K with a constant flow of LN_2 . The germanium window temperature was monitored by platinum resistors embedded in the surrounding housing. The thin-film interference model on which the optical property determinations were based required that only the front surface of the germanium window be coated by the contaminant material. Therefore, special precautions were taken to ensure that nothing was deposited on the rear surface. Two LN_2 -cooled baffles were located behind the rear surface to scavenge any gases that otherwise would be incident on it. One was a rectangular flat plate located directly behind the germanium surface when it was in position for film deposition. The other was a hollow LN_2 -cooled cylinder which shielded the rear surface when it was rotated into the IR transmittance measurement position. The IR beam used in making the transmittance measurements passed through the center of the hollow tube.

2.1.1 Effusion Cell

The outgassing products for contaminating the sample surface were generated using an effusion cell. The cell has a cylindrical aluminum body 3.5 in. (8.89 cm) long with an internal bore diameter of 1.75 in. (4.45 cm). The material used to produce the outgassing flux was loaded into the closed end of the effusion cell, and the outgassing products exited through the open end. A Teflon® -coated heating element covered most of the outside surface of the

cylinder. A temperature-controlled power supply was used to maintain the temperature of the cell at a constant value (usually 125°C). Cell temperatures were sensed by a thermocouple and controlled within $\pm 3^\circ\text{C}$ of the set point. The effusion cell exit was positioned 2 in. (5.08 cm) from the germanium window and quartz crystal microbalance (QCM). The QCM is an instrument used to measure the mass of the deposited contaminant. The centerline of the effusion cell was located midway between the centers of the germanium window and the QCM so that the deposition rates on the two were equal.

The effusion cell was lined with disposable aluminum foil liners. The liners and aluminum foil sample boat were baked out at 125°C for 24 hr prior to each material test. This ensured that the deposited contaminants came from the material being investigated and not the peripheral components. New aluminum foil liners and boats were installed for each material investigated.

2.1.2 Germanium Window Deposition Surface

Germanium was picked for the deposition surface because it has good thermal conductance and a flat transmittance spectrum over the 700–4,000 cm^{-1} (2.5–14 μm) wavenumber range. The window was 2.75 in. (6.99 cm) square and was 0.157 in. (4 mm) thick. Nominally, the transmittance (Fig. 3) of the window (at room temperature) was 47–48 percent over most of the wavenumber range. At 77 K, the transmittance increased to about 49 percent in the flat portion of the spectrum. The refractive index of germanium (Ref. 4) is given by

$$n_g(\nu) = A + BL + CL^2 + D\nu^{-2} + E\nu^{-4} \quad (1)$$

where

ν = wavenumber

A = 3.88

B = 0.391707

C = 0.163492

D = -0.000006

E = 0.000000053

L = $(\nu^{-2} - 0.028)^{-1}$

2.1.3 Infrared Transmittance Measurement Equipment

A commercially made Michelson interferometer was utilized in making infrared transmittance measurements of the deposited contaminant film on the germanium window. A graphite radiation source was located inside the interferometer housing. The inter-

ferometrically modulated infrared beam was collimated and allowed to pass through a housing port. The exit beam was then passed through a KBr window on the chamber port, through the germanium test window, through another KBr window on the opposite side of the chamber, and finally to a box containing the detector optics and detector. The detector was Hg-Cd-Te, which was sensitive to wavelengths from $4,000\text{--}450\text{ cm}^{-1}$ ($2\text{--}22\text{ }\mu\text{m}$). Typically, 32 scans were co-added (averaged) for both the sample and reference measurements with a resolution of 2 cm^{-1} . A reference measurement was made before each sample measurement. Data were initially stored on the system hard disk and then on magnetic tape.

2.1.4 QCM Configuration

For measuring the mass deposition, a QCM was used. The QCM had a mass sensitivity of $4.3 \times 10^{-9}\text{ gm/Hz}$. The unit was made up of two crystals, the reference surface and the sensing surface. The surfaces had crystal cuts of 39° , $40'$ to minimize temperature effects at near LN_2 temperature. One of the crystals served as the sensing surface, whereas the other was not exposed to mass flux and was the reference. Any material that adhered to the sensing crystal altered the oscillator operating frequency. This change in frequency was proportional to the mass of material condensed on the crystal surface.

The QCM electronic controller was set up so four outputs from the QCM were possible (mass, temperature, frequency, and mass rate). Knowing the rate and temperature at which mass accumulated (or evaporated) aided in interpreting the QCM data and identifying the species condensed or evaporated. The mass deposited on the sensing crystal was determined by recording the change in mass directly or by monitoring the frequency of the sensing crystal. The relation between the frequency change (Δf) and the deposited mass (Δm) can be expressed as (Ref. 5)

$$\Delta m = 1.4 \times 10^{-9} \Delta f \text{ gm/Hz} \quad (2)$$

or

$$\Delta m/S = 4.43 \times 10^{-9} \Delta f \text{ gm/cm}^2 * \text{Hz} \quad (3)$$

where S = surface area of the sensing crystal electrode, 0.316 cm^2 . If a density of 1.0 gm/cm^3 is assumed for the condensed film, then the change in film thickness (Δt) can be calculated from the frequency change (Δf) using the equation

$$\Delta t = 4.43 \times 10^{-9} \Delta f \quad (4)$$

where Δt is given in cm and Δf is given in Hertz.

QCM cooling to LN_2 temperature was accomplished by conduction as it was mounted directly to the LN_2 -cooled housing holding the germanium window. Even so, the cooling

rate was less than that of the germanium window. Temperature equilibrium was established for both the QCM and germanium window before the deposition of contaminants was begun.

3.0 EXPERIMENTAL TEST PROCEDURE

3.1 FILM THICKNESS MEASUREMENT

The thin-film thickness measurement technique has been described previously (Refs. 6-7) and will only be reviewed here. To make accurate n, k measurements, the transmittance must be measured for carefully determined film thicknesses. The thin-film interference technique provides a method for calculating the discrete film thicknesses. As a thin film forms on a reflecting (or transmitting) substrate, a reflected or transmitted beam of radiation will exhibit a sinusoidally varying signal. Using the thin-film interference equations, the maxima and minima locations can be used to accurately calculate the thin-film thickness from

$$t = m \lambda / 2n(1 - \{\sin^2/n^2\})^{0.5} \quad (5)$$

where

- t = film thickness, microns
- λ = wavelength, microns
- n = real part of refractive index at wavelength λ
- θ = incidence angle, deg
- m = order of interference

However, to make these calculations, the film refractive index n must be known for the incident wavelength. The He-Ne laser wavelength of $0.6328 \mu\text{m}$ was used. Since germanium does not transmit this wavelength, the technique was used in the reflective mode. Two He-Ne laser beams were incident at two angles (24.0 and 67.5 deg), and interference fringes were observed as the contaminant film was deposited. The refractive index at $0.6328 \mu\text{m}$ was determined from the interference patterns observed on a strip chart recorder trace for the two solar cell detector outputs. This was done by fringe (interference maxima or minima) counting for each of the incidence angles and using the equation from Ref. 8:

$$n = [\{\sin^2 \theta_1 - (m_1/m_2)^2 * \sin^2 \theta_2\} / (1 - (m_1/m_2)^2)]^{0.5} \quad (6)$$

where θ_1 and θ_2 were the two incidence angles and m_1 and m_2 were the numbers of interference peaks counted for the angles θ_1 and θ_2 , respectively.

Knowing the refractive index at $0.6328 \mu\text{m}$, the film thicknesses at the interference maxima and minima peaks were easily calculated using Eq. (5). Either incidence angle could be used,

but the smaller angle provided smaller thickness increments. For a sample thickness calculation, let $n = 1.4$, $\theta_1 = 24$ deg, $\lambda = 0.6328 \mu\text{m}$, and $m = 1$ (for the first interference maxima). From Eq. (5), then, $t = 0.2474 \mu\text{m}$. Similarly, calculations for the first minima ($m = 1/2$) yield a film thickness of $0.1237 \mu\text{m}$.

3.2 MATERIAL DOCUMENTATION AND PREPARATION

Sample material time of preparation, cure time, mixture ratio, batch number, and preconditioning time were all carefully documented. The adhesives and potting compounds were contained in an aluminum foil boat which was 3 in. \times 1.5 in. \times 1.5 in. (7.62 cm \times 3.81 cm \times 3.81 cm). The empty aluminum foil boat was outgassed for 24 hr prior to filling with material. Composites were placed in the effusion cell in the "as received" condition. All materials were preconditioned by placing them in a 50-percent (± 5 percent) relative humidity (R.H.) cell for 24 hr prior to installation in the chamber.

3.3 CONTAMINANT OPTICAL PROPERTIES (COP) CHAMBER TEST PROCEDURES

After the test material had been preconditioned, the boat containing the sample material was inserted into the effusion cell and installed in the COP chamber. He-Ne laser alignment checks were carried out to ensure that the laser beams reflected from the germanium window were incident on the solar cell detectors. Also, the transmittance of the germanium window was inspected to ensure that no contaminant film had remained after cleaning. The housekeeping data program (See Ref. 2) was started for monitoring the QCM frequency, mass, temperature, and mass deposition rate. The effusion cell temperatures, the solar cell outputs for the two incidence angles, and the germanium window temperatures were also monitored. The chamber was evacuated using a mechanical pump and a turbomolecular pump. Once the chamber pressure was reduced to the 10^{-5} torr level, the chamber liner was cooled to LN_2 temperature. After the liner reached LN_2 temperature, the LN_2 flow to the germanium window and QCM was started. The germanium window cooled down much quicker than the QCM because of the better thermal conductivity. When the chamber pressure reached the mid- to high- 10^{-7} torr range, heating of the effusion cell was started. The effusion cell was thermostatically controlled to 125°C , and the outgassed components were condensed on the germanium window and the QCM. The centers of the germanium window and the QCM were aligned equidistant from the effusion cell centerline so that the two surfaces would experience the same flux rate. The solar cell outputs were documented versus time using a strip chart recorder. As the outgassed products condensed on the germanium window, the thin-film interference caused the solar cell outputs to exhibit sinusoidally varying values. Deposition continued until the first interference minimum (quarter wavelength) occurred. The transmittance of the germanium window with the deposited film was then measured.

This required rotating the germanium out of the deposition position into the transmittance measurement position. In making the transmittance measurement, a set of 32 scans was taken with the germanium rotated out of the infrared interferometer beam. This was the 100-percent transmittance, or reference, beam. The germanium window was then rotated into position so the interferometer beam was incident normal to it, and another 32 scans were taken. The transmittance was determined by a ratio of the Fourier transforms of the two sets of interferograms.

Once the transmittance measurements were completed, the germanium was rotated back into deposition position, and the film buildup and transmittance measurements continued. This procedure was repeated for as many thicknesses as could be obtained before the deposition rate decreased to a minimal value. Transmittance measurements were made for as many thicknesses as possible to maximize the accuracy of the n, k calculations.

4.0 DATA REDUCTION

4.1 OPTICAL PROPERTIES OF SATELLITE MATERIALS OUTGASSING PRODUCTS

Most contaminant problems encountered in space involve contaminant thicknesses of a few micrometers or less. Therefore, thin-film interference equations are generally used to predict contaminant effects on the reflectance or transmittance of an optical element. These calculations require knowledge of the contaminant film refractive and absorptive indices, n and k . They are components of the more general expression for the complex refractive index given by $n^* = n - ik$. In order to determine the complex refractive index of the thin, solid contaminant films, an analytical model of film plus substrate transmittance has been developed at AEDC by Roux (Refs. 6, 7, 10, 11). Most of the model follows the expressions given by Heavens in Ref. 12 for thin-film transmittance and reflectance. The model assumes the germanium window is a thick film and there is no phase coherence between multiple, internally reflected rays. All interference occurs within the thin contaminant film. An expression is derived for the normal transmittance of a thin film on a nonabsorbing substrate, and its derivation is shown by Roux (Refs. 5, 9). The resulting expression for the transmittance is summarized as

$$T = T(n, k, \theta, N_g, \nu, d) \quad (7)$$

where n and k represent the film refractive and absorptive indices, θ is the incidence angle, N_g is the real part of the substrate refractive index, ν is the wavenumber, and d is the film thickness. Expressions for the partially absorbing substrate cases are also available but were not used in this study.

The optical constants of the contaminant films were determined using the experimentally measured transmittance values over the 4,000–700 cm^{-1} wavenumber range and for as many film thicknesses as possible. Generally at least 10 film thicknesses (and preferably more) were required to determine n and k . The transmittance values for all film thicknesses were input into the computer program TRNLIN which uses the analytical thin-film interference transmittance model, and a nonlinear least-squares convergence routine for determining n and k . In some instances, the program did not converge upon a unique value of n . This usually occurred in regions of strong absorption or low wavenumber or where it was only possible to form a few thicknesses of contaminant. The n value appears to be primarily defined by the period of the transmittance versus thickness curve at each wavenumber. At small thicknesses, high absorption, or low wavenumbers, the transmittance versus thickness (for each wavenumber) curve is not well defined, i.e., the period of the interference as a function of thickness is not well defined. The k value, which is primarily defined by the magnitude of the transmittance, was well defined for the entire spectral range (700 to 4,000 cm^{-1}). Therefore, for cases where the n values were not uniquely defined, the k values were used with the Subtractive Kramers-Kronig relationship to compute n .

The Subtractive Kramers-Kronig expression is given by

$$n(\nu) = n(\nu_m) + (2/\pi) P \int_0^{\infty} \frac{k(\nu') - k(\nu)\nu}{(\nu')^2 - (\nu)^2} - \frac{k(\nu')\nu' - k(\nu_m)\nu_m d\nu'}{(\nu')^2 - (\nu_m)^2}$$

where ν_m is a reference frequency and P is the Cauchy principal integral value. The $k(\nu')$ values used in Eq. (8) were those determined using TRNLIN. These new n values were then used in the analytical model (along with the k values) to check the agreement with the transmittance data. Generally, the Subtractive Kramers-Kronig n values yielded good agreement when the analytical model results and actual transmittance data were compared. The n values, derived using TRNLIN, were usually larger in areas of strong absorption than the Kramers-Kronig values. This may be caused by the Subtractive Kramers-Kronig integration being carried out over the wavenumber range (700–4,000 cm^{-1}) instead of from zero to + infinity as specified in the integration limits of Eq. (8).

4.2 TRANSMITTANCE CALCULATIONS USING CALCRT

To realize the maximum utility of the data (n 's and k 's) generated from the experimental and analytical studies, it was necessary to develop another computer program, CALCRT (calculations of reflectance and transmittance). This program was written for AEDC by Dr. Kent Palmer of Westminster College in Fulton, Missouri. CALCRT, written in FORTRAN, calculates the reflectances and transmittances of a radiation beam that strikes a film and substrate system which has planar interfaces. The interfaces are, ideally, infinite in extent.

The film and substrate are sandwiched between semi-infinite vacuums, so that the refractive indices on each side of the film-substrate are identically equal to one.

The user must supply the substrate optical constants and thicknesses, the contaminant optical constants and thicknesses, and the radiation beam incidence angle. Transmittance or reflectance can be calculated as functions of contaminant film thickness or wavenumber.

5.0 RESULTS AND DISCUSSION

5.1 TORRSEAL SEALANT

Torrseal samples were prepared by mixing equal lengths of resin and hardener as suggested by the manufacturer. The mixture was applied to 10 aluminum foil strips and allowed to cure for 15 days. The total material mass was 34.83 gm prior to the measurements. Transmittance measurements were made for 13 film thicknesses from 0.121 to 1.82 μm . The calculated refractive and absorptive indices are shown in Fig. 4. Using these n 's and k 's, transmittance values versus wavenumber were calculated and are shown in Figs. 5-7 for the film thicknesses 0.12, 0.61, and 1.82 μm , respectively. Transmittance as a function of film thickness is shown in Figs. 8-10 for the wavenumbers 800, 2,000, and 3,250 cm^{-1} , respectively. Measured transmittances are plotted with the calculated values for comparison.

For the thinnest contaminant film (Fig. 5) only H_2O (3,250 cm^{-1}) and CO_2 (2,340 cm^{-1}) can be identified. For the thickest film (Fig. 7) weak hydrocarbon bands at 2,800-3,000 cm^{-1} and 1,000-1,600 cm^{-1} are seen. The band at 1,018 cm^{-1} is probably caused by a silicone. The broad bands centered at 832 and 1,674 cm^{-1} are also caused by H_2O .

5.2 POLYCLAD LAMINATE

Polyclad FR-4 epoxy laminate was cut into pieces that fit the aluminum foil boat used in the effusion cell. Total material mass before testing was 108.465 gm. Transmittance measurements were made for 11 film thicknesses from 0.132 to 2.9 μm . The calculated refractive and absorptive indices are shown in Fig. 11. Using the n 's and k 's, transmittance values versus wavenumber were calculated and are shown in Figs. 12-14 for the film thicknesses 0.132, 0.922, and 2.9 μm , respectively. Transmittance as a function of film thickness is shown in Figs. 15-17 for the wavenumbers 800, 2,000, and 3,250 cm^{-1} , respectively. Measured transmittances are plotted with the calculated values for comparison.

For the thinnest contaminant film (Fig. 12) only H_2O (3,250 cm^{-1}) and CO_2 (2,340 cm^{-1}) can be identified. For the thickest film (Fig. 14) the broad bands centered at 832 and 1,674 cm^{-1} are also caused by H_2O .

5.3 NVF LAMINATE

NVF epoxy/glass laminate was cut into pieces that fit the aluminum foil boat used in the effusion cell. Total material mass before testing was 98.94 gm. Transmittance measurements were made for 16 film thicknesses from 0.132 to 4.21 μm . The calculated refractive and absorptive indices are shown in Fig. 18. Using the n 's and k 's, transmittance values versus wavenumber were calculated and are shown in Figs. 19–21 for the film thicknesses 0.132, 1.05, and 4.21 μm , respectively. Transmittance as a function of film thickness is shown in Figs. 15–17 for the wavenumbers 800, 2,000, and 3,250 cm^{-1} , respectively. Measured transmittances are plotted with the calculated values for comparison.

For the thinnest contaminant film (Fig. 19) only H_2O (3,250 cm^{-1}) and CO_2 (2,340 cm^{-1}) can be identified. For the thickest film (Fig. 21) the broad bands centered at 832 and 1,674 cm^{-1} are also caused by H_2O .

5.4 URALANE

Uralane 5753-A/B (LV) urethane casting compound was mixed by adding 20 parts by weight of 5753-A to 100 parts by weight of 5753-B. The mixture was cured for 8 hr at 95°C plus 24 hr at 25°C. Total material mass was 28.427 gm prior to the measurements. Transmittance measurements were made for 8 film thicknesses from 0.11 to 0.91 μm . The calculated refractive and absorptive indices are shown in Fig. 25. Using the n 's and k 's, transmittance values versus wavenumber were calculated and are shown in Figs. 26–28 for the film thicknesses 0.11, 0.45, and 0.91 μm , respectively. Transmittance as a function of film thickness is shown in Figs. 29–31 for the wavenumbers 1,100, 2,000, and 3,250 cm^{-1} , respectively. Measured transmittances are plotted with the calculated values for comparison.

For the thinnest contaminant film (Fig. 26) only H_2O (3,250 cm^{-1}) and CO_2 (2,340 cm^{-1}) can be identified. For the thickest film (Fig. 28) weak hydrocarbon bands at 2,800–3,000 cm^{-1} and 1,000–1,600 cm^{-1} are seen.

5.5 RTV-566

RTV-566 silicon sealant was prepared by mixing an amount of RTV-566B curing agent equal to 0.1 percent by weight of RTV-566A base compound. The total material mass was 34.83 gm prior to the measurements. Transmittance measurements were made for 11 film thicknesses from 0.11 to 1.48 μm . The calculated refractive and absorptive indices are shown in Fig. 32. Using the n 's and k 's, transmittance values versus wavenumber were calculated and are shown in Figs. 33–35 for the film thicknesses 0.11, 0.68, and 1.48 μm , respectively. Transmittance as a function of film thickness is shown in Figs. 36–38 for the wavenumbers

1,100, 2,000, and 3,250 cm^{-1} , respectively. Measured transmittances are plotted with the calculated values for comparison.

For the thinnest contaminant film (Fig. 33) only H_2O (3,250 cm^{-1}) and CO_2 (2,340 cm^{-1}) can be identified. For the thickest film (Fig. 35) strong hydrocarbon bands at 2,800–3,000 cm^{-1} and 1,000–1,600 cm^{-1} are seen. The band at 1,018 cm^{-1} is probably caused by a silicone. The broad bands centered at 832 and 1,674 cm^{-1} are also caused by H_2O .

5.6 MIXTURES

Contaminant films on optical surfaces of spacecraft are rarely condensed from a single source. To predict the effects of a mixture of contaminants on the transmittance or reflectance of an optical surface, the optical properties of the individual sources must be combined in a way to generate n and k values for the contaminant mixture. An attempt to calculate values for a two component mixture was made.

Transmittance measurements were made for contaminant films from three mixtures of Uralane and RTV-566. Refractive indices were determined for each mixture. The refractive index values for Uralane and RTV-566 were combined using a simple algorithm based on the ratio of components in each mixture. Mixture ratios of the films were determined from measurements of the mass loss of each component after the test and the density of the components. Mixture one ratio was 65-percent Uralane, 35-percent RTV; mixture two was 47-percent Uralane, 53-percent RTV; and mixture three was 28-percent Uralane, 72-percent RTV. Refractive and absorptive indices, and calculated and measured transmittance data for the three mixtures are plotted in Figs. 39–59.

Transmittance values were calculated for two film thicknesses using the combined n and k values obtained for each mixture ratio. The calculated transmittance values are compared to measured data for each mixture in Figs. 60–65. The calculated values are shifted from the measured values. Calculated values for mixture one and three are higher than the measured values. Calculated values for mixture two are lower than the measured values. The results indicate that an algorithm for combining optical property data based on the physics of thin-film interference is needed. This need will be addressed in subsequent work.

6.0 SUMMARY

Optical property measurements of condensed contaminant films on cryogenically cooled substrates have previously been reported in Refs. 2 and 3. Measurements for five additional individual materials and three material mixtures are presented in this report. Infrared spectral transmittance measurements were made for thin films of contaminant deposited on a 77 K

germanium window under vacuum conditions. Material temperatures were controlled at 125°C to provide the outgassing source. The objective of this report is to present the refractive and absorptive indices of the condensed outgassing products of satellite materials which were determined from the experimental measurements of the infrared transmittance spectra, and to describe an effort to combine optical property data from two materials to provide values that can be used to calculate the surface effects for contaminant mixtures.

The n, k values for each material and mixture were used to calculate transmittance values as a function of wavenumber and film thickness. The average difference between measured and calculated values was 1.24 percent. This result indicates that the TRNLIN inversion program provides optical property data that can be used for prediction of contamination surface effects on cryogenic optical systems.

Optical property data from two materials were combined to provide values that can be used to calculate the surface effects for contaminant mixtures. Calculated transmittance values were compared to measurements for the three mixtures. The calculated values are shifted from the measured values. The results indicate that an algorithm for combining optical property data based on the physics of thin-film interference is needed. This need will be addressed in subsequent work.

REFERENCES

1. Storer, Roberta A., Editor. ASTM E595-84, "Standard Test Method for Total Mass Loss and Collected Volatile Condensable Material from Outgassing in a Vacuum Environment." 1988 Annual Book of ASTM Standards, Section 15, Vol. 15.03, ASTM Headquarters, Philadelphia, Pennsylvania, 1988.
2. Wood, B. E., Bertrand, W. T., Bryson, R. J., and Seiber, B. L. "Surface Effects of Satellite Outgassing Products." AEDC-TR-87-8, September 1987 (Also *AIAA Journal of Thermophysics and Heat Transfer*, Vol. 2, No. 4, October 1988, pp. 289-295).
3. Wood, B. E., Bertrand, W. T., Kiech, E. L., Holt, J. D., and Falco, P. M. "Surface Effects of Satellite Material Outgassing Products." AEDC-TR-89-2, June 1989
4. Herzberger, M. and Salzberg, C. D. "Refractive Indices of Infrared Optical Materials and Color Correction of Infrared Lenses." *Journal of the Optical Society of America*, Vol. 52, No. 4, April 1962, pp. 420-426.

5. "Operation and Service Manual for Quartz Crystal Microbalance, QCM Sensor Mark 9." QCM Research, Laguna Beach, California.
6. Wood, B. E. and Roux, J. A. "Infrared Optical Properties of Thin H₂O, NH₃, and CO₂ Cryofilms." AEDC-TR-79-57, September 1979.
7. Roux, J. A., Wood, B. E., Smith, A. M., Pipes, J. G. and Scott, H. E. "IR Optical Properties of Bipropellant Cryocontaminants." *Proceedings of the USAF/NASA International Spacecraft Contamination Conference*, Ed. J. M. Jemiola, AFML-TR-78-190 and NASA-CP-2039, March 1978, pp. 412-455.
8. Wood, B. E. and Smith, A. M. "Infrared Reflectance of Condensed Gas Films," *AIAA Progress in Astronautics and Aeronautics: Thermophysics and Thermal Control*, Vol. 65, Ed. Raymond Viskanta, 1979, pp. 22-38.
9. Campbell, William A. Jr., Marriott, Richard S., and Park, John J. "Outgassing Data for Selecting Spacecraft Materials." NASA Reference Publication 1124, June 1984.
10. Alt, R. E., Roux, J. A., Wood, B. E., Frazine, D. F., Dawbarn, R., and Scott, H. E. "Bipropellant Engine Plume Contamination Program, Volume 1 Chamber Measurements—Phase I." AEDC-TR-79-28, December 1979.
11. Wood, B. E. and Roux, J. A. "Infrared Optical Properties of Thin CO, NO, CH₄, HCl, N₂O, O₂, N₂, and Ar Cryofilms." *Progress in Astronautics and Aeronautics, Spacecraft Contamination: Sources and Prevention*, Vol. 91, Eds. J. A. Roux and T.D. McCay, 1984, pp. 139-161.
12. Heavens, O. S. *Optical Properties of Thin Films*. Dover Publications, Inc., New York, 1965.

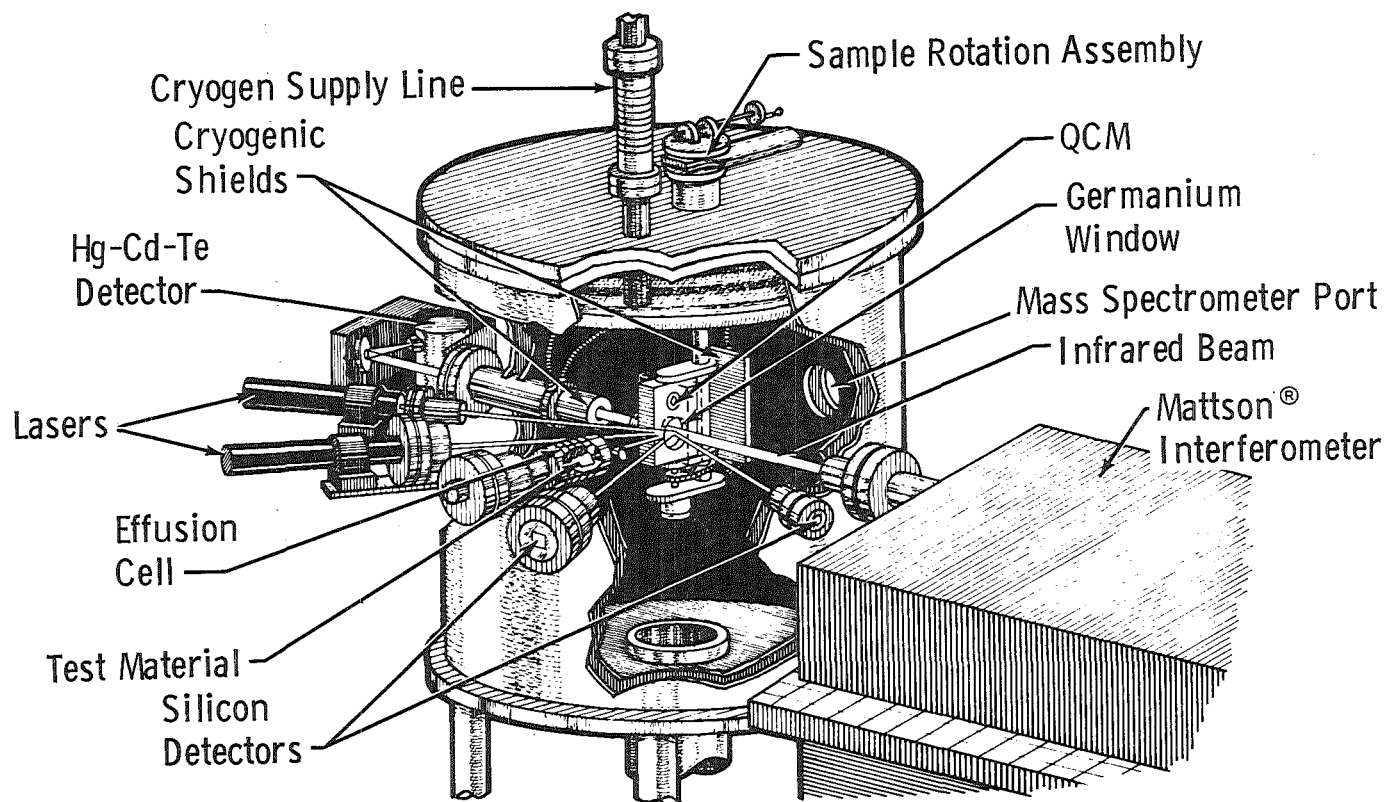


Figure 1. Schematic of the COP chamber.

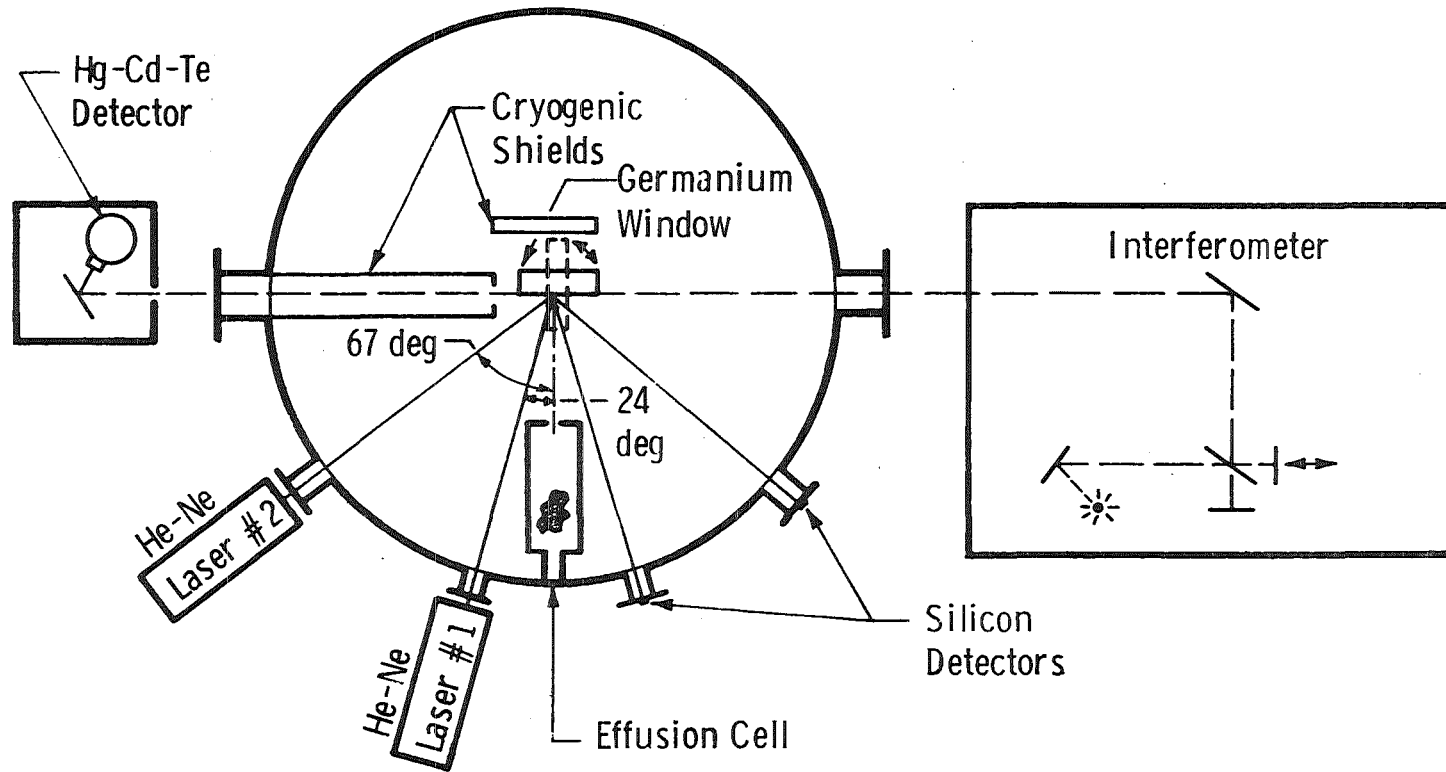


Figure 2. Schematic of COP chamber components.

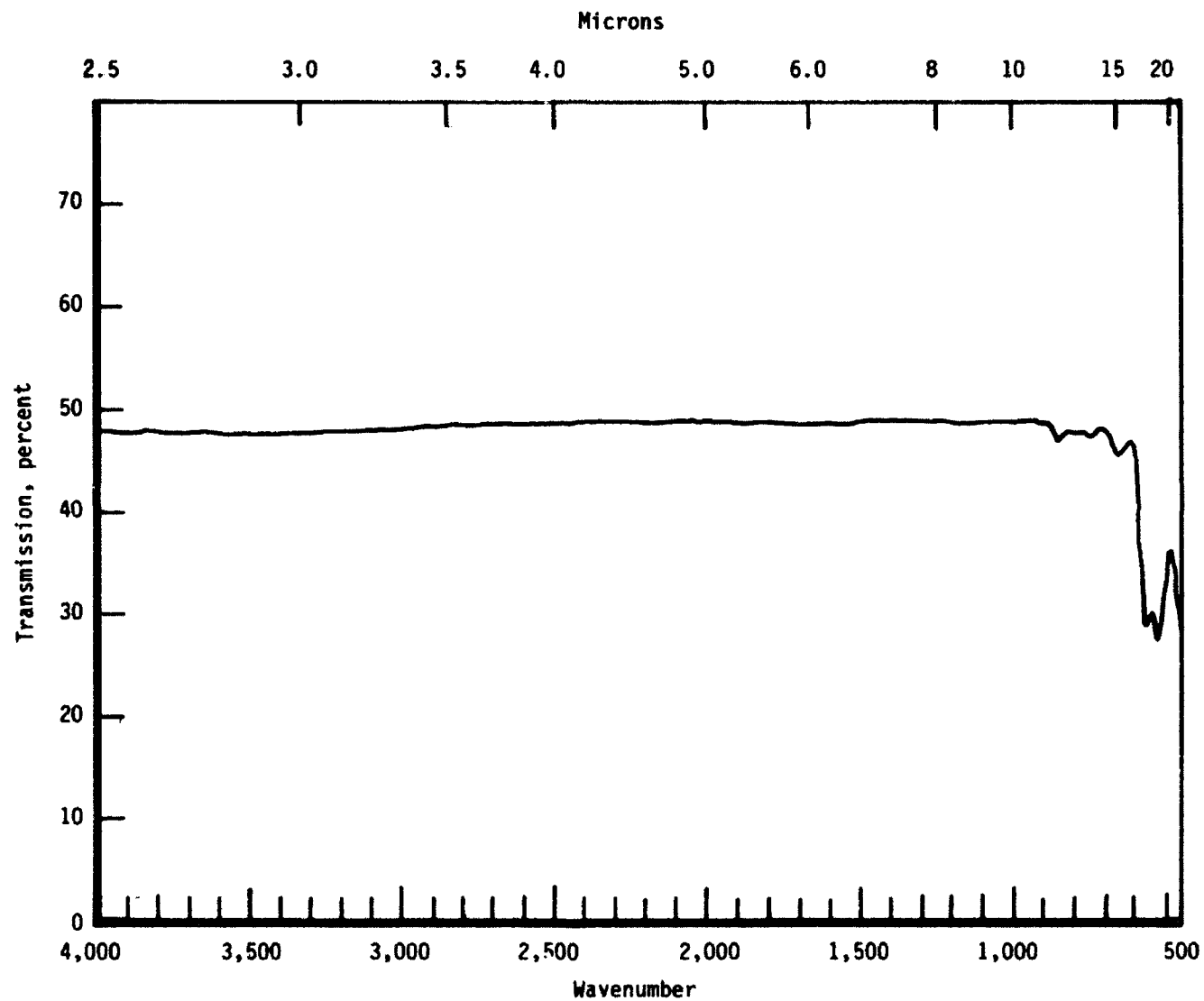
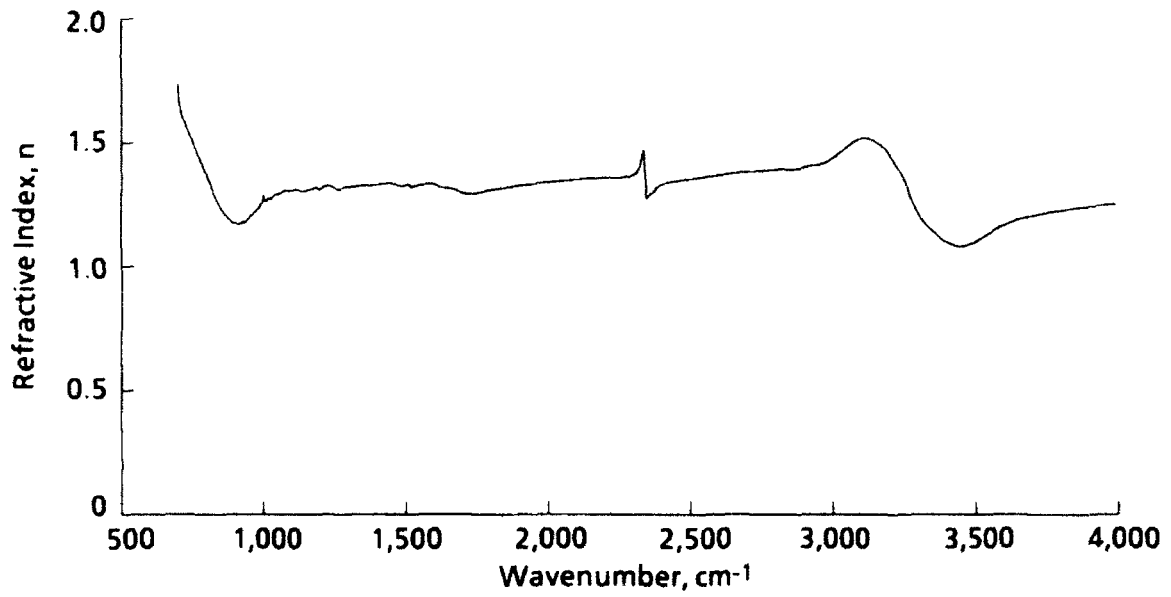
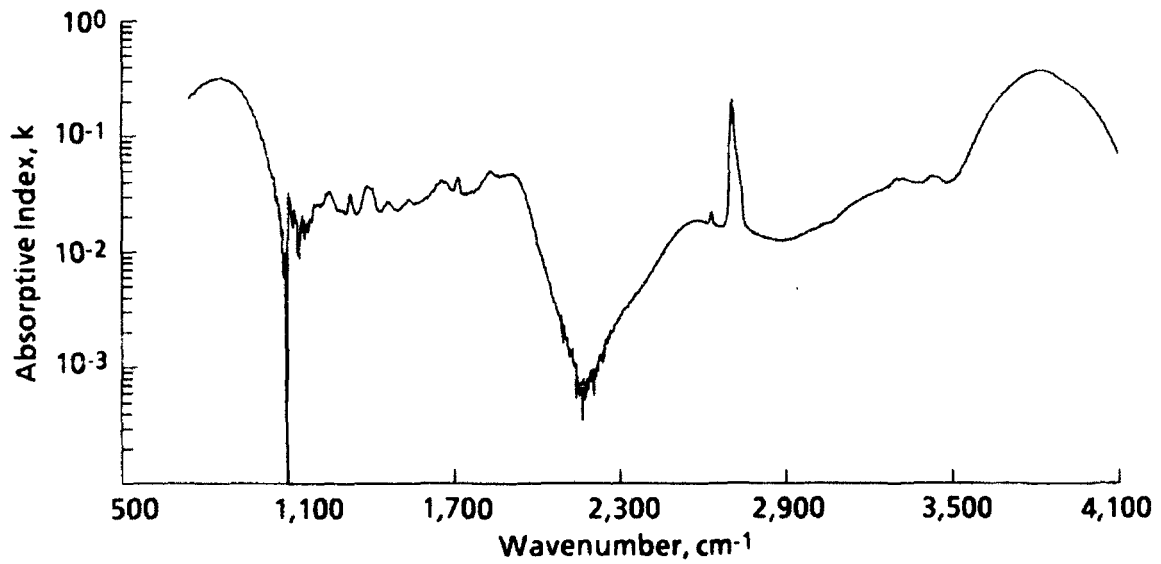


Figure 3. Transmittance of a bare germanium window at 77 K.



a. Refractive index



b. Absorptive index

Figure 4. Optical properties for Torrseal.

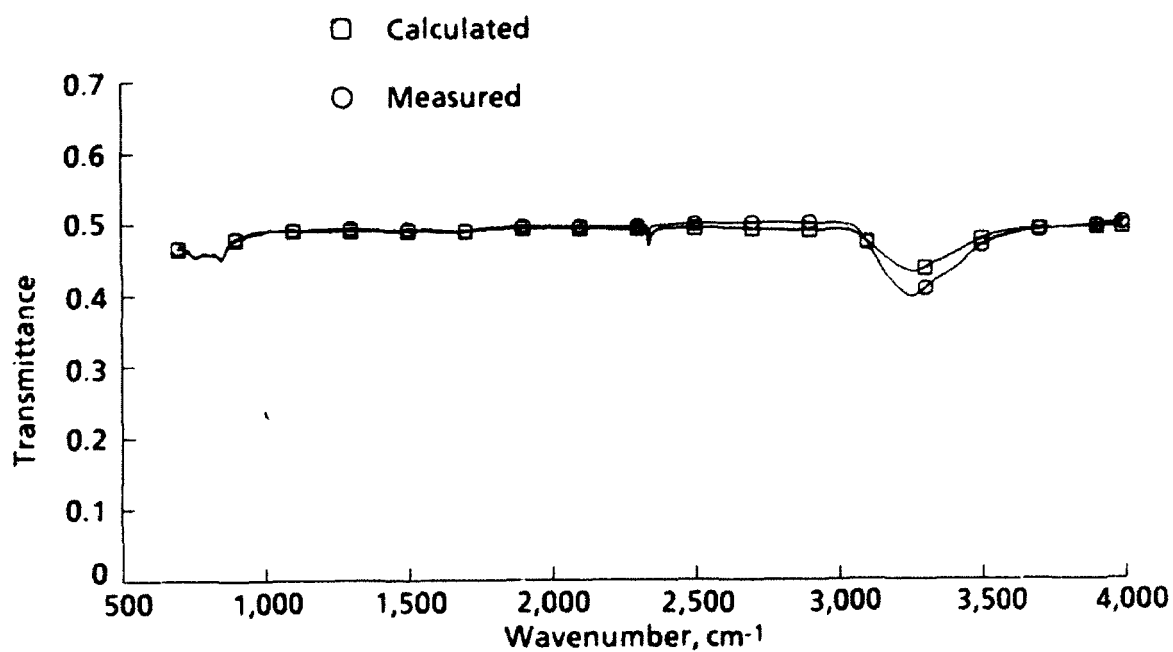


Figure 5. Transmittance for 0.12- μm -thick Torrseal.

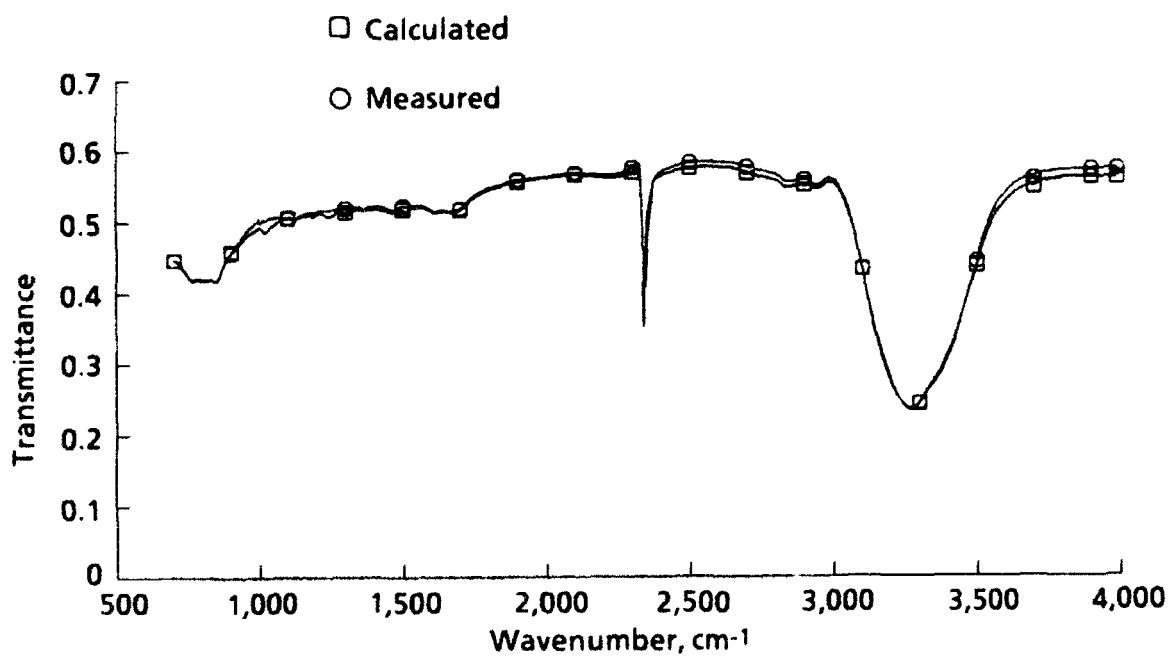


Figure 6. Transmittance for 0.61- μm -thick Torrseal.

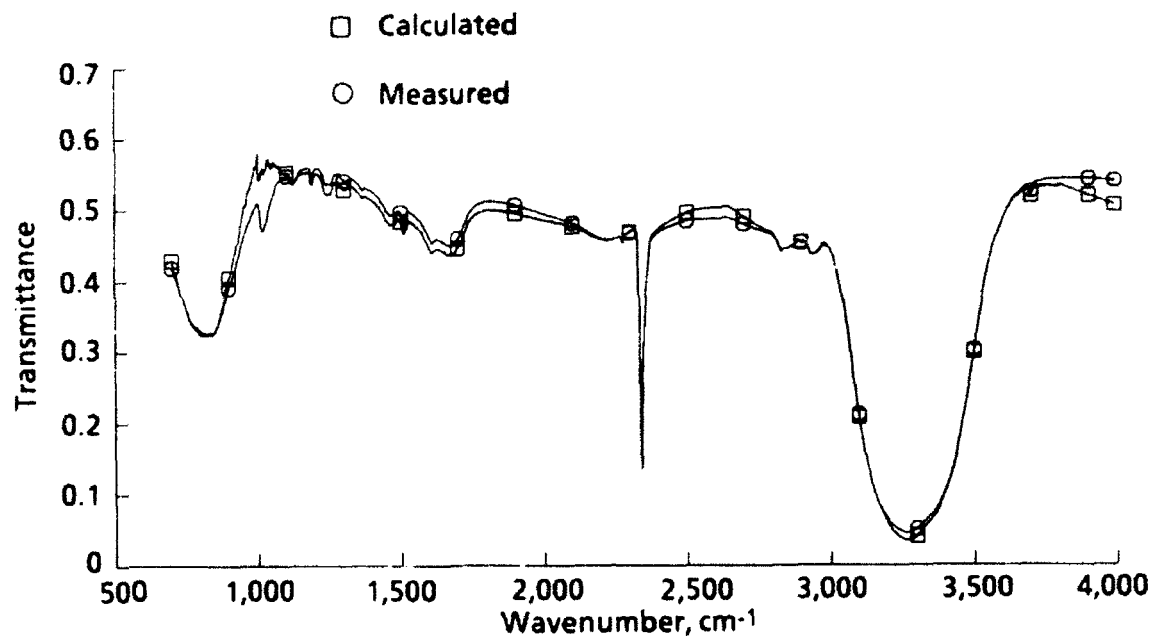


Figure 7. Transmittance for 1.82- μm -thick Torrseal.

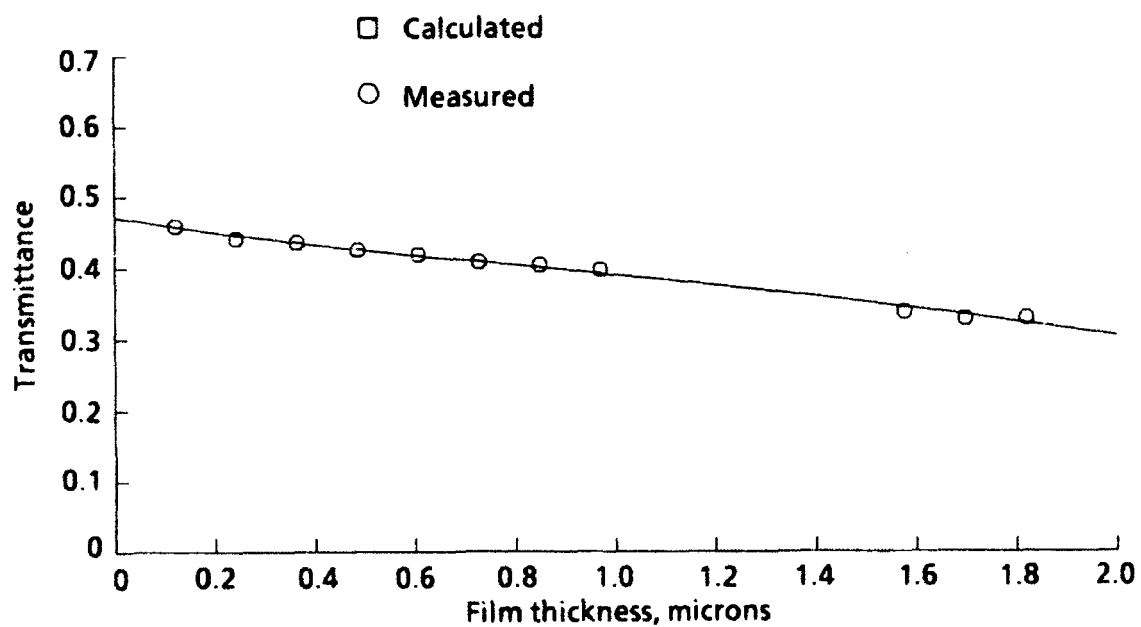


Figure 8. Transmittance at 800 cm^{-1} for Torrseal.

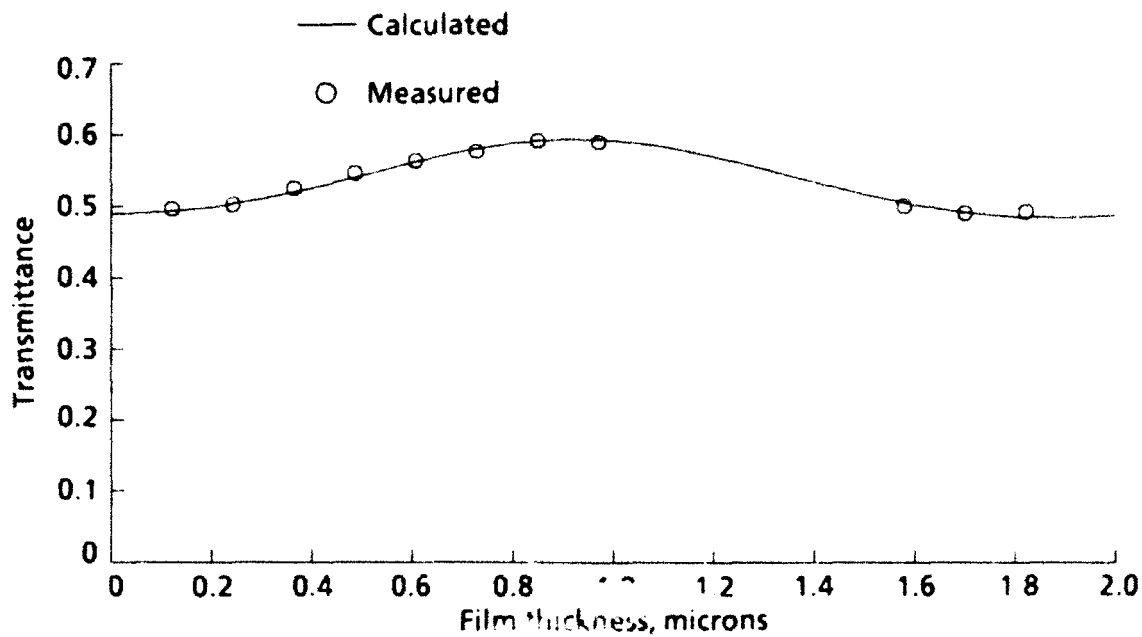


Figure 9. Transmittance at $2,000\text{ cm}^{-1}$ for Torrseal.

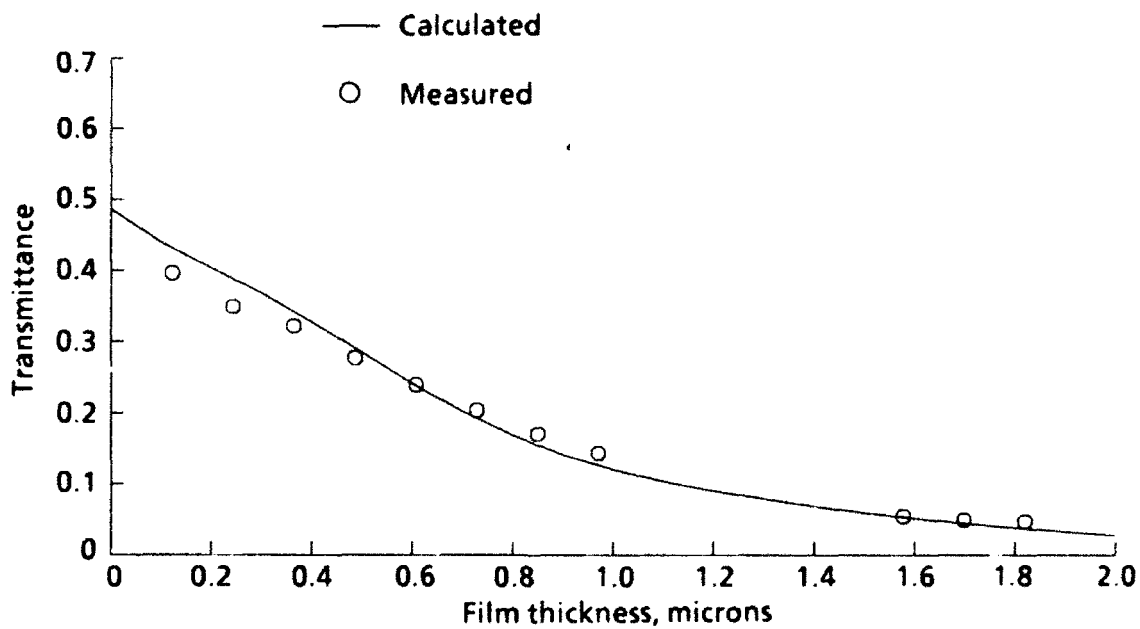


Figure 10. Transmittance at $3,250\text{ cm}^{-1}$ for Torrseal.

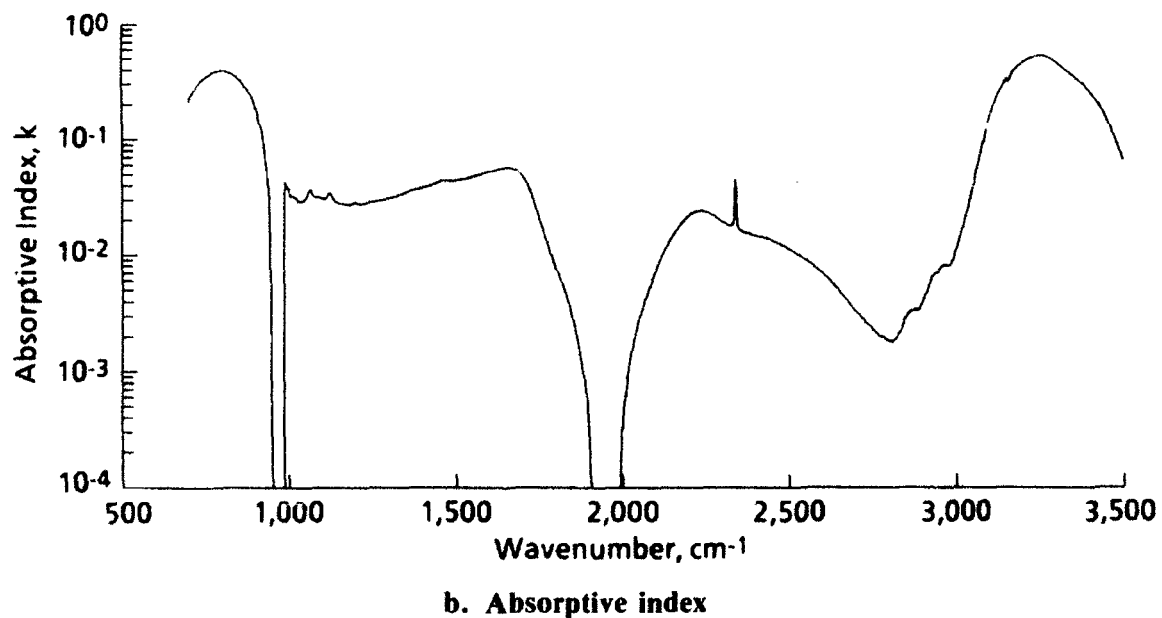
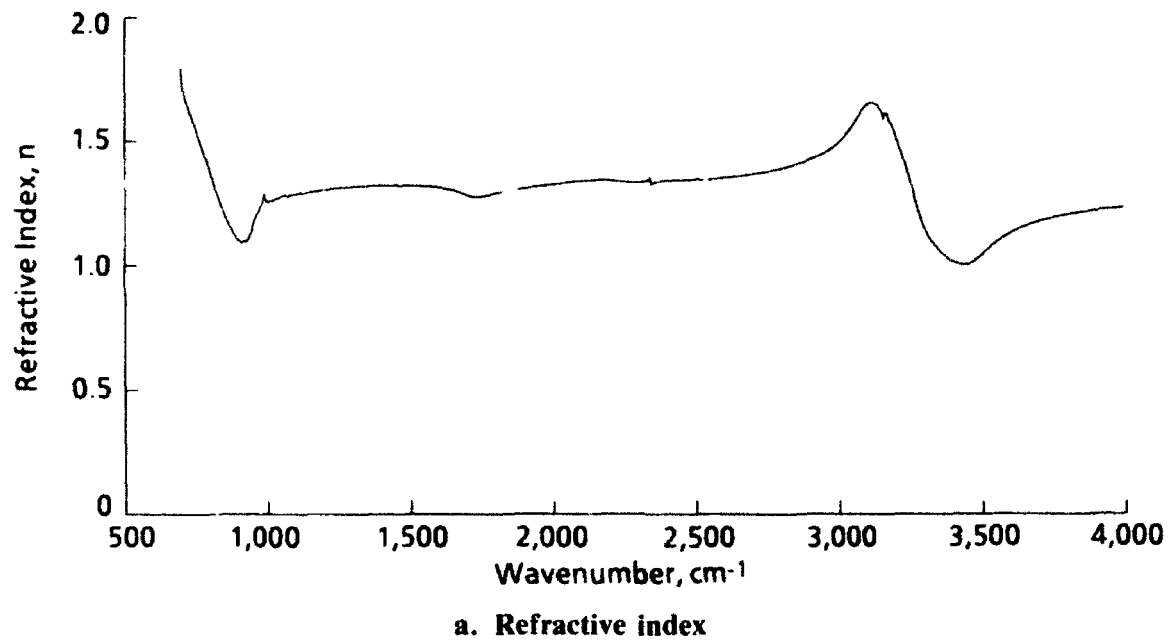


Figure 11. Optical properties for Polyclad.

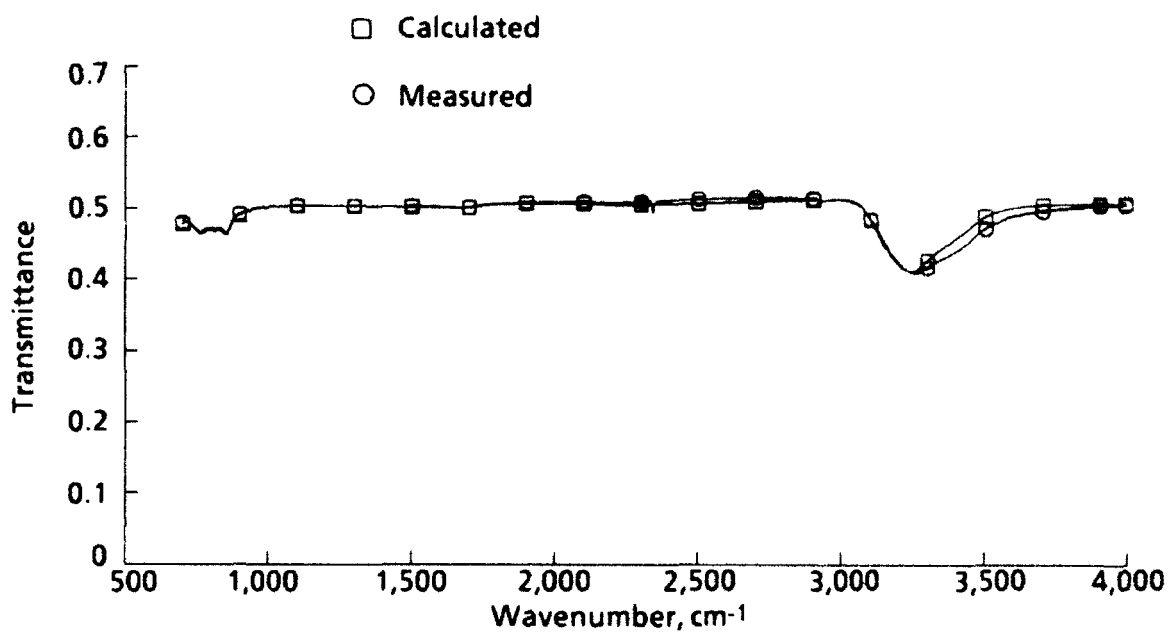


Figure 12. Transmittance for 0.13- μm -thick Polyclad.

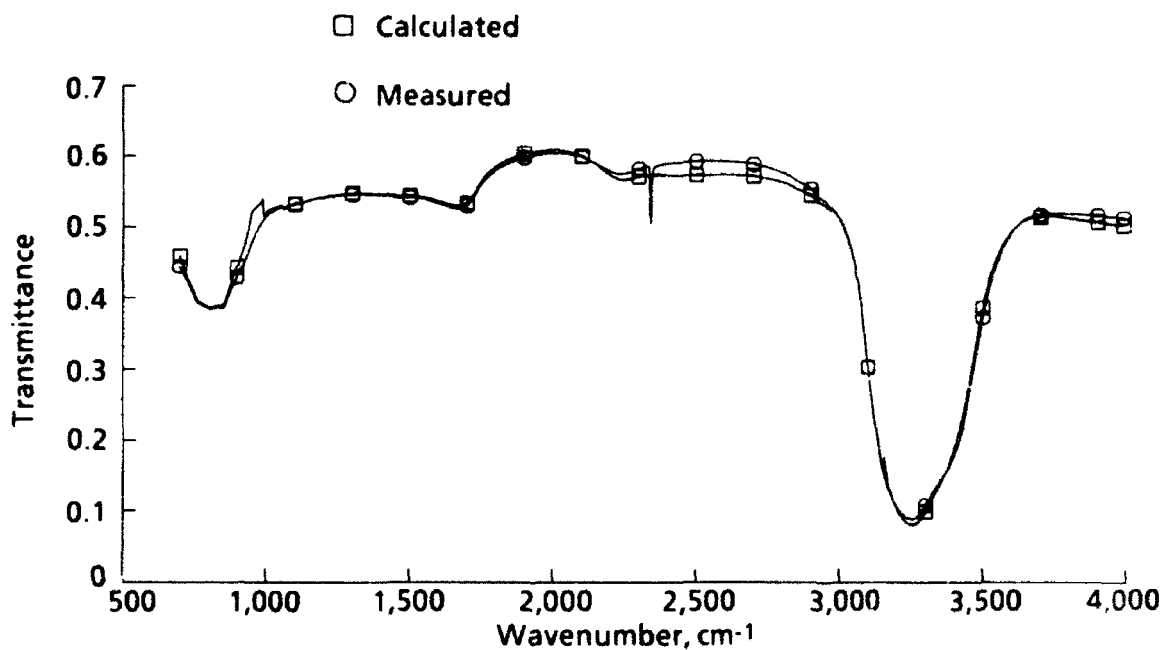


Figure 13. Transmittance for 0.92- μm -thick Polyclad.

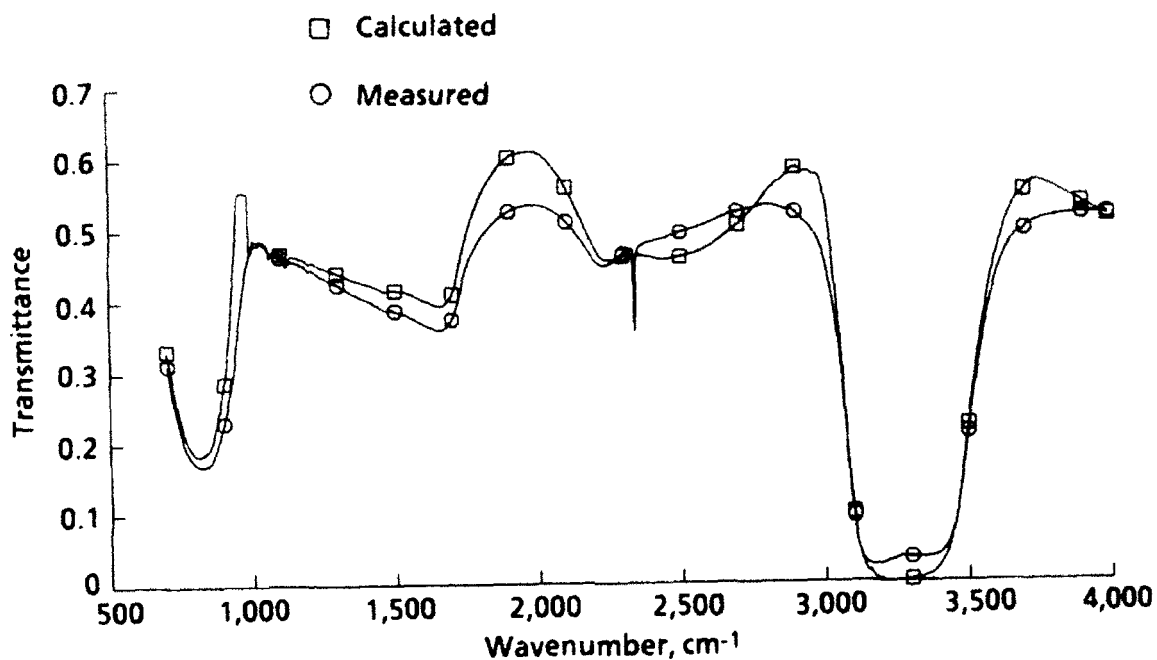


Figure 14. Transmittance for 2.90- μm Polyclad.

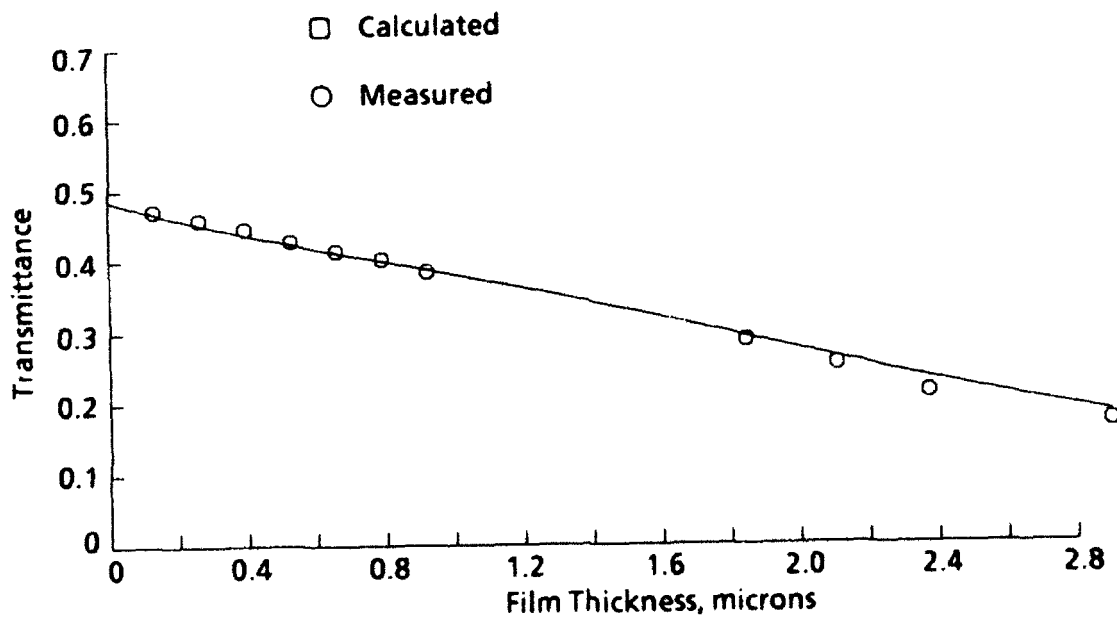


Figure 15. Transmittance at 800 cm^{-1} for Polyclad.

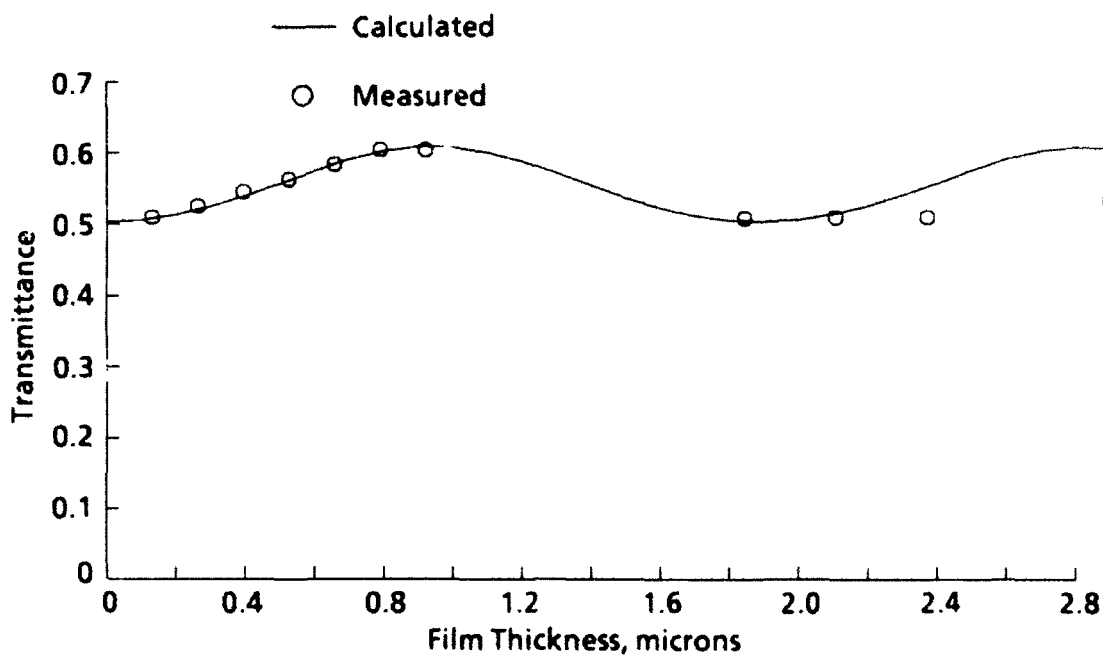


Figure 16. Transmittance at $2,000\text{ cm}^{-1}$ for Polyclad.

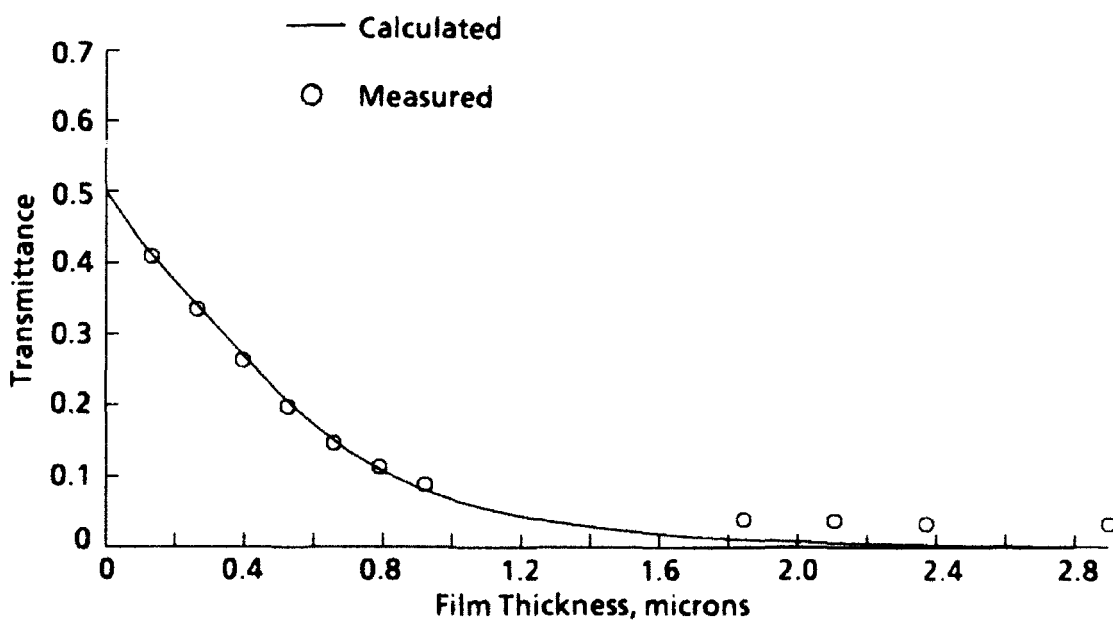
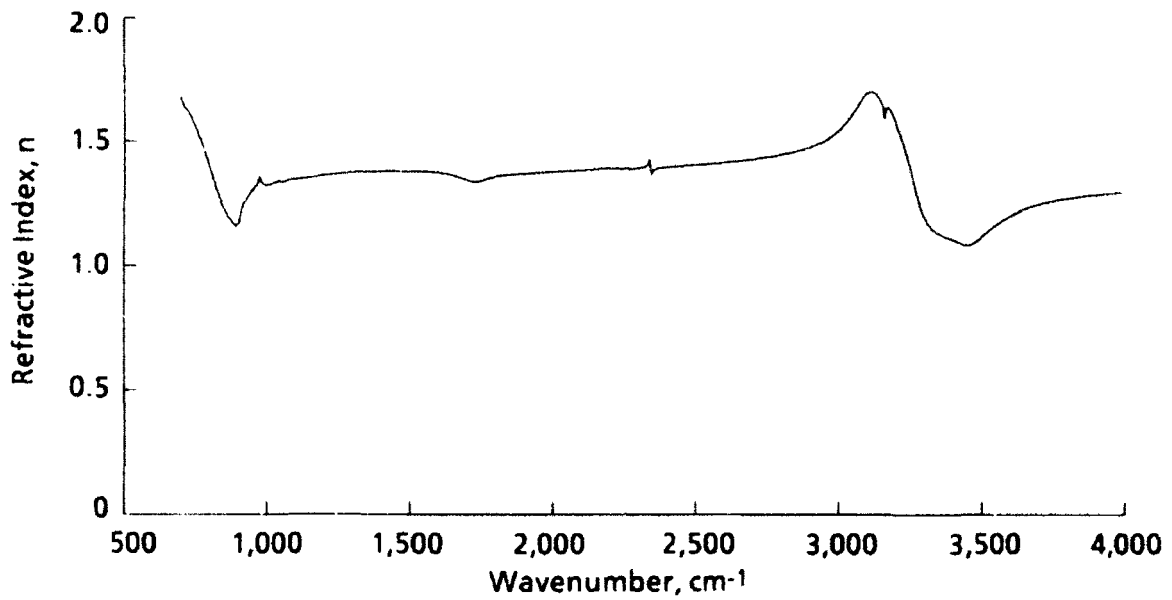
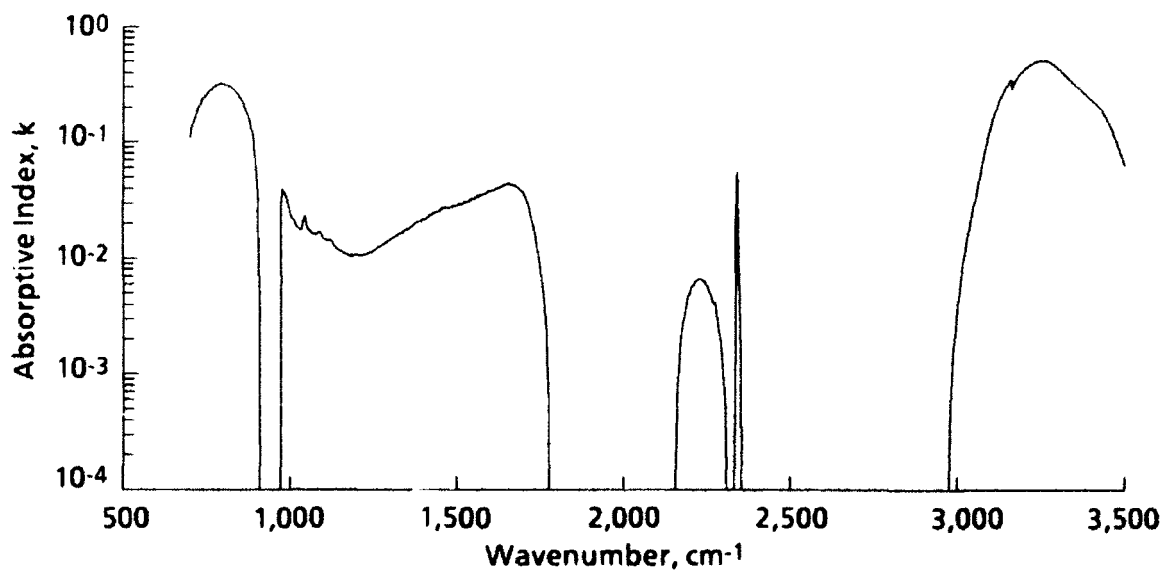


Figure 17. Transmittance at $3,250\text{ cm}^{-1}$ for Polyclad.



a. Refractive index



b. Absorptive index

Figure 18. Optical properties for NVF.

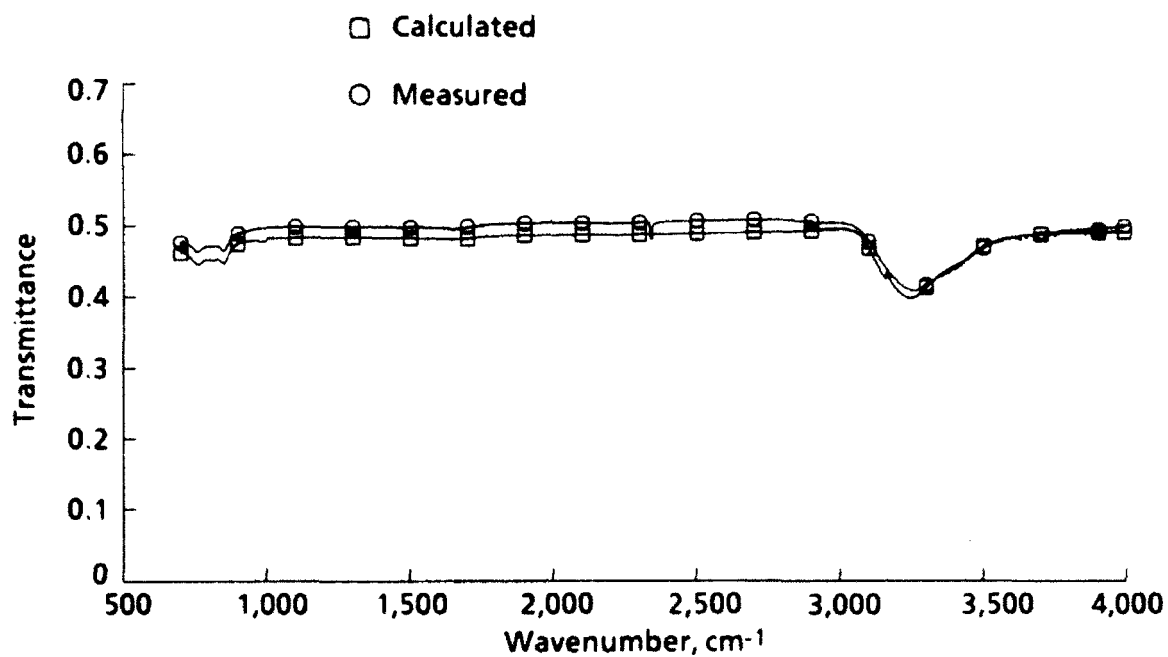


Figure 19. Transmittance for 0.13- μm -thick NVF.

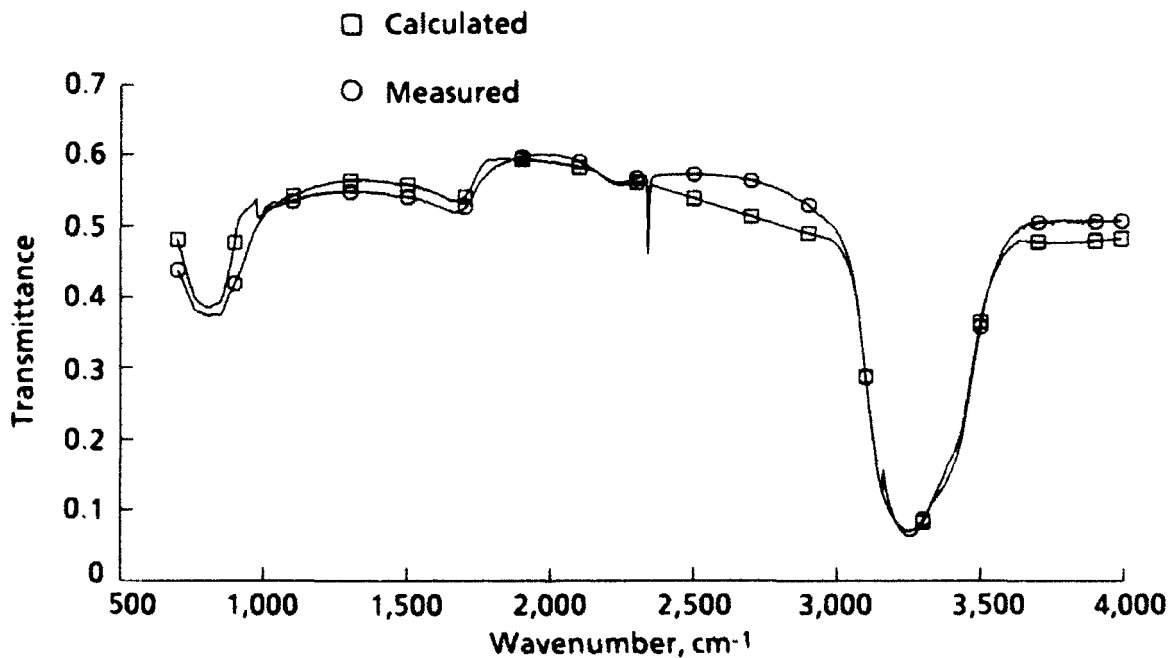


Figure 20. Transmittance for 1.05- μm -thick NVF.

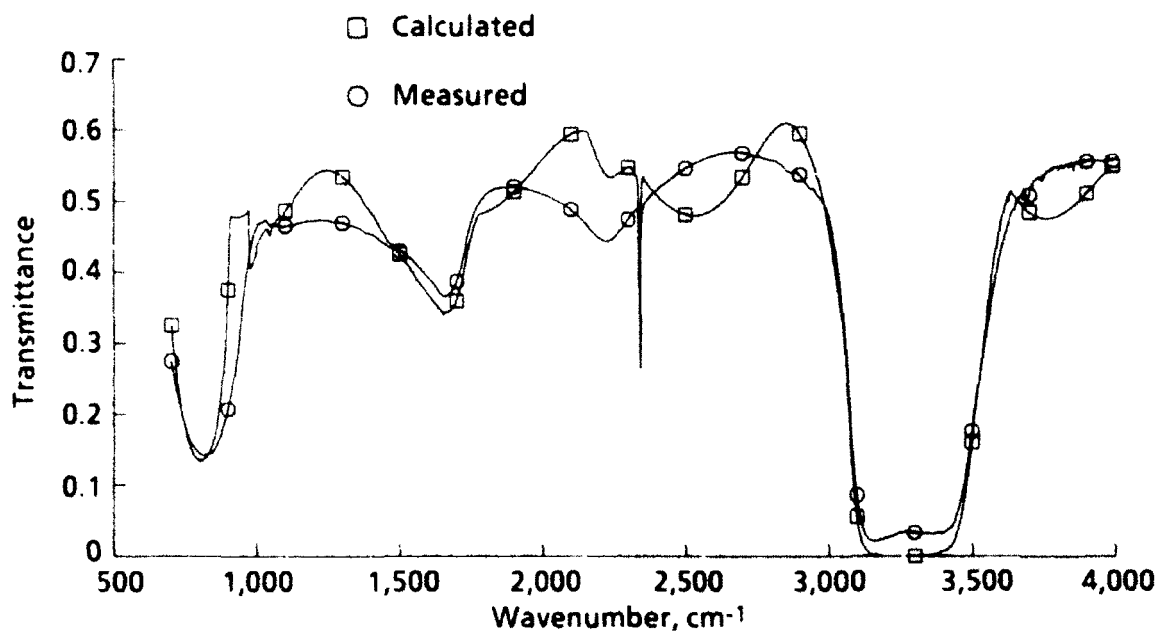


Figure 21. Transmittance for 4.21- μm -thick NVF.

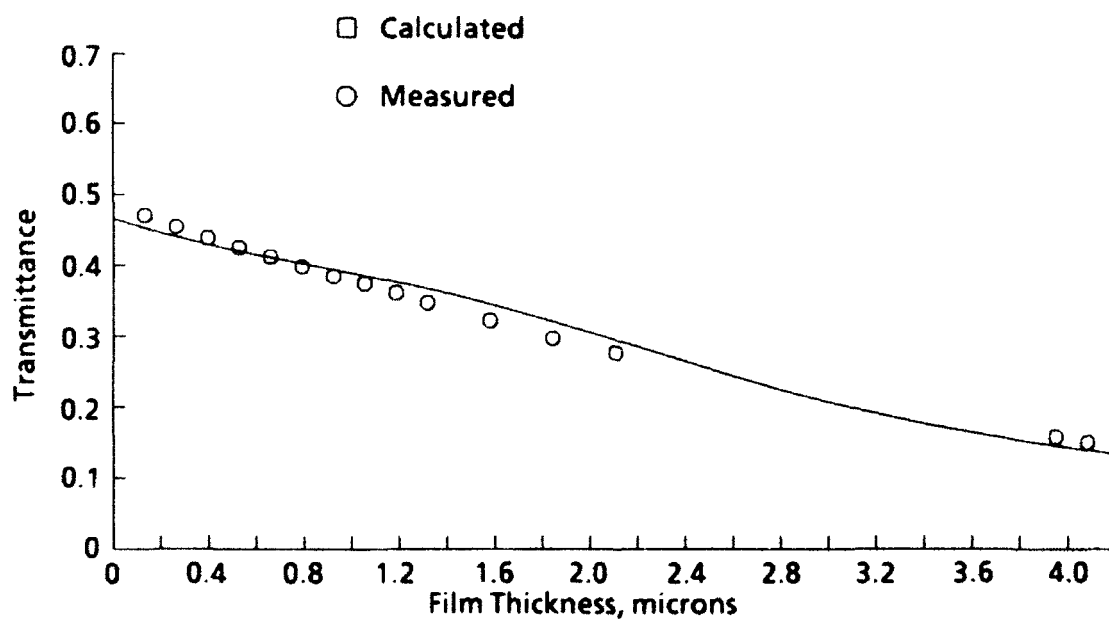


Figure 22. Transmittance at 800 cm^{-1} for NVF.

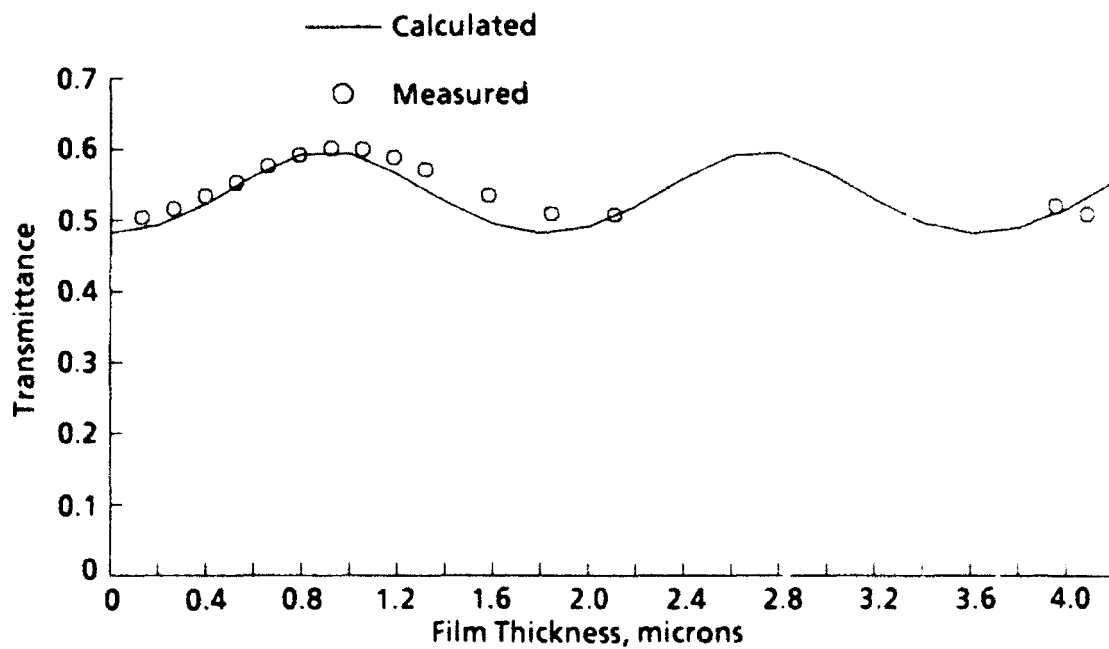


Figure 23. Transmittance at 2,000 cm⁻¹ for NVF.

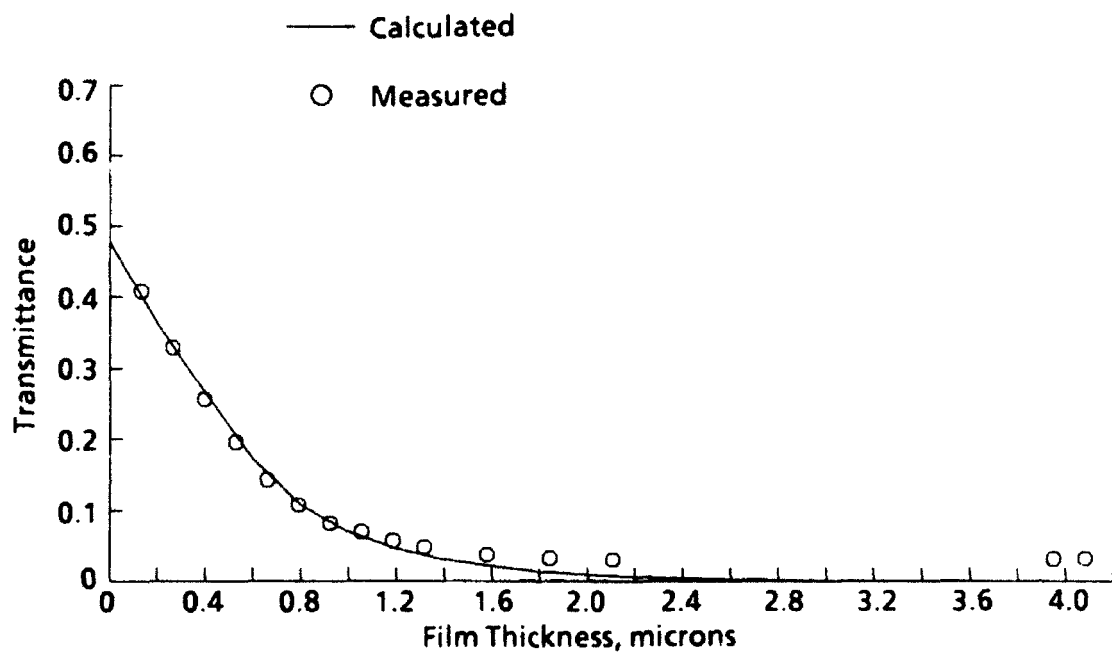
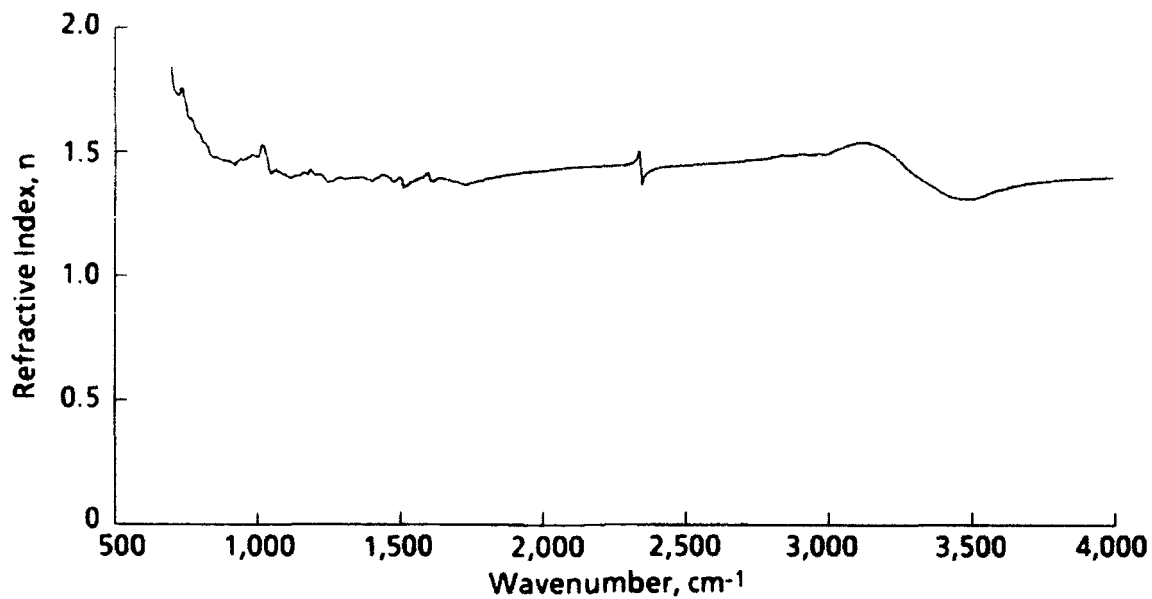
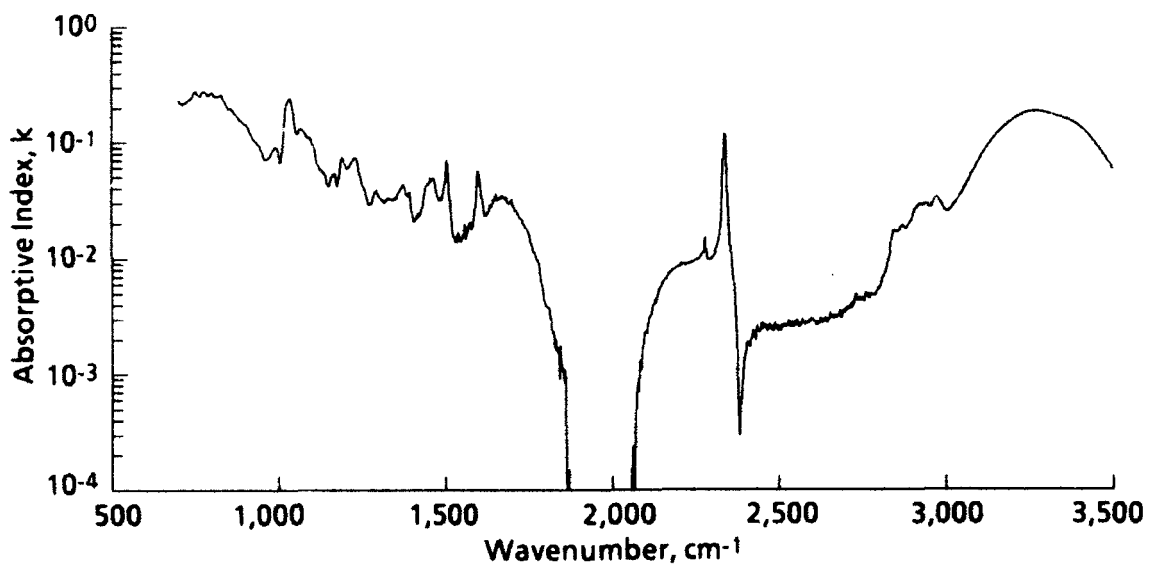


Figure 24. Transmittance at 3,250 cm⁻¹ for NVF.



a. Refractive index



b. Absorptive index

Figure 25. Optical properties for Uralane®.

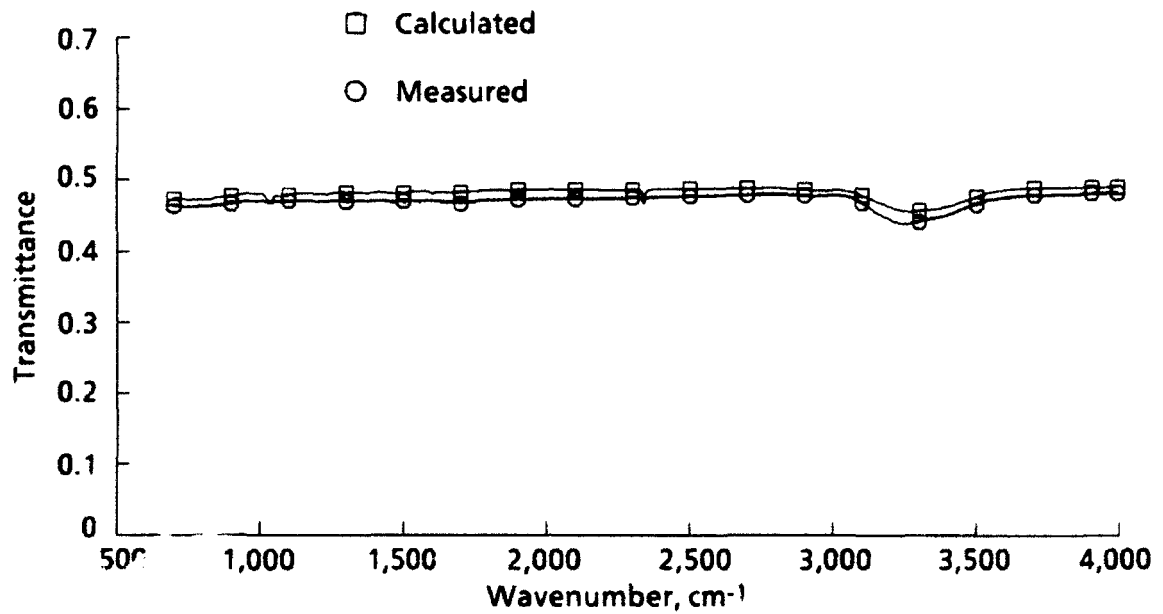


Figure 26. Transmittance for 0.11- μm -thick Uralane®.

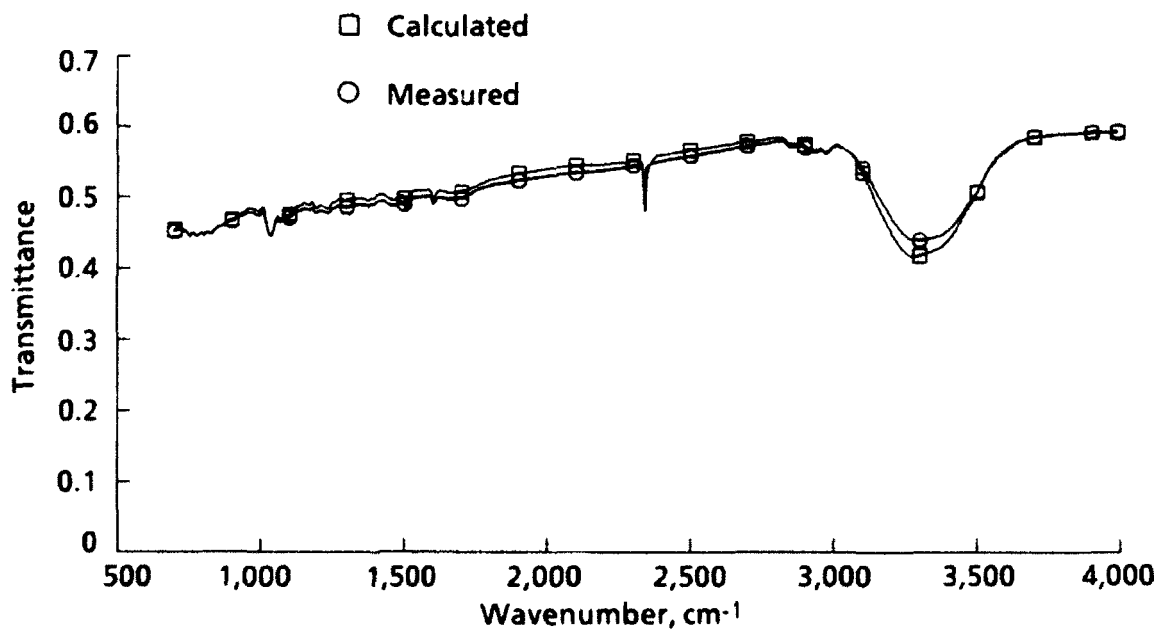


Figure 27. Transmittance for 0.45- μm -thick Uralane®.

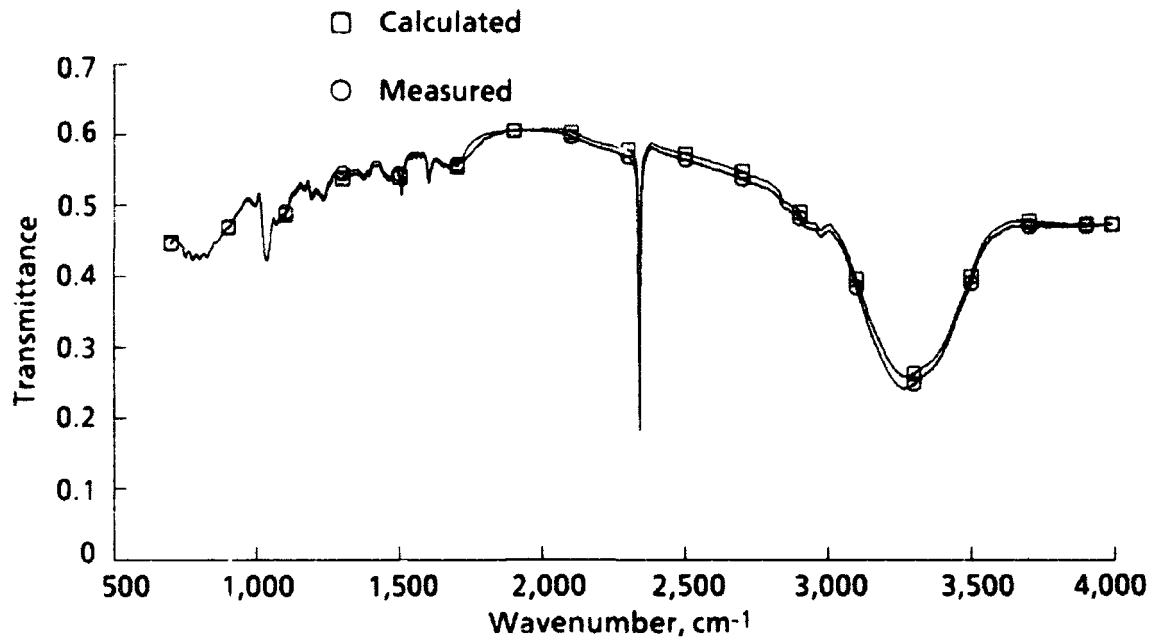


Figure 28. Transmittance for 0.91- μm -thick Uralane®.

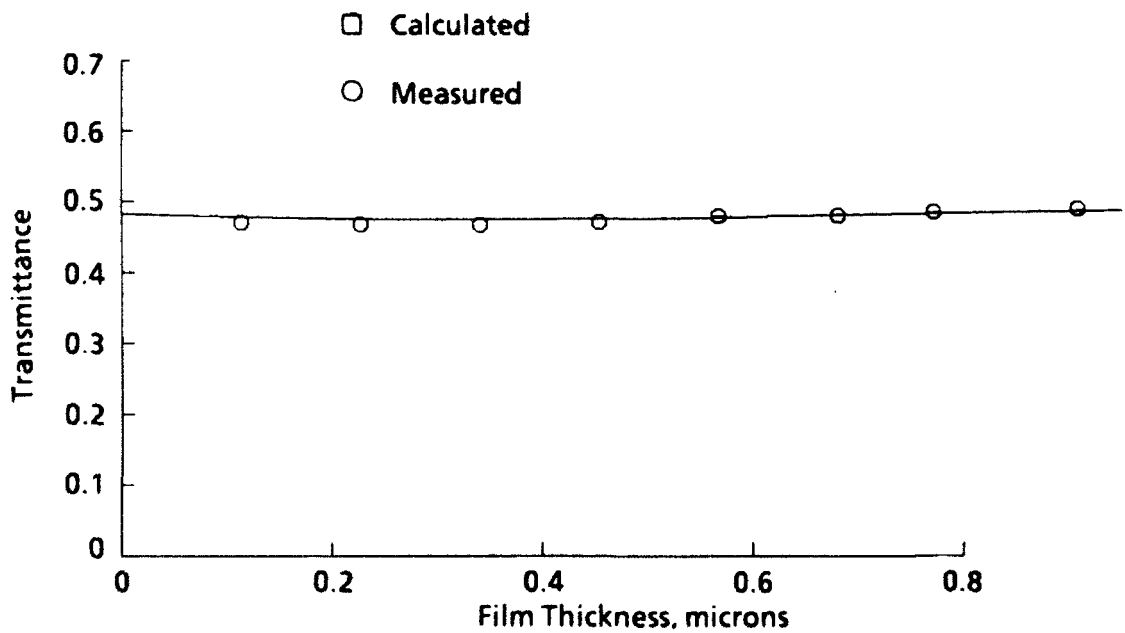


Figure 29. Transmittance at 1,110 cm^{-1} for Uralane®.

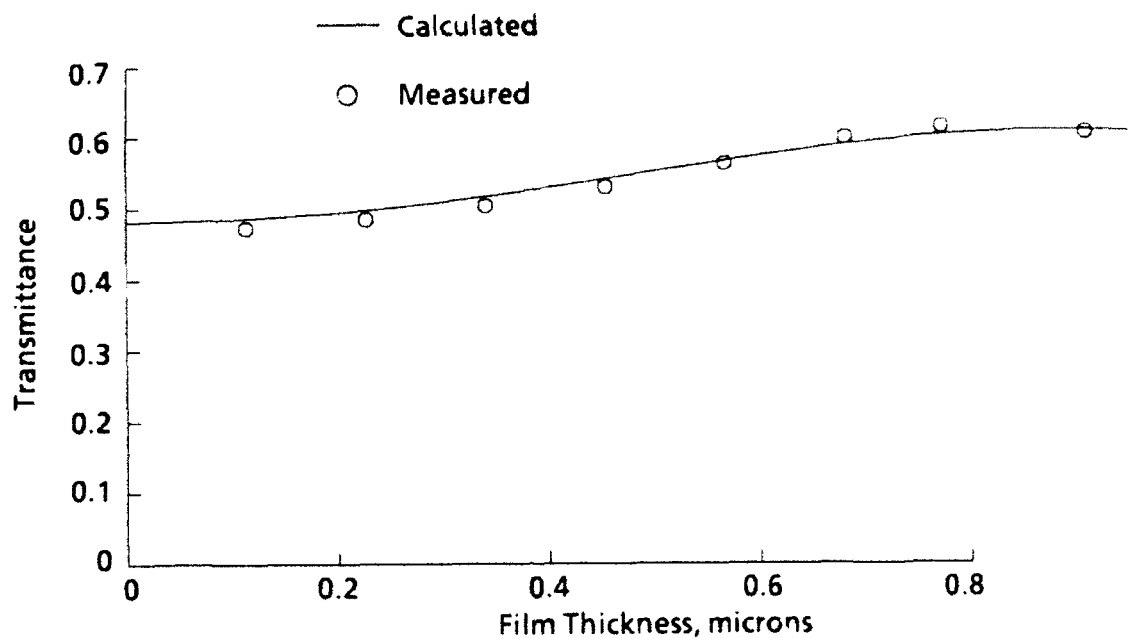


Figure 30. Transmittance at 2,000 cm⁻¹ for Uralane®.

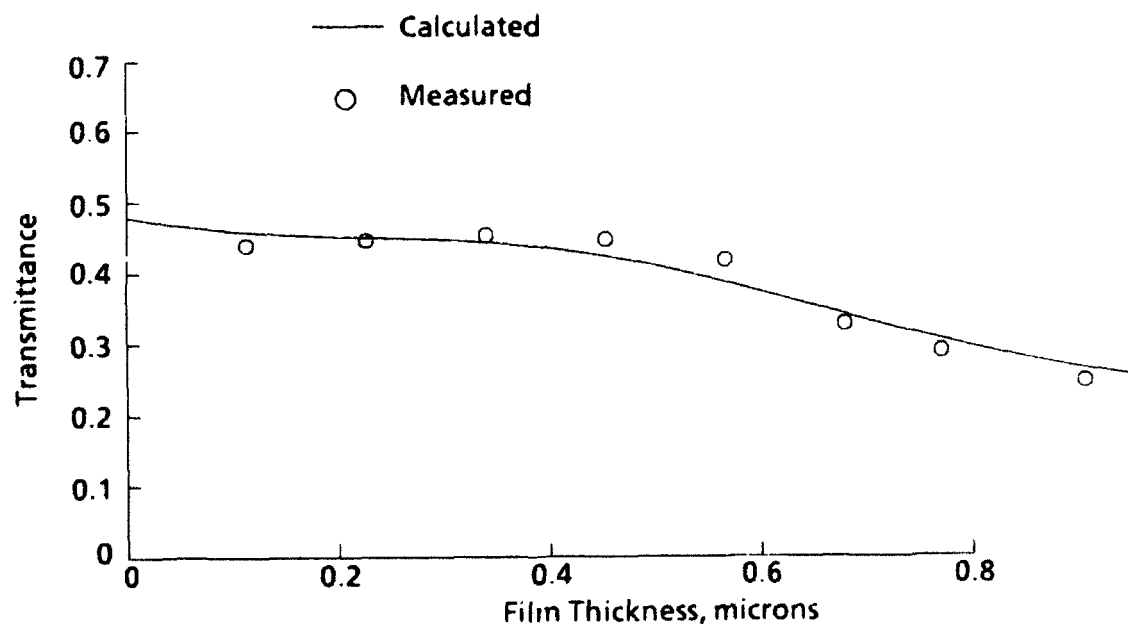
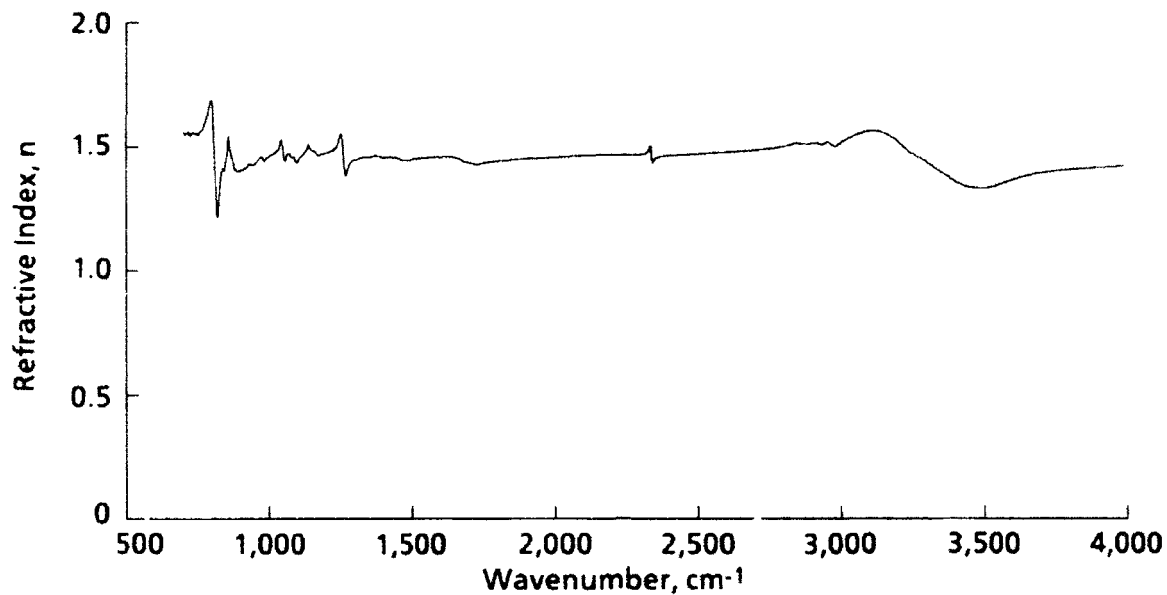
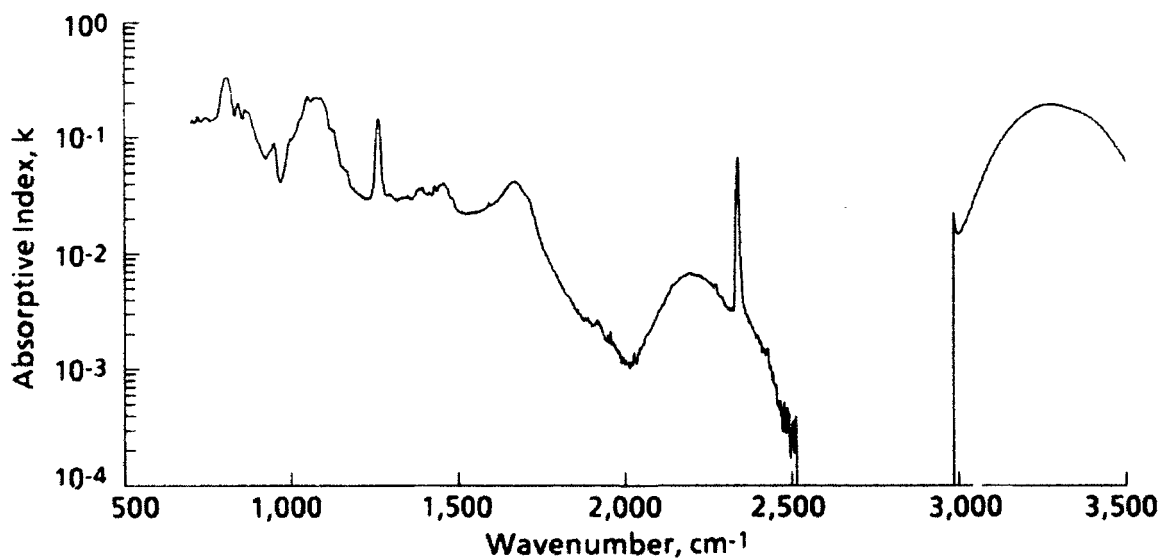


Figure 31. Transmittance at 3,250 cm⁻¹ for Uralane®.



a. Refractive index



b. Absorptive index

Figure 32. Optical properties for RTV®-566.

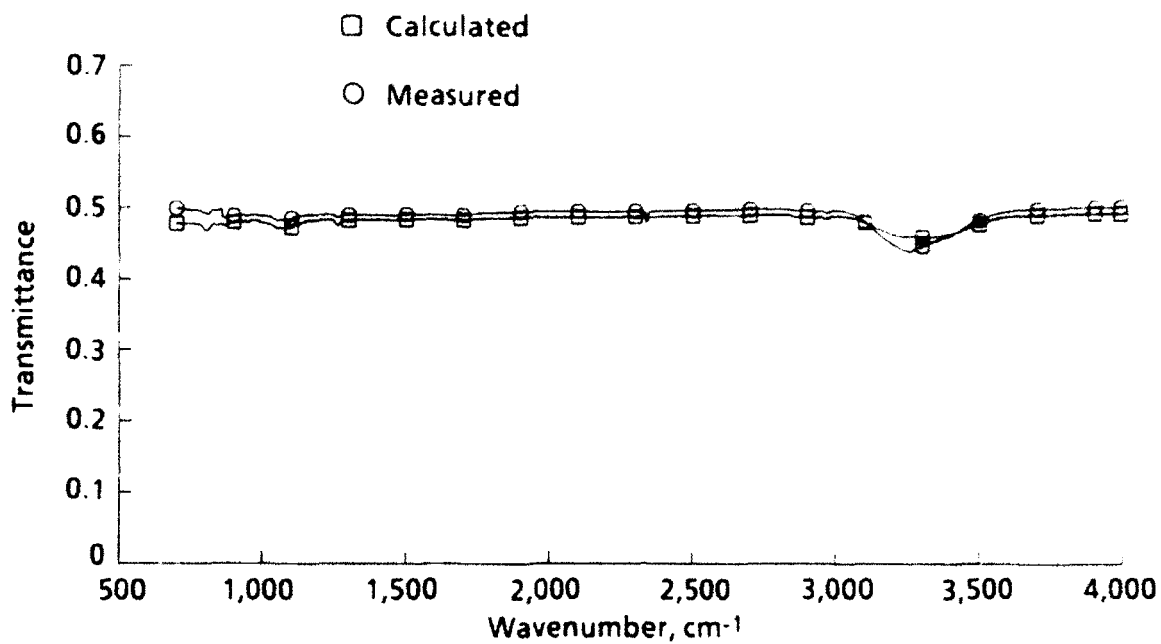


Figure 33. Transmittance for 0.11- μm -thick RTV[®]-566.

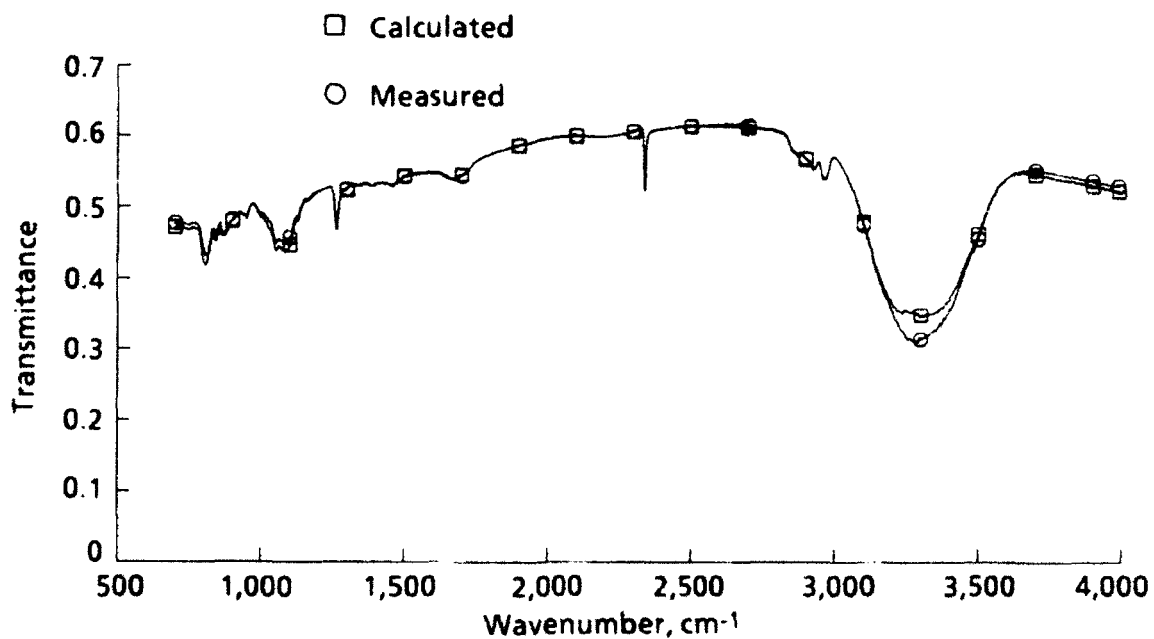


Figure 34. Transmittance for 0.68- μm -thick RTV[®]-566.

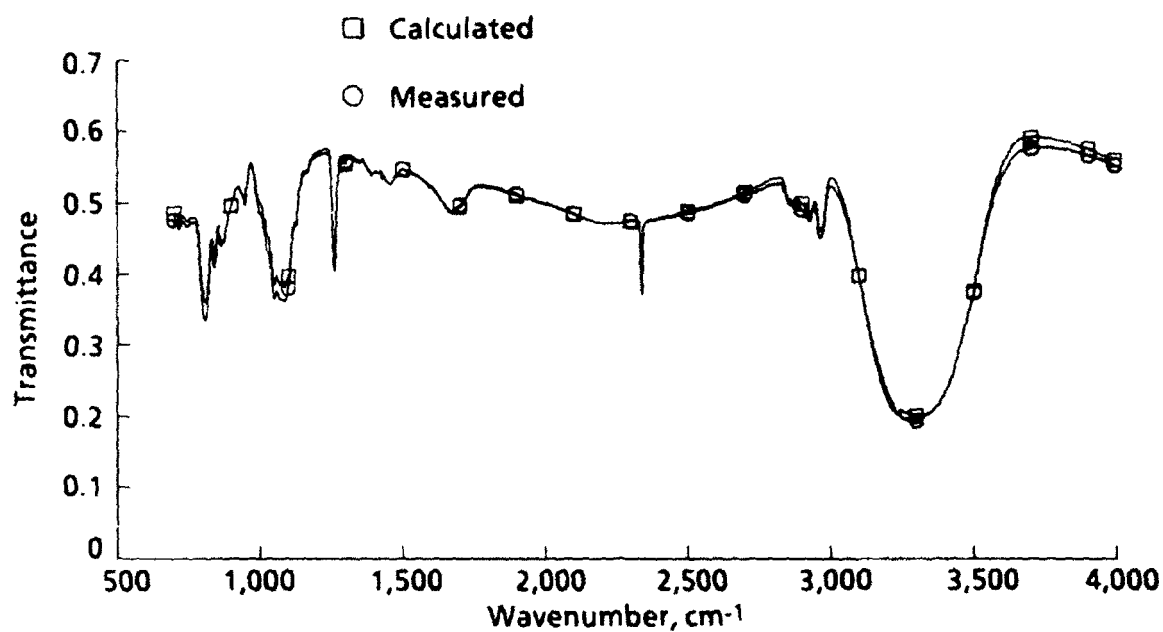


Figure 35. Transmittance for 1.48- μm -thick RTV[®]-566.

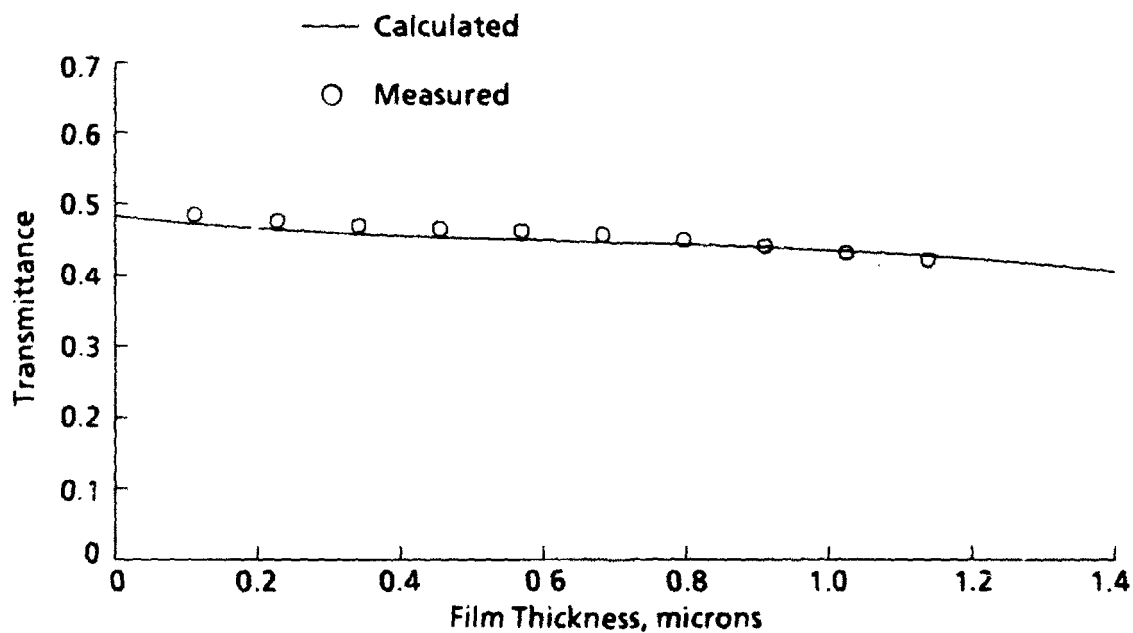


Figure 36. Transmittance at 1,100 cm^{-1} for RTV[®]-566.

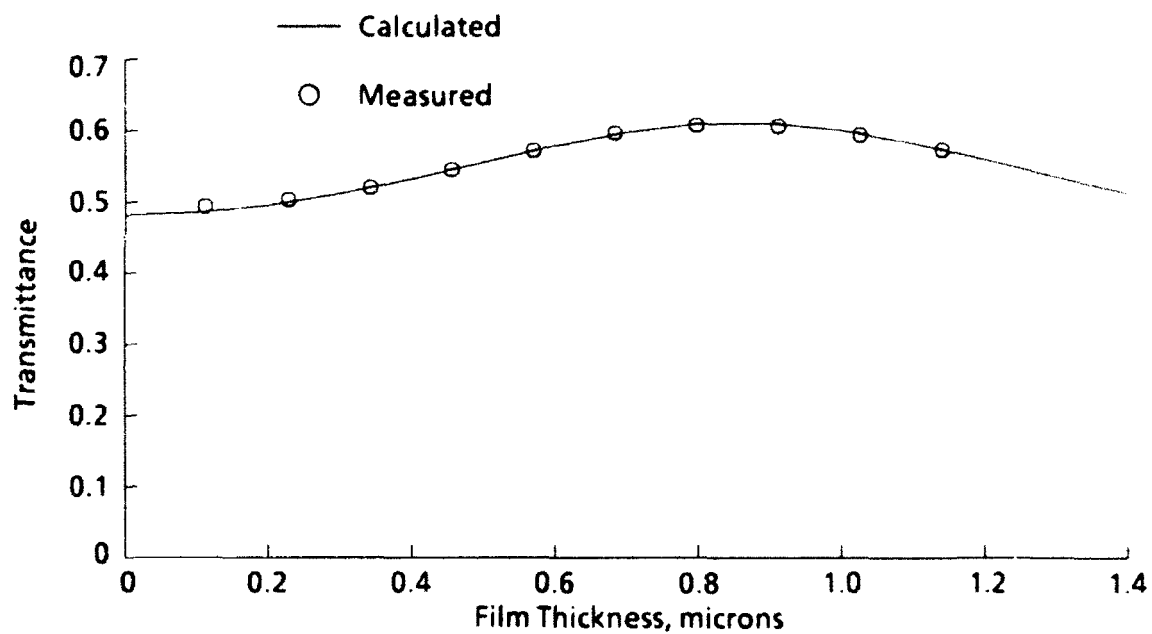


Figure 37. Transmittance at 2,000 cm⁻¹ for RTV®-566.

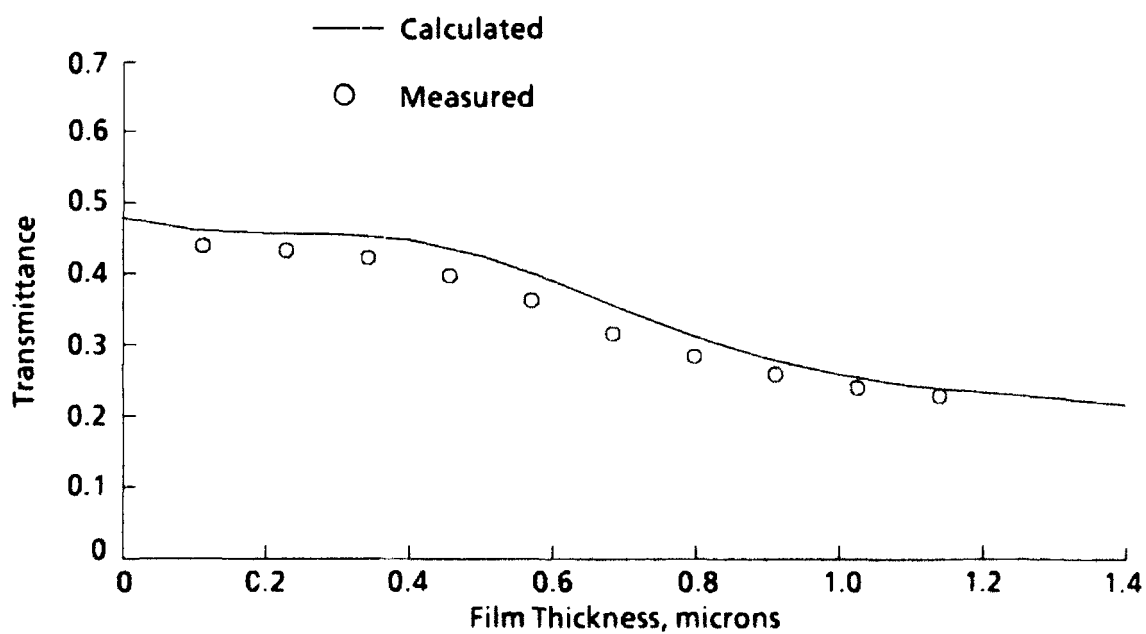
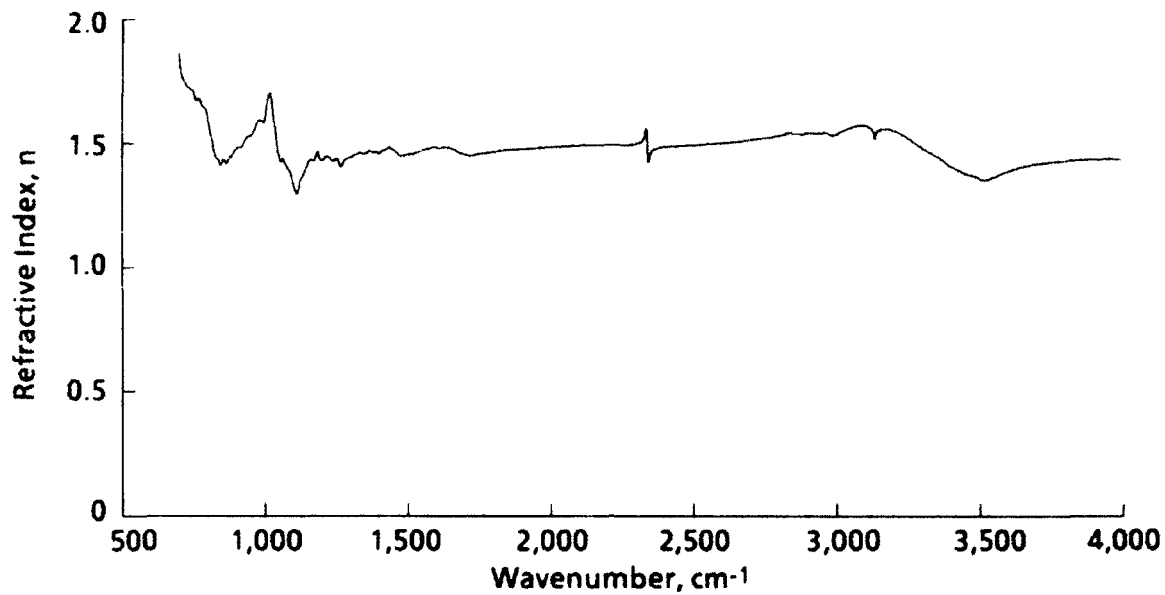
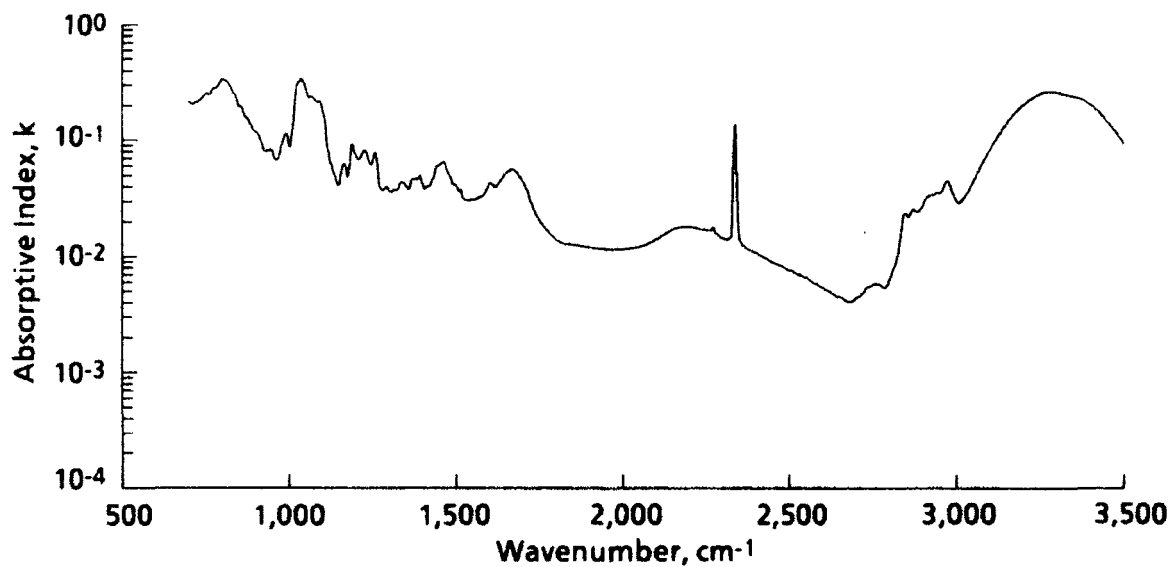


Figure 38. Transmittance at 3,250 cm⁻¹ for RTV®-566.



a. Refractive index



b. Absorptive index

Figure 39. Optical properties for mix 1.

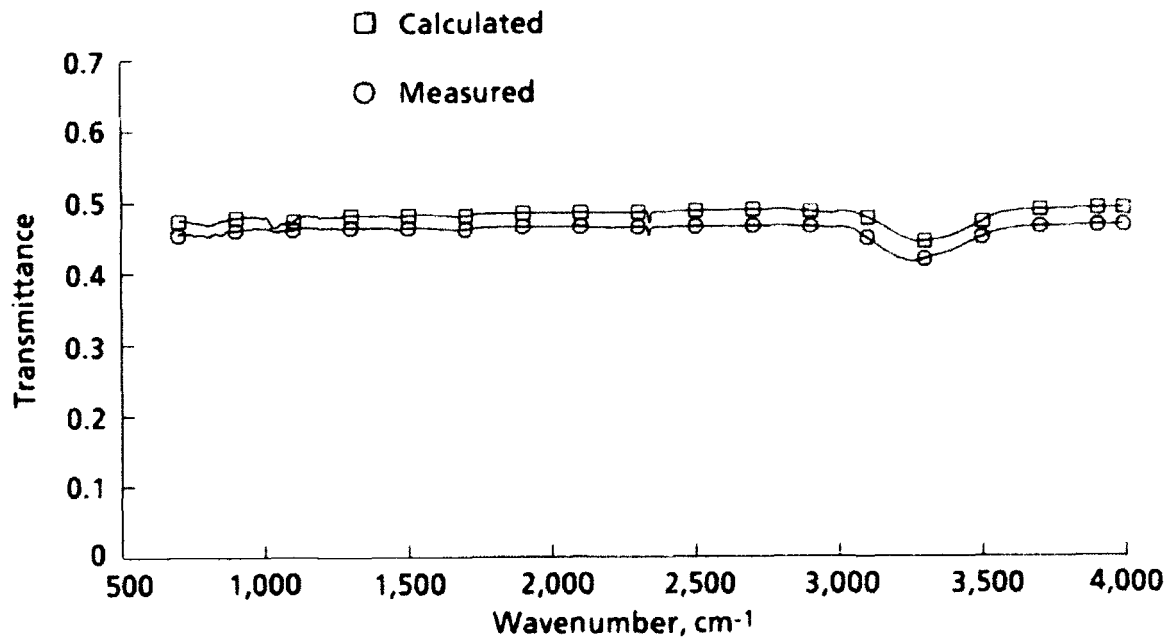


Figure 40. Transmittance for 0.11- μm -thick mix 1.

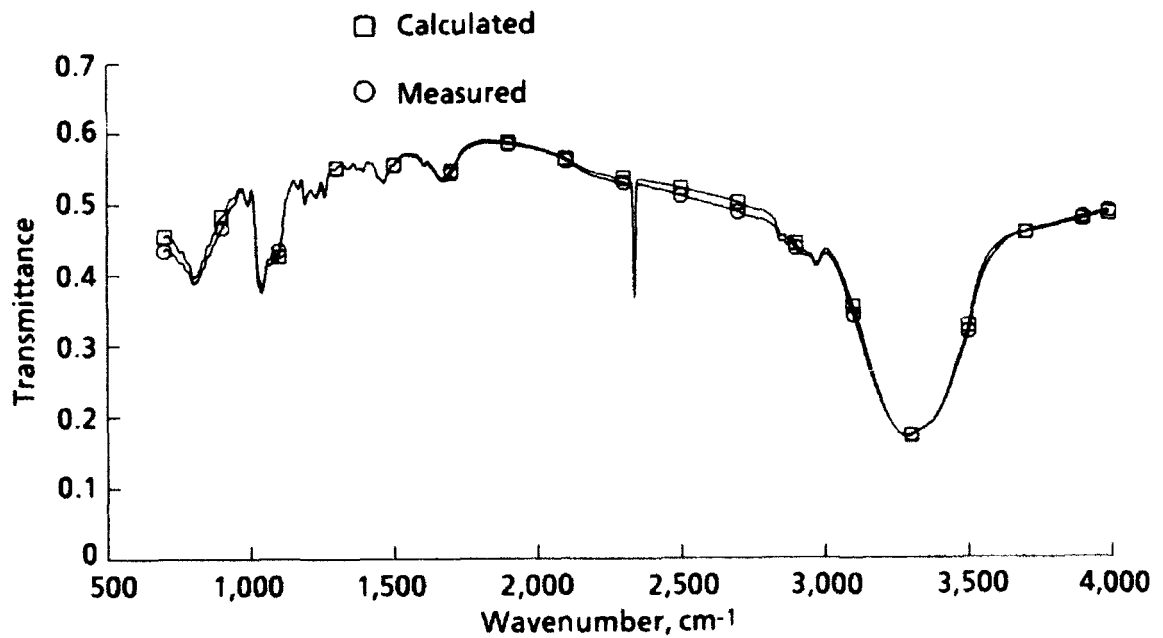


Figure 41. Transmittance for 1.02- μm -thick mix 1.

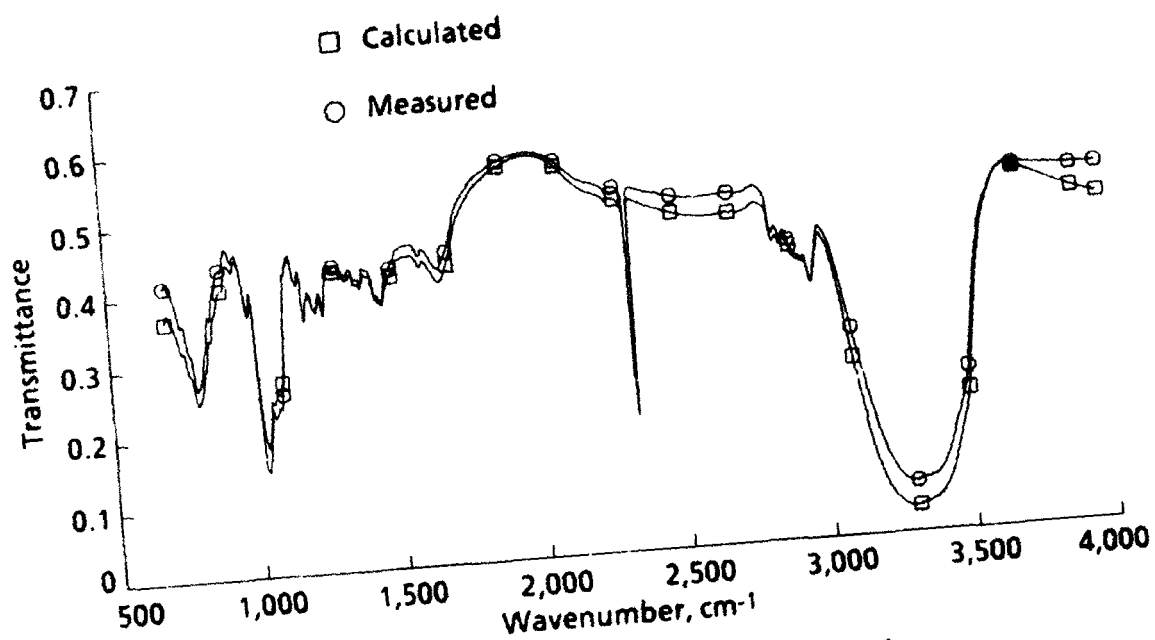


Figure 42. Transmittance for 2.50- μm -thick mix 1.

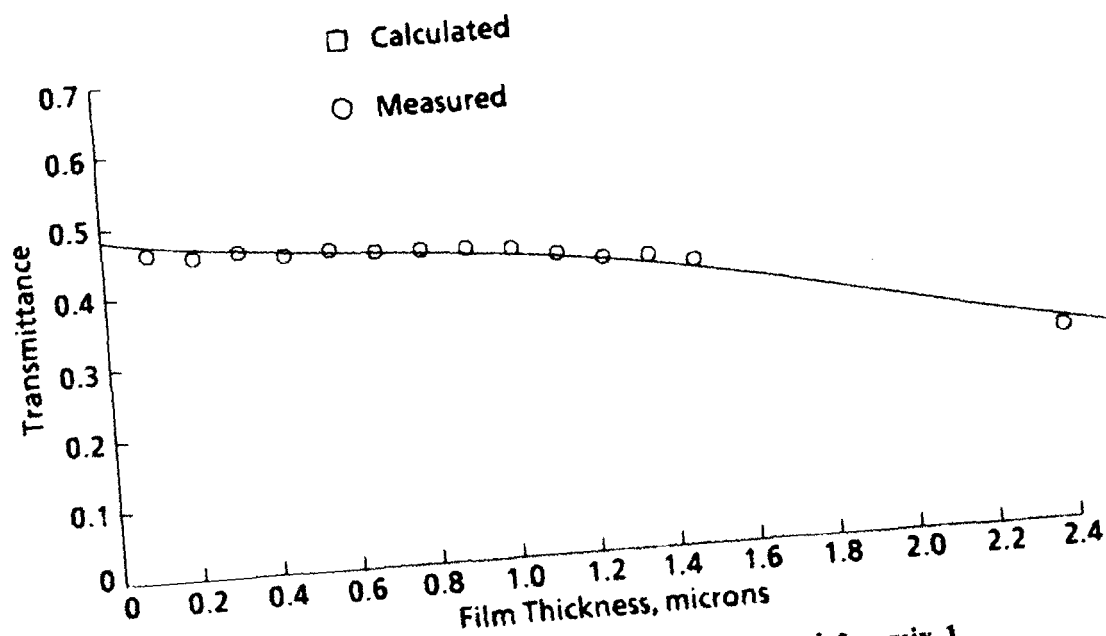


Figure 43. Transmittance at 1,100 cm^{-1} for mix 1.

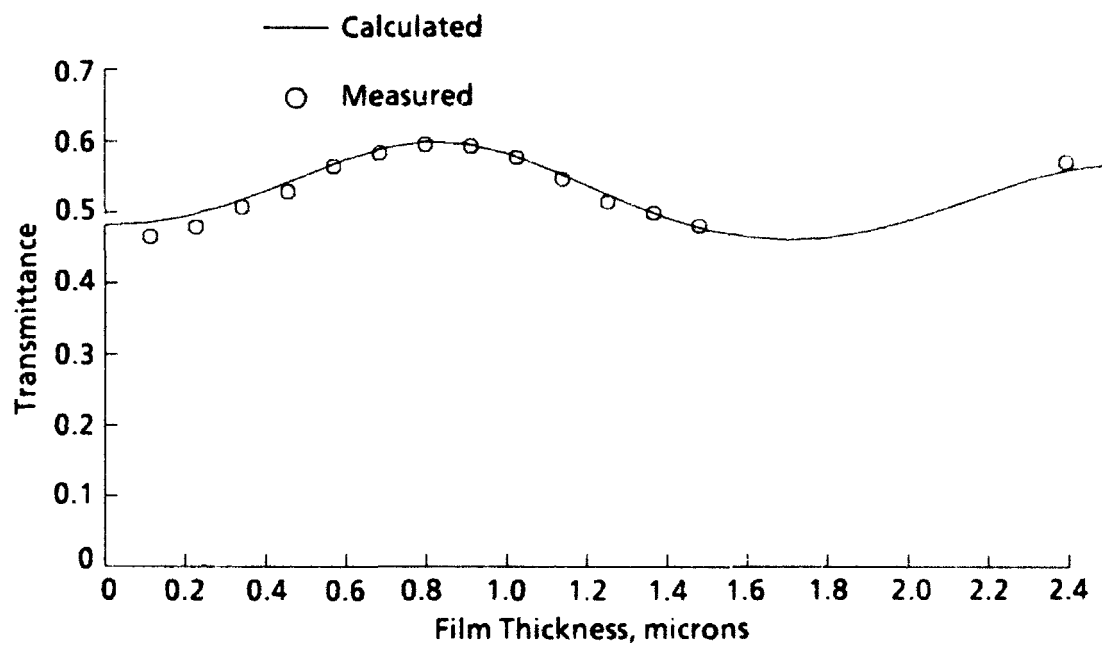


Figure 44. Transmittance at $2,000\text{ cm}^{-1}$ for mix 1.

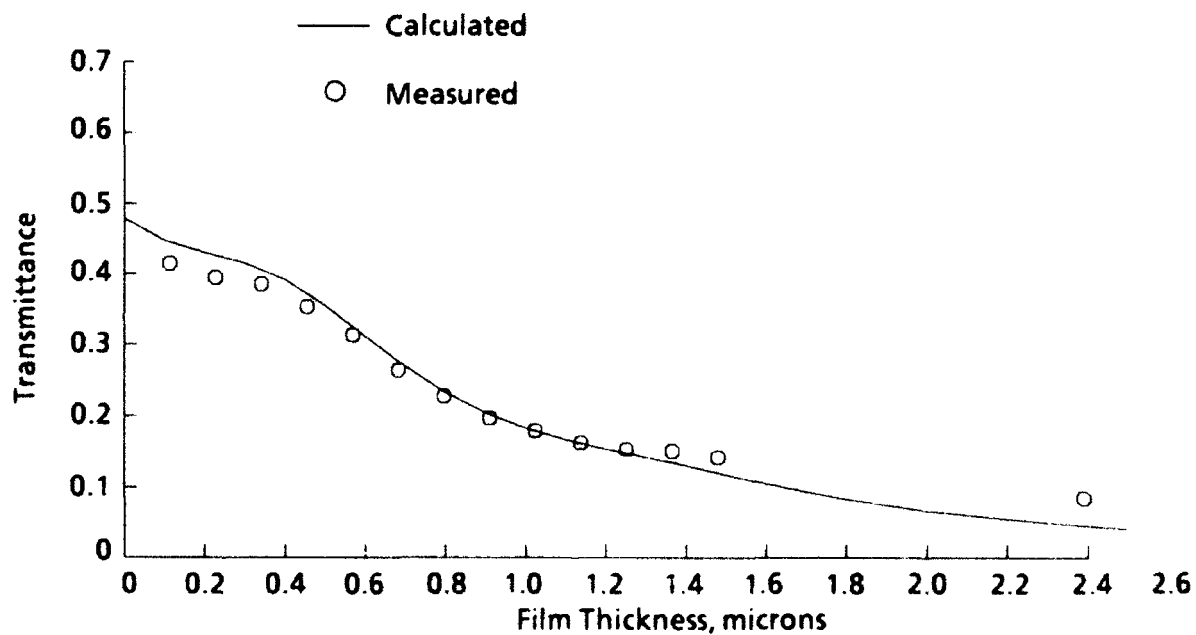
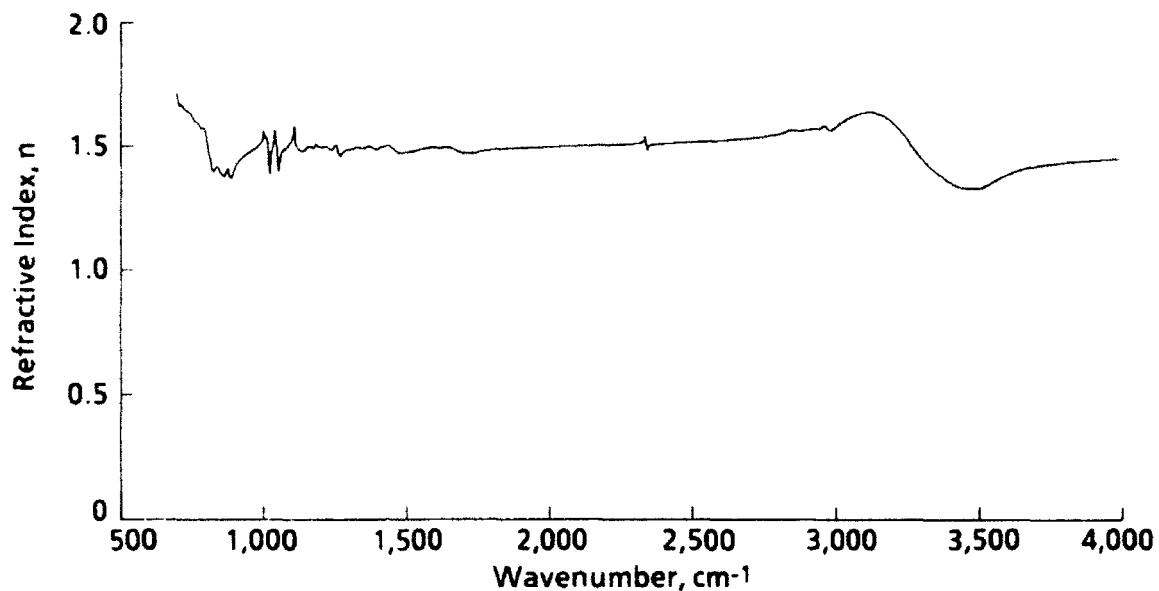
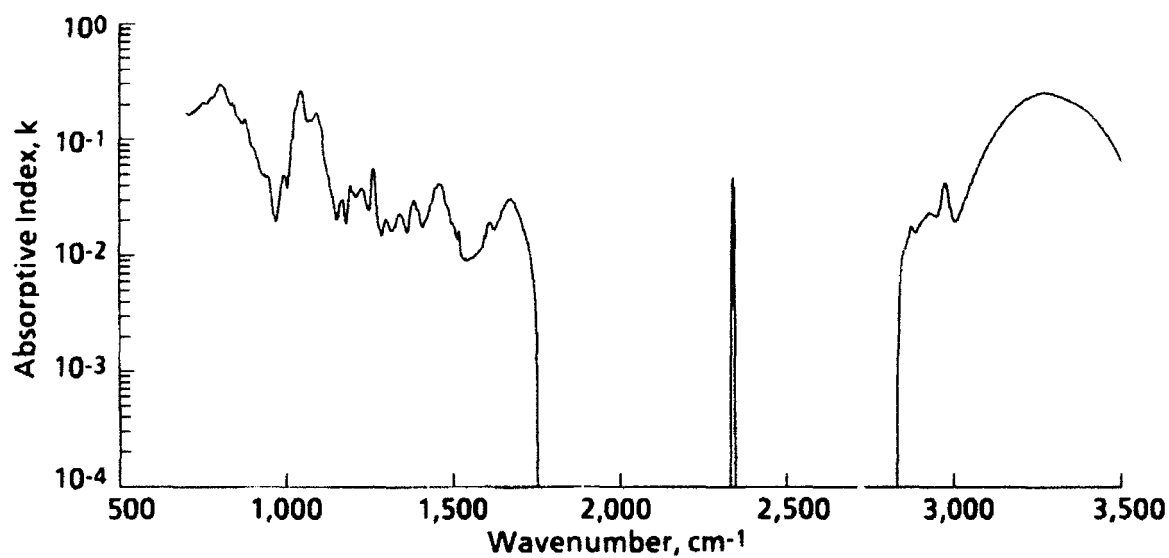


Figure 45. Transmittance at $3,250\text{ cm}^{-1}$ for mix 1.



a. Refractive index



b. Absorptive index

Figure 46. Optical properties for mix 2.

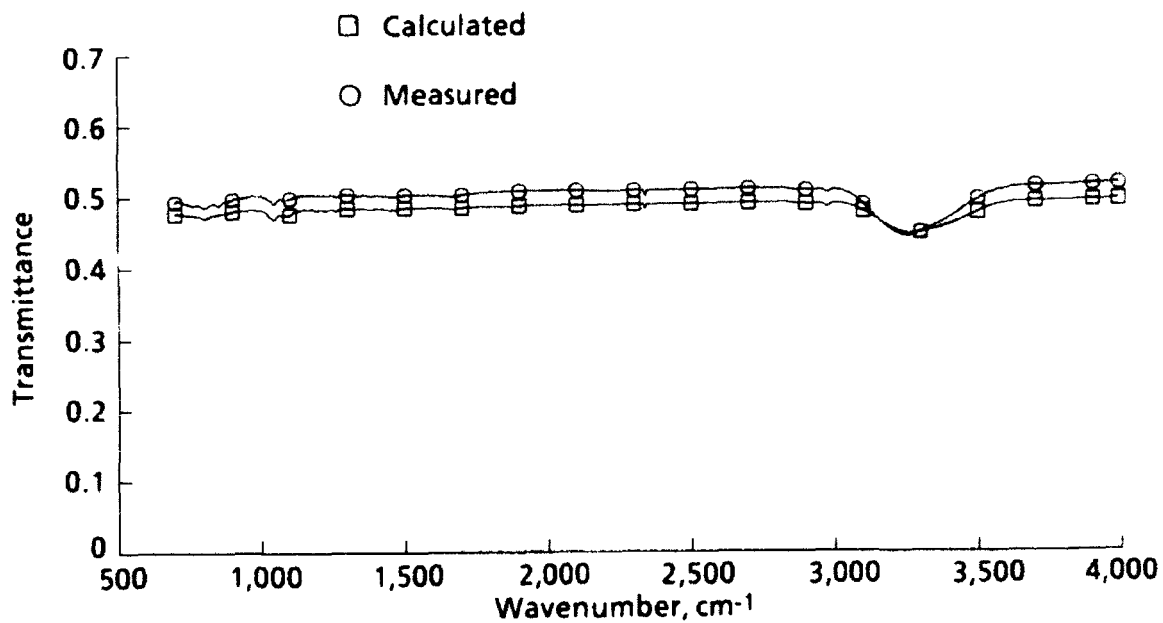


Figure 47. Transmittance for 0.11- μ m-thick mix 2.

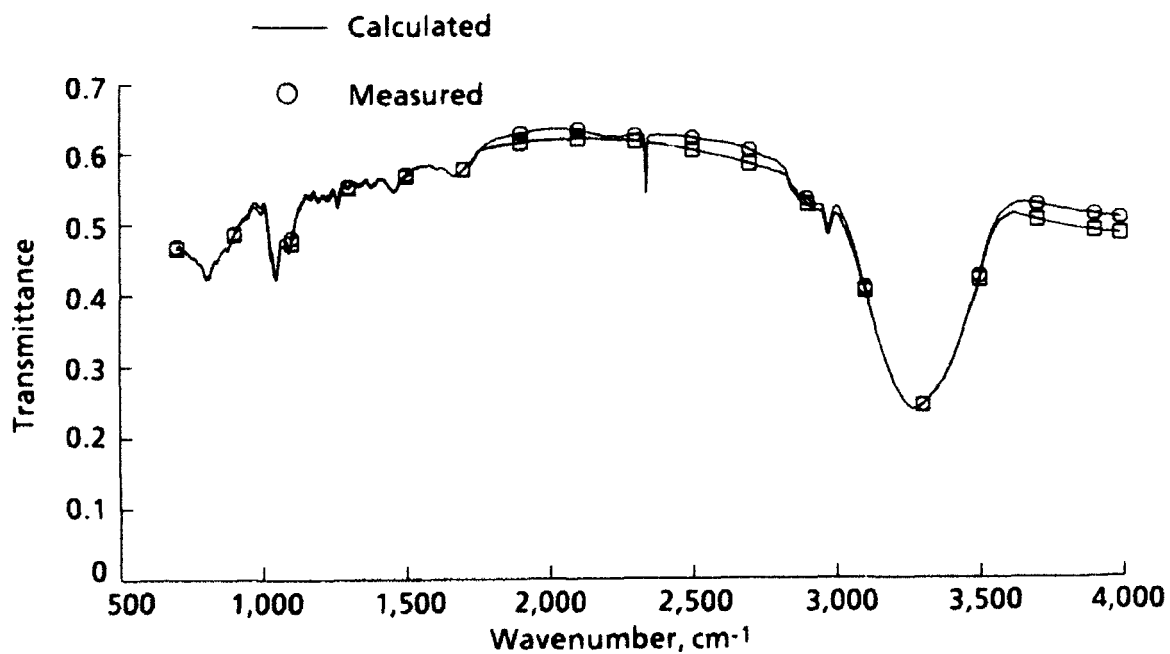


Figure 48. Transmittance for 0.79- μ m-thick mix 2.

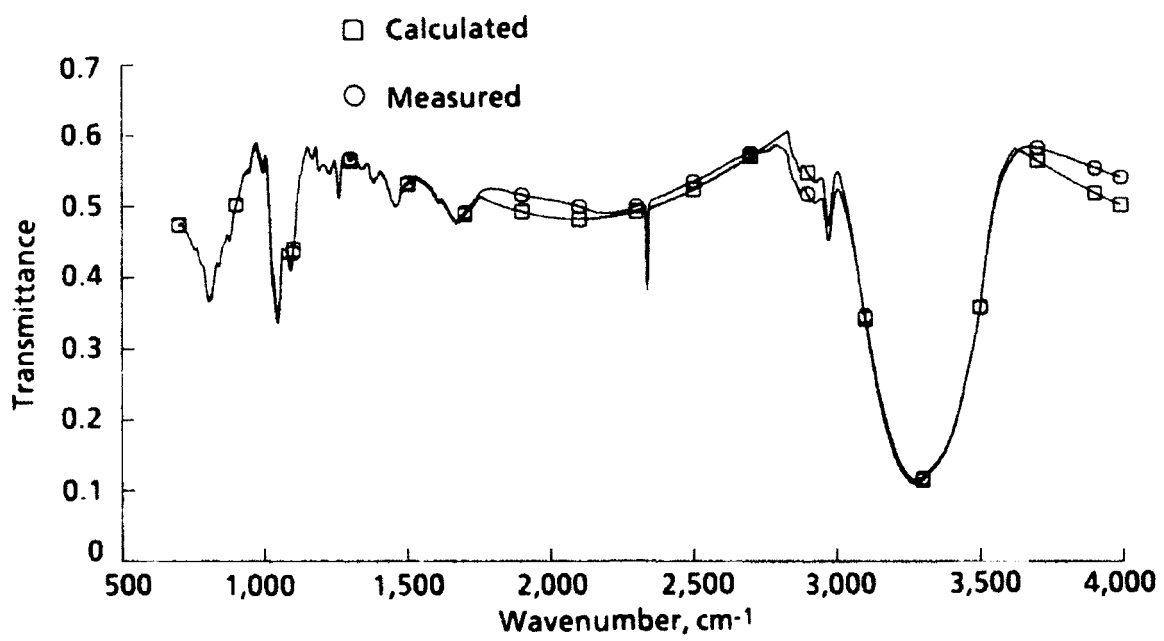


Figure 49. Transmittance for 1.59- μm -thick mix 2.

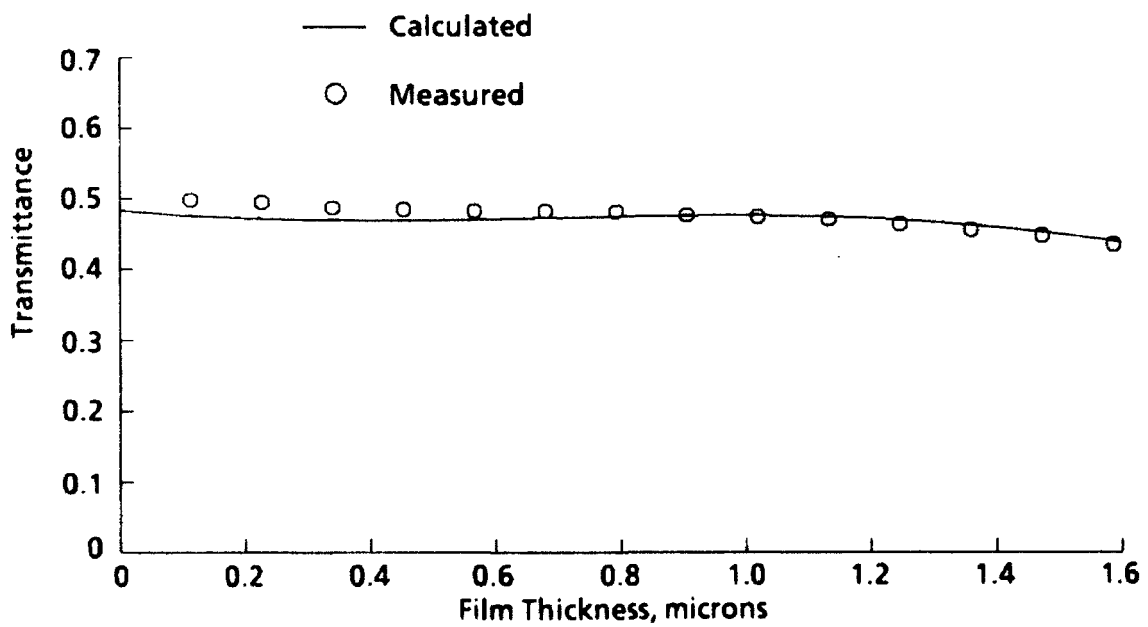


Figure 50. Transmittance at 1,100 cm^{-1} for mix 2.

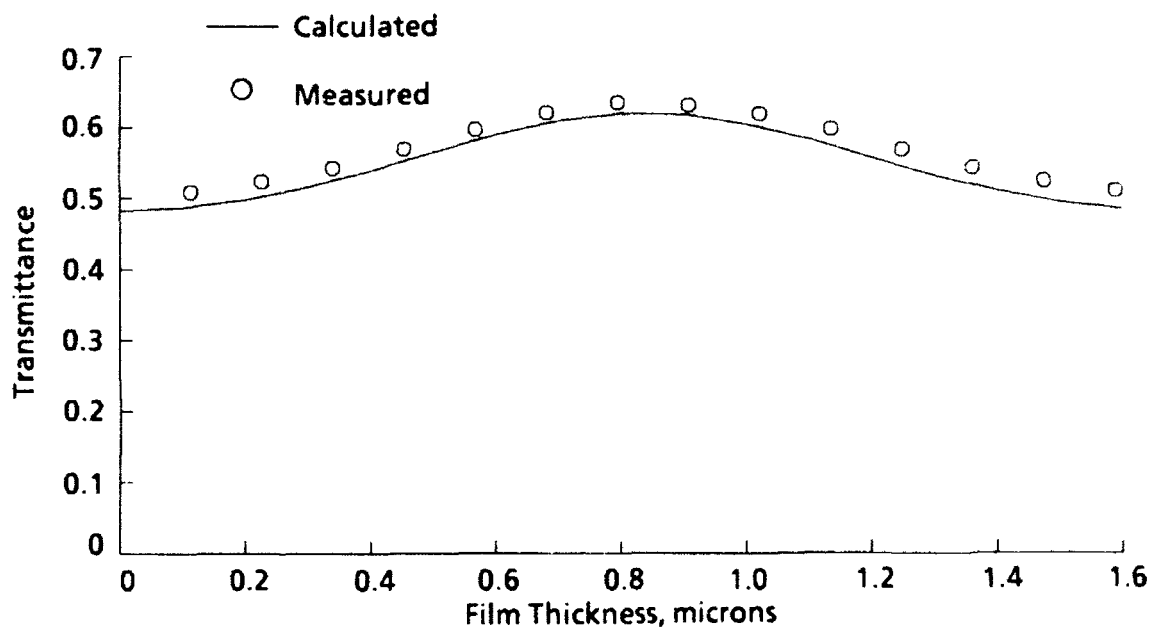


Figure 51. Transmittance at $2,000\text{ cm}^{-1}$ for mix 2.

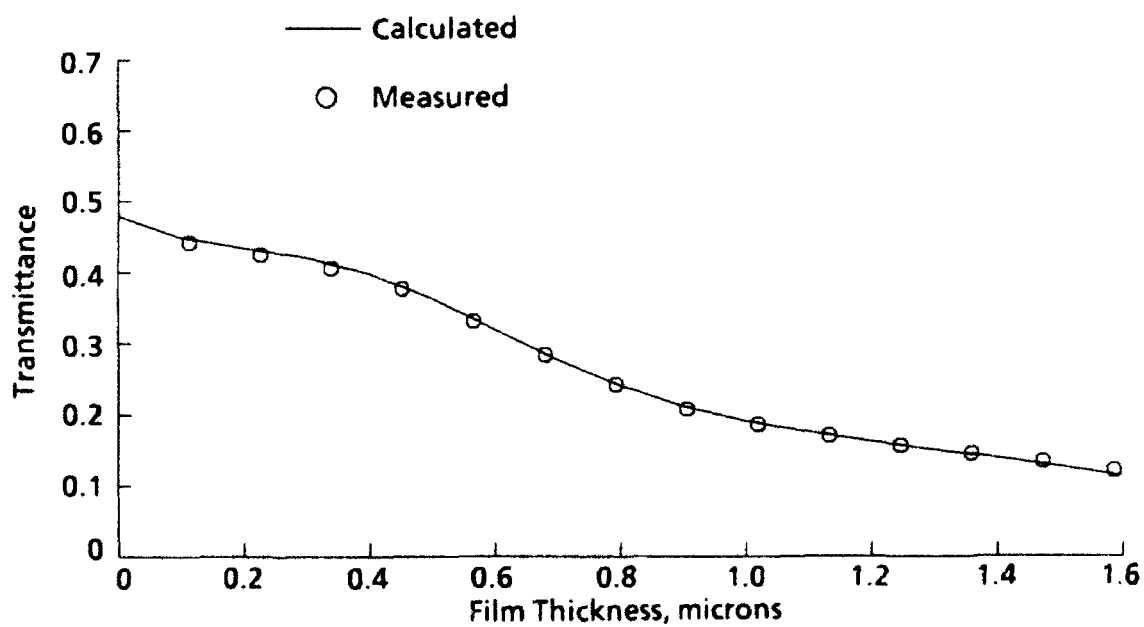
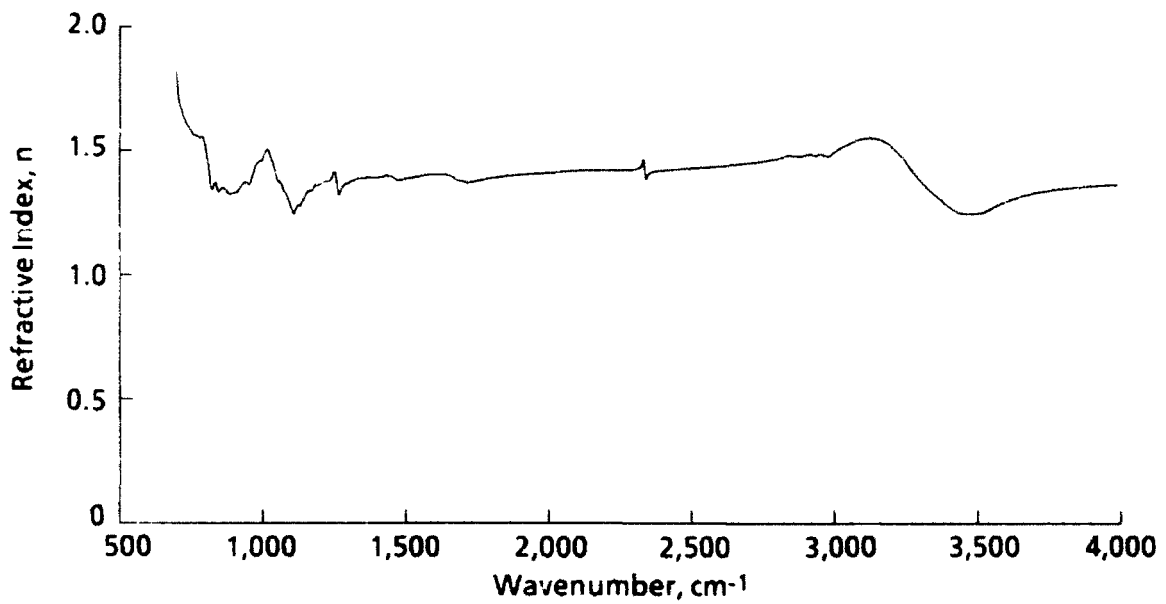
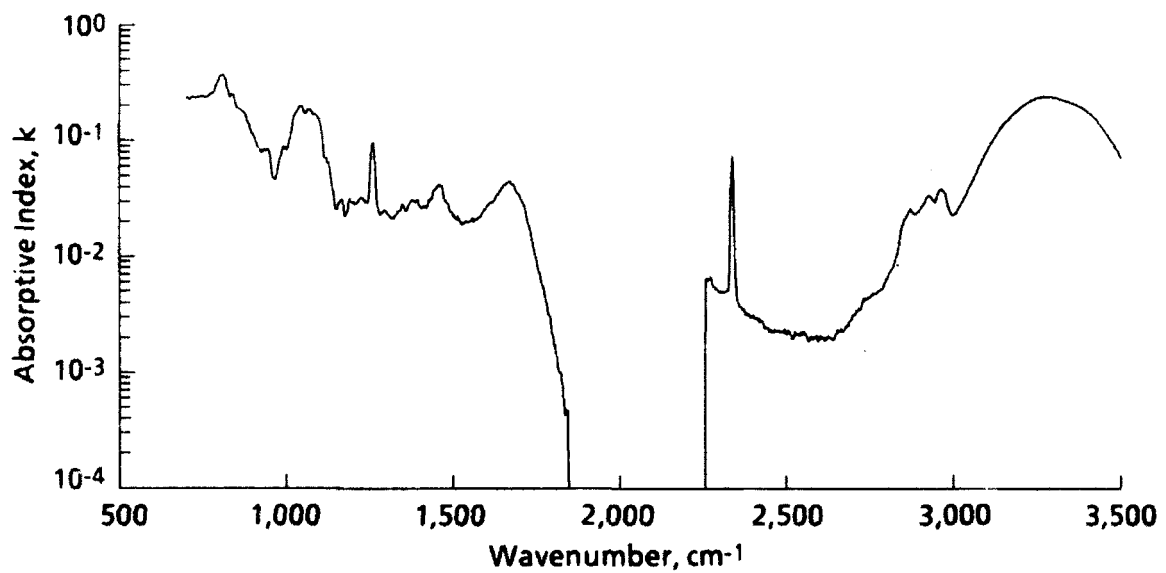


Figure 52. Transmittance at $3,250\text{ cm}^{-1}$ for mix 2.



a. Refractive index



b. Absorptive index

Figure 53. Optical properties for mix 3.

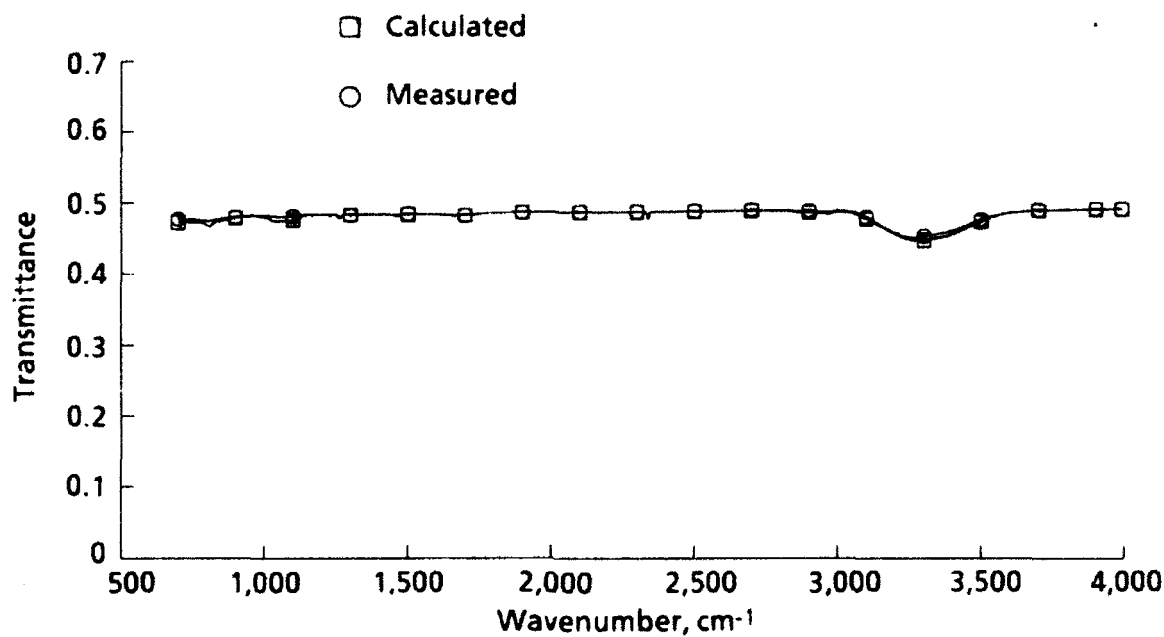


Figure 54. Transmittance for 0.12- μm -thick mix 3.

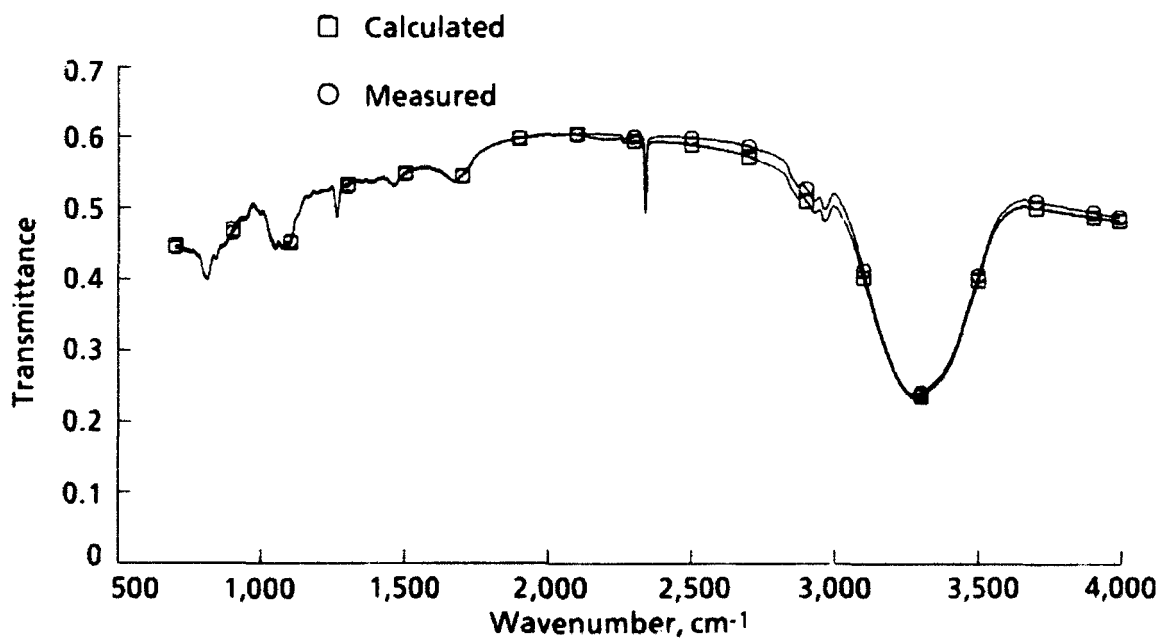


Figure 55. Transmittance for 0.83- μm -thick mix 3.

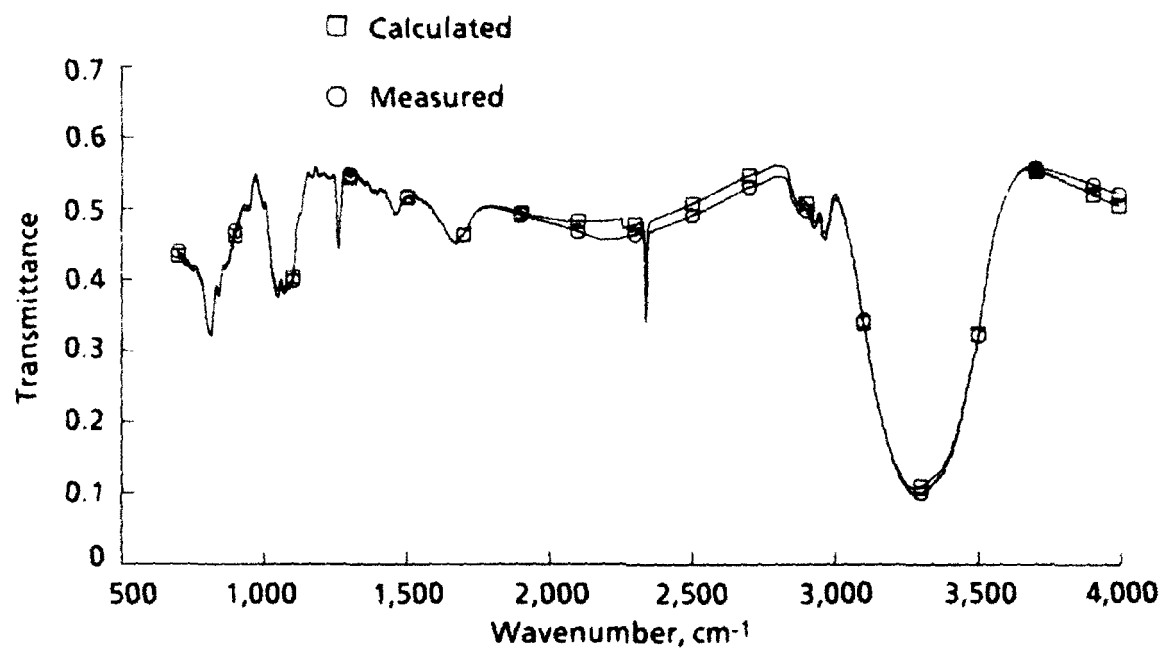


Figure 56. Transmittance for 1.66- μm -thick mix 3.

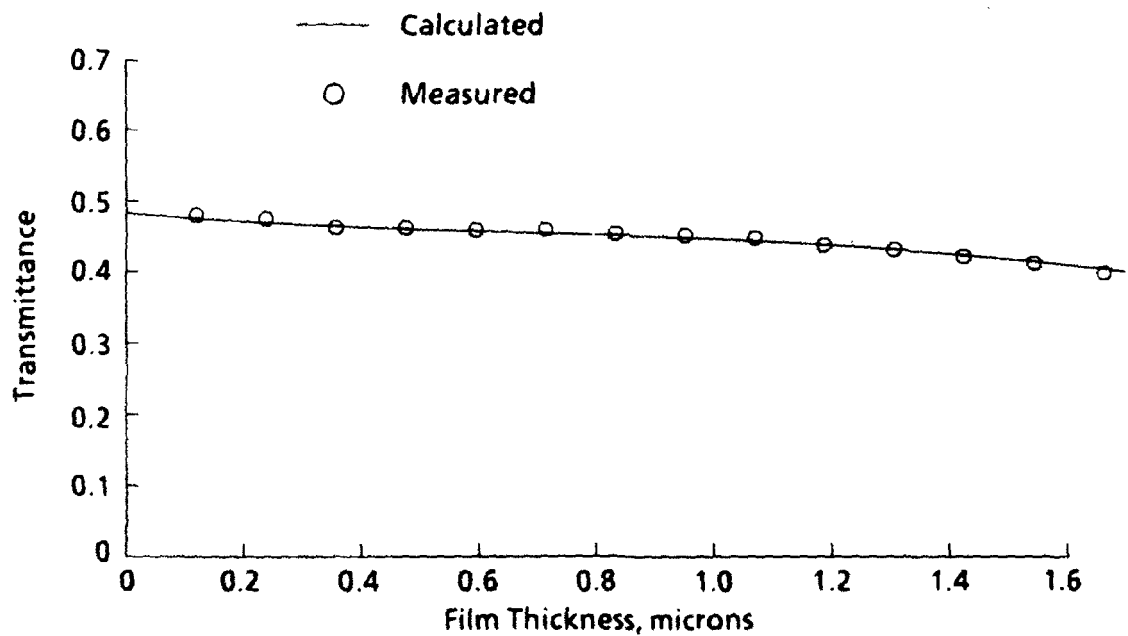


Figure 57. Transmittance at 1,100 cm^{-1} for mix 3.

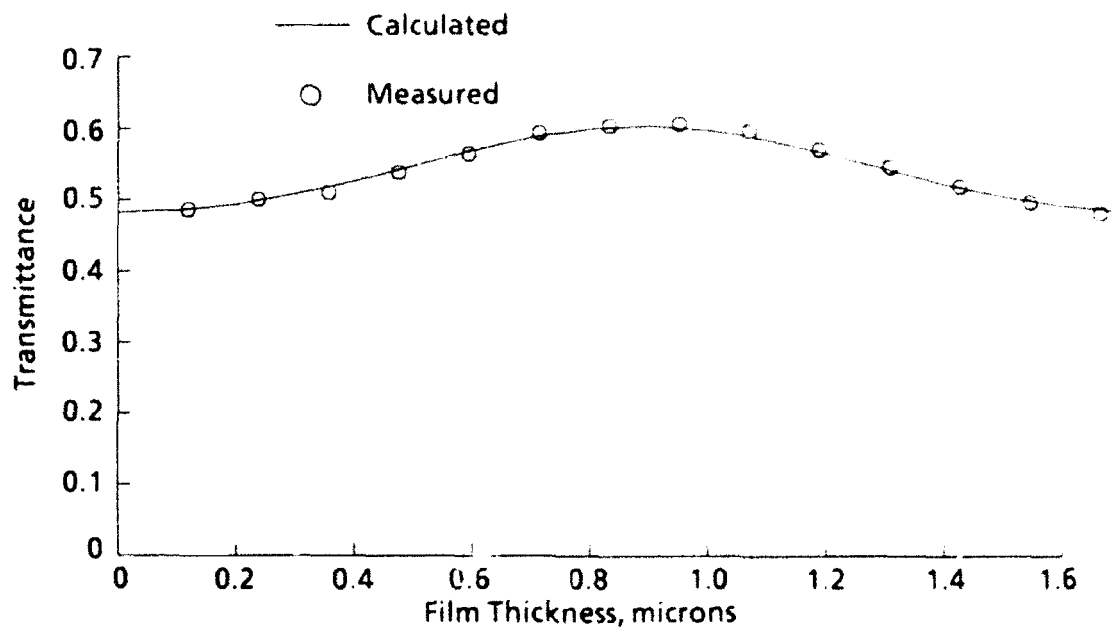


Figure 58. Transmittance at $2,000\text{ cm}^{-1}$ for mix 3.

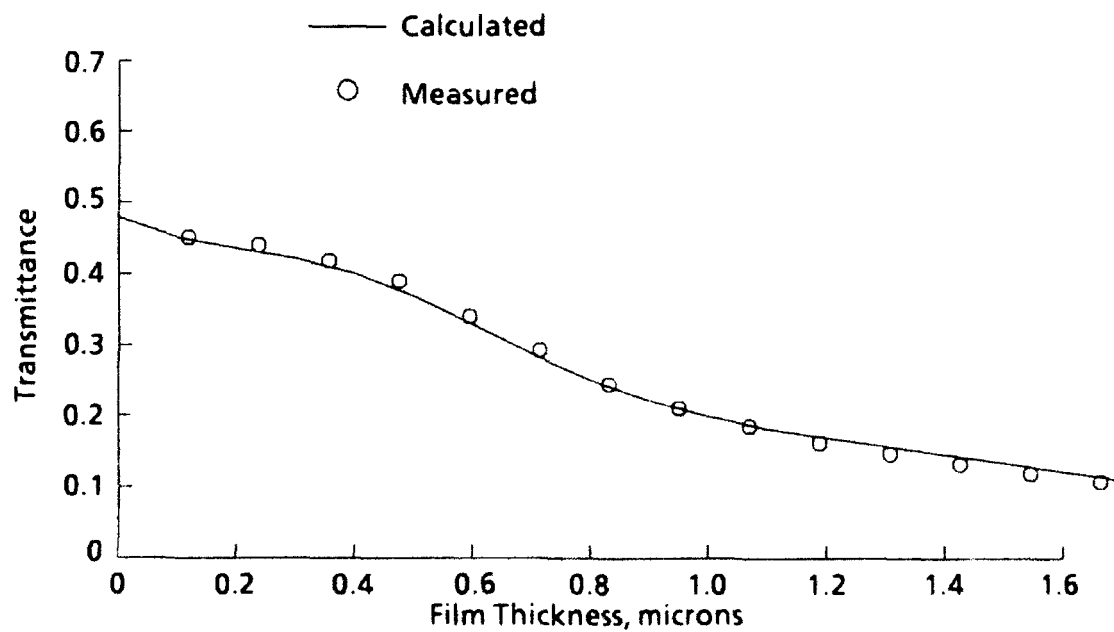


Figure 59. Transmittance at $3,250\text{ cm}^{-1}$ for mix 3.

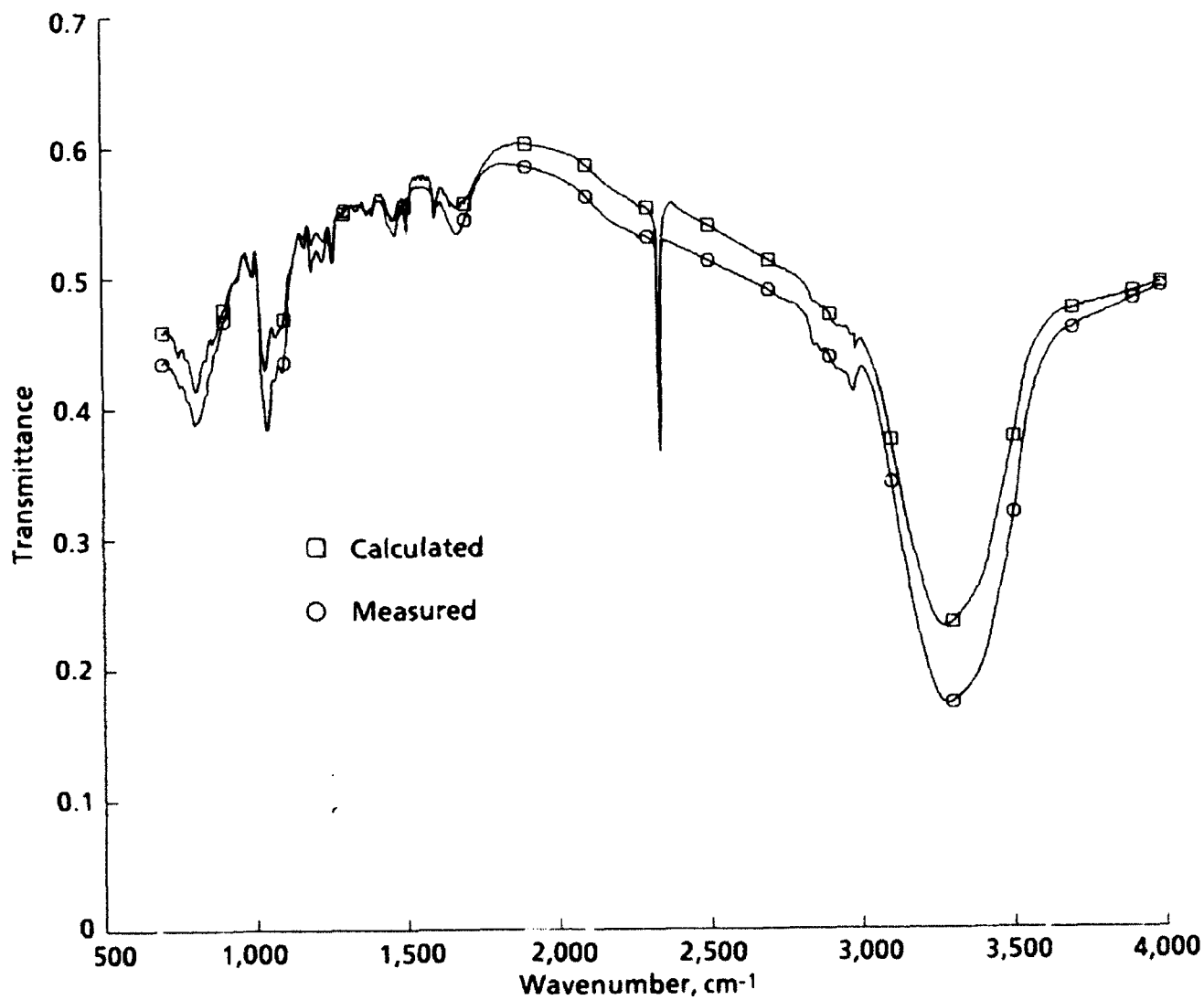


Figure 60. Transmittance for 1.02-μm-thick combined mix 1.

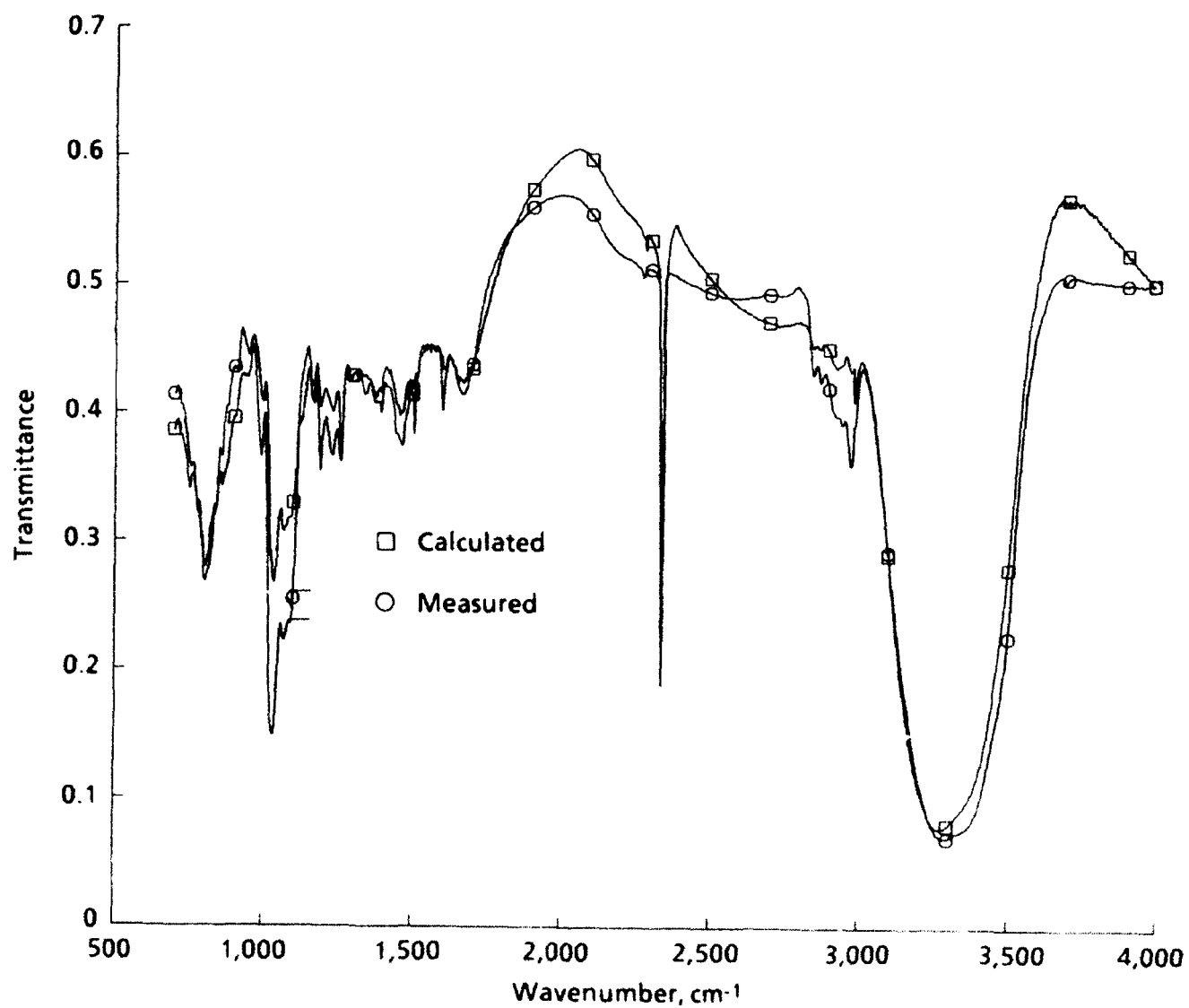


Figure 61. Transmittance for 2.50- μ m-thick combined mix 1.

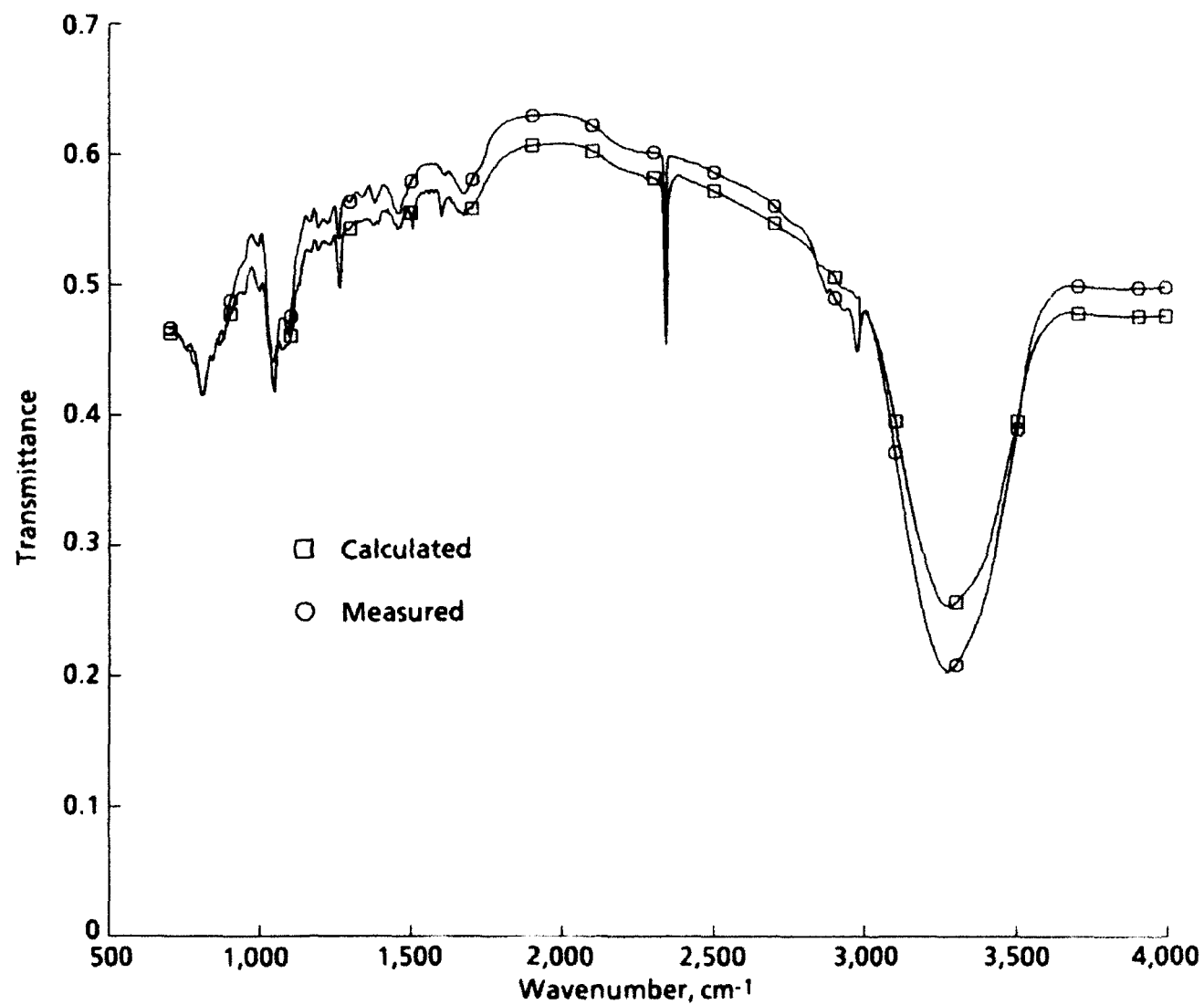


Figure 62. Transmittance for 0.91-μm-thick combined mix 2.

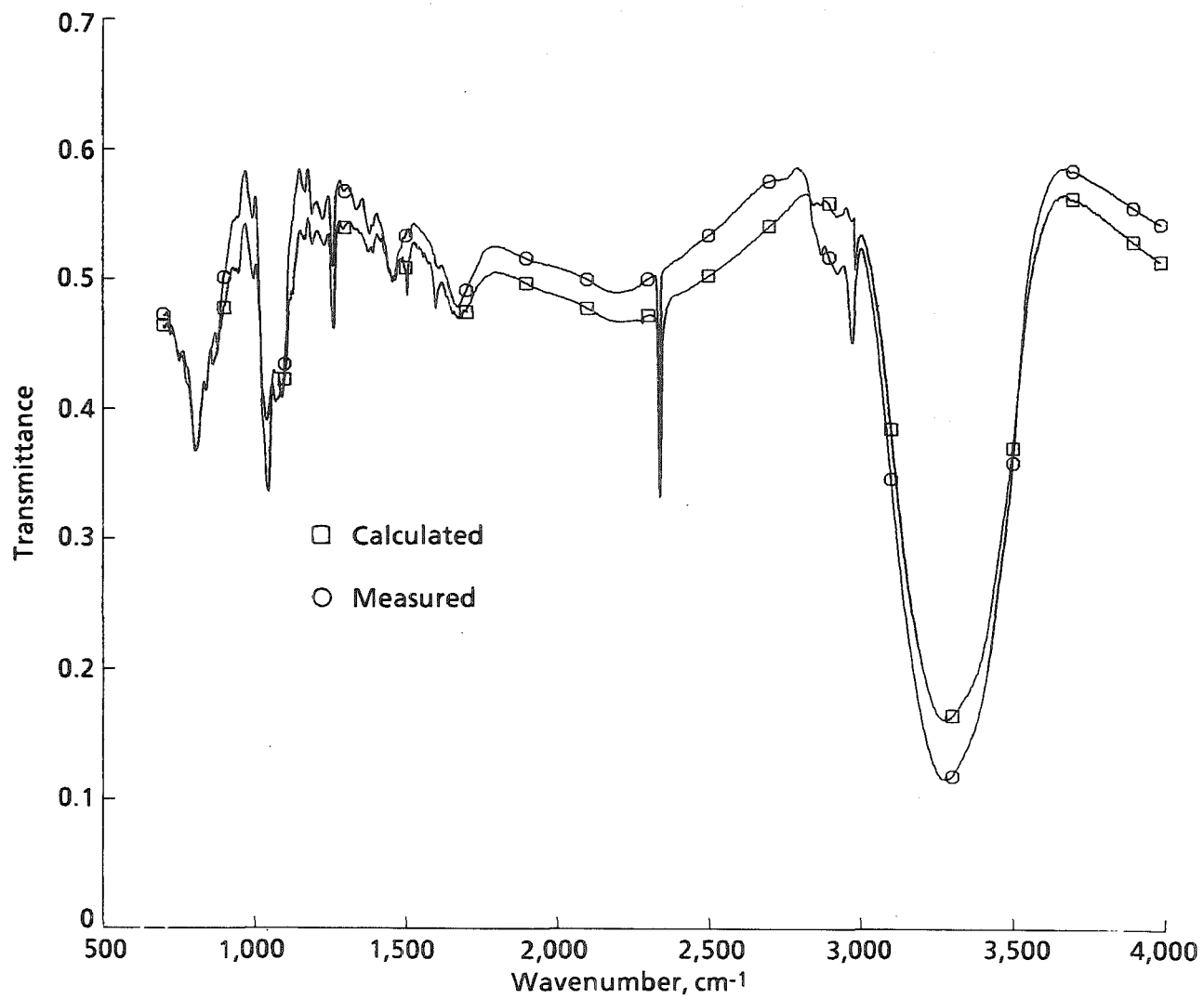


Figure 63. Transmittance for 1.59-μm-thick combined mix 2.

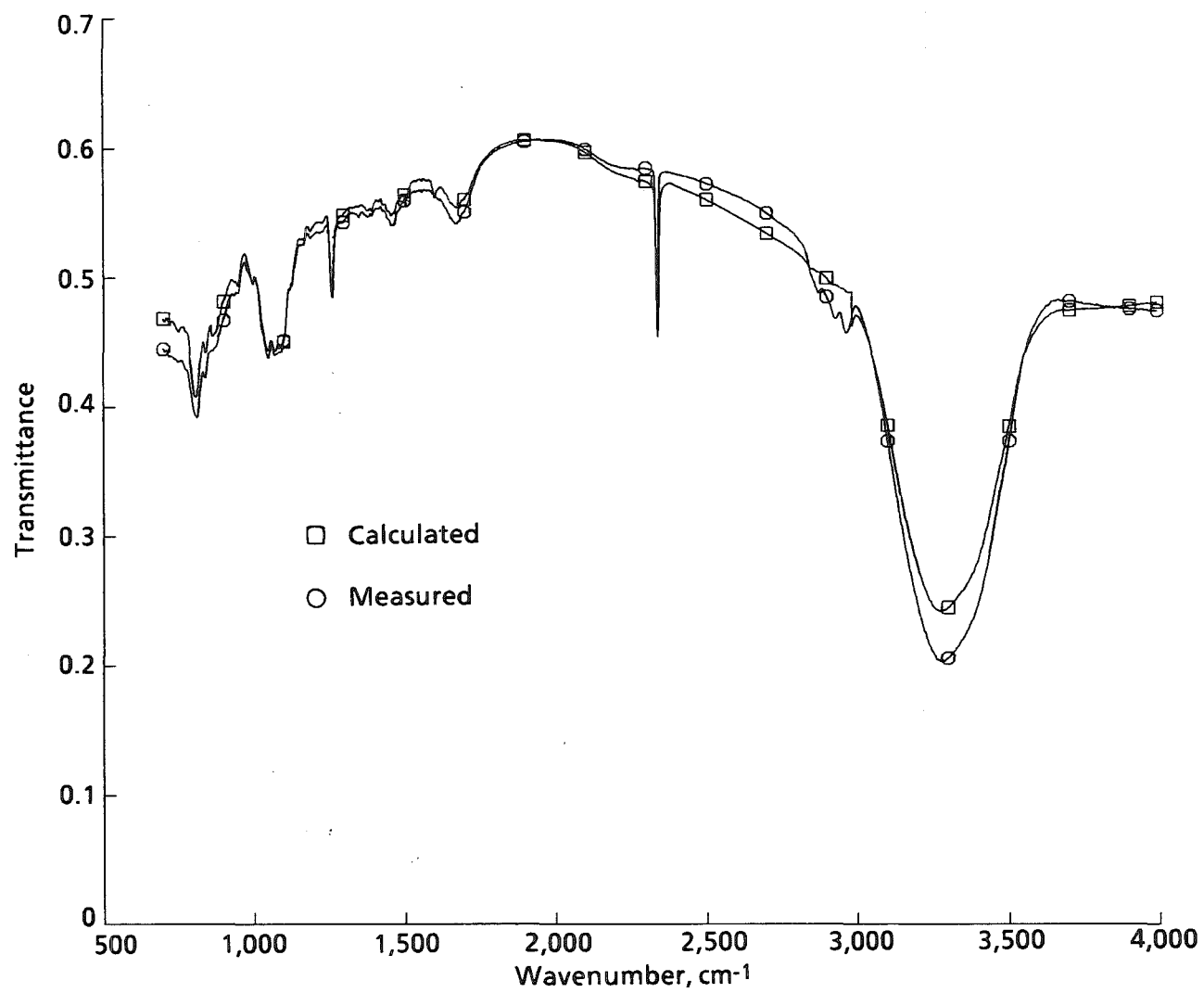


Figure 64. Transmittance for 0.95- μm -thick combined mix 3.

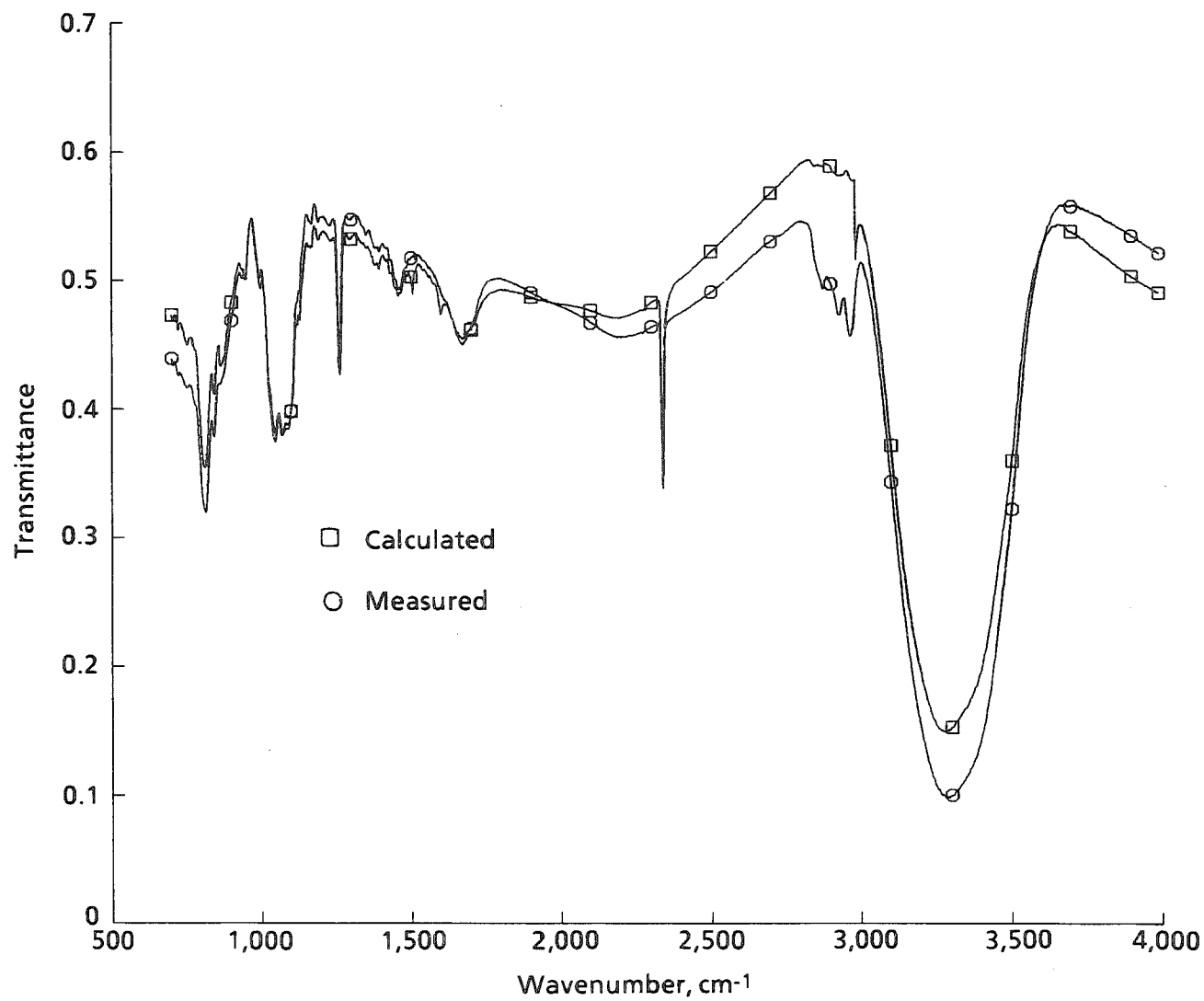


Figure 65. Transmittance for 1.66- μm -thick combined mix 3.